THE ASTROPHYSICAL JOURNAL SUPPLEMENT SERIES, 79:507–568, 1992 April

RADIATIVE ATOMIC ROSSELAND MEAN OPACITY TABLES

FORREST J. ROGERS AND CARLOS A. IGLESIAS
Lawrence Livermore National Laboratory, P.O. Box 808, Livermore, CA 94550
Received 1991 May 29; accepted 1991 September 12

ABSTRACT

For more than two decades the astrophysics community has depended on opacity tables produced at Los Alamos. In the present work we offer new radiative Rosseland mean opacity tables calculated with the OPAL code developed independently at LLNL. We give extensive results for the recent Anders-Grevesse mixture which allow accurate interpolation in temperature, density, hydrogen mass fraction, as well as metal mass fraction. The tables are organized differently from previous work. Instead of rows and columns of constant temperature and density, we use temperature and follow tracks of constant R, where R = density/(temperature)^3. The range of R and temperature are such as to cover typical stellar conditions from the interior through the envelope and the hotter atmospheres. Cool atmospheres are not considered since photoabsorption by molecules is neglected. Only radiative processes are taken into account so that electron conduction is not included. For comparison purposes we present some opacity tables for the Ross-Aller and Cox-Tabor metal abundances. Although in many regions the OPAL opacities are similar to previous work, large differences are reported. For example, factors of 2–3 opacity enhancements are found in stellar envelop conditions.

Subject headings: atomic data — atomic processes — stars: interiors

1. INTRODUCTION

The transport of energy in the interior of stars is primarily through photon radiation, convection, and electron conduction. Of the three processes, the radiative transport is perhaps the most essential in governing the structure and evolution of a star. However, there are no direct measurements of the radiative opacity at stellar interior conditions so that one must rely on theoretical calculations. The first comprehensive tables of Rosseland mean opacities were produced by Cox, Stewart, & Eilers (1965) and Cox & Stewart (1965). Refinements and extensions of this pioneering effort were carried out by several groups at Los Alamos (Cox & Stewart 1969, 1970a,b; Cox & Tabor 1976; Magee, Merts, & Huebner 1975; Huebner et al. 1977). A compendium of Los Alamos results produced since 1977 is given by Weiss, Keady, & Magee (1990). Although Los Alamos opacities (here collectively called LAO) have become the standard, opacity tables by Carson have also been used in a number of applications (e.g., Carson & Stothers 1976, 1988; Carson, Stothers, & Vermury 1981). Note that past discrepancies between Carson and LAO have been resolved (Carson et al. 1984).

In the development of the LAO opacities several approximations were introduced such as hydrogenic formulas and scaling of photoionization cross sections in the atomic data. To a large extent these approximations were imposed by computer limitations of that time, but the uncertainties in the opacity caused by these compromises were not known. As observational and modeling capabilities progressed, it became apparent that a number of serious discrepancies existed between stellar models and observations which could possibly be attributed to inaccuracies in opacity.

For example, the possibility that opacity enhancements could be the energizing mechanism for pulsations in β Cephei stars was first examined by Stellingwerf (1978). He increased the Cox-Tabor (1976, hereafter CT) opacity by as much as 70% in the region 10^5 K $< T < 4 \times 10^5$ K and obtained an instability strip in good agreement with observations. Later, Simon (1982) noticed that increasing the opacity of the metals by factors of 2–3 for 10^5 K $< T < 10^6$ K in classical Cepheid models reproduced observed period ratios at evolutionary masses and luminosities. Inspired by this result, he suggested that the opacity may indeed be underestimated for temperatures above 10^5 K and speculated that the deficiency was due to approximations in the calculation of photon absorption processes of heavy elements.

Magee, Merts, & Huebner (1984) responded to Simon's plea for a reexamination of the metal opacity and concluded that such large opacity increases were incompatible with atomic physics. Contrary to their claims, Simon's speculation has been subsequently substantiated by Iglesias, Rogers, & Wilson (1987, 1990) and Iglesias and Rogers (1991b), and the opacity enhancement attributed to improved atomic physics. Independently, Rozsnyai (1989) has bracketed the opacities using an approximate treatment to account for the large number of spectral lines and obtained minima and maxima compatible with Simon's speculation.

Using the opacity study of Simon (1982) and the preliminary opacity calculations of Iglesias et al. (1987) as a guide, Andreasen and Petersen (1988; Andreasen 1988; Petersen 1989, 1990) artificially enhanced the opacity by a factor λ in the temperature range 1.5×10^5 K $< T < 8 \times 10^5$ K. They were able to reproduce observed period ratios for double-mode Cepheids and δ Scuti variables with $\lambda = 2.5$. They also found that the same opacity increase offered an attractive solution to the mass anomaly in bump Cepheids. Although the preliminary calculation by Iglesias et al. (1987), done at too high a density for these models and consisting of a seven element mixture,

suggested an increase of only 1.4 over LAO, more recent calculations at more appropriate matter conditions with a 14 element mixture support the $\lambda = 2.5$ increase (Iglesias et al. 1990; Iglesias & Rogers 1991b). Furthermore, very recent calculations by Moskalik, Buchler, & Marom (1991) using actual opacity tables in Iglesias & Rogers (1991b) have essentially removed the beat mass discrepancies.

Andreasen (1988) also found that a more modest opacity increase of $\lambda = 1.5$ is sufficient to resolve the mass anomalies for the lower metallicity RR Lyrae stars. Again, the $\lambda = 1.5$ opacity enhancement in Population II stars is supported by recent opacity calculations (Iglesias & Rogers 1991b). Recently, however, these low-metallicity variable stars have been reexamined (Simon & Cox 1991, and references therein). These authors conclude that in view of the extremely low metallicity very large opacity enhancements seem necessary in order to resolve the mass anomalies. Interestingly, Cox (1991) has shown that opacity decreases near $T \approx 3 \times 10^4$ K (Iglesias & Rogers 1991b) accompanied with modest opacity increases near $T \approx 2 \times 10^5$ K essentially eliminate the inconsistencies between evolution and pulsation theories.

A number of other studies demonstrate sensitivity to opacity. Several groups have considered the p-mode eigenfrequencies in the Sun (Christensen-Dalsgaard et al. 1985; Korzennik & Ulrich 1989; Cox, Guzik, & Kidman 1989; Cox, Guzick, & Raby 1990), and all concluded that increases in the LAO opacities of 10%–20% near the bottom of the convection zone brings models and observations into better agreement. Again, such an increase in opacity has been substantiated (Iglesias & Rogers 1991a). The lithium depletion problem in the Hyades cluster has been addressed by Swenson, Stringfellow, & Faulkner (1990) who showed that increasing the CT opacities by 37% near $T = 4 \times 10^6$ K reduces the computed lithium abundances to values consistent with observational constraints.

Finally, not all attempts to resolve the discrepancies between models and observations depend on opacity changes. For example, Carson & Stothers (1988) suggest a luminosity increase to bring into virtually perfect agreement pulsation models with observed ridgelike classical bump Cepheids. Nevertheless, the existing discrepancies are sensitive to the opacity, and they will be difficult to eliminate until uncertainties in opacity calculations are better understood and substantially reduced. As a result, at least two major independent efforts are underway to recompute opacity tables. One is the Opacity Project (Seaton 1987; Berrington et al. 1987). The other is our own, which we refer to as OPAL. There are two OPAL tables already available but these are somewhat specialized. The first is for the solar radiative interior (Iglesias & Rogers 1991a), and the second is for Cepheid variables (Iglesias & Rogers 1991b). Here, we offer more extensive results.

The present paper is organized as follows. In § 2 we briefly describe the OPAL code. This is followed by a description of the opacity tables in § 3 and estimates of the expected errors due to interpolation in § 4. The OPAL results are compared to previous work in § 5, and uncertainties in the large opacity enhancements near $\log T \approx 5.4$ are discussed in § 6. Final conclusions are offered in § 7. The opacity tables are collected in the Appendix. It is important to note that even though we emphasize the Anders-Grevesse (1989) metal composition, opacities for mixtures with different relative metal abundances can be made available.

2. THE OPAL CODE

The OPAL code removes several approximations in the equation of state and atomic data generation present in past calculations. Although there are equation of state issues which can affect the opacity, the most significant opacity enhancements reported here are due to improvements in the atomic physics.

2.1. *Equation of State*

The opacity calculations begin with the equation of state (EOS) to obtain occupation numbers. In the OPAL code we use the "physical picture" approach which starts from the grand canonical ensemble of a system of electrons and nuclei interacting through the Coulomb potential (Rogers 1981, 1991). Configurations corresponding to bound clusters of ions, atoms, and molecules are sampled in this ensemble. Any effects of the plasma environment on the internal states is obtained directly from the statistical mechanical analysis rather than by assertion as is the case in the so-called chemical picture (e.g., Hummer & Mihalas 1988; Mihalas, Dappen, & Hummer 1988). Our approach avoids the ad hoc cutoff procedures necessary in free energy minimization schemes. The method also provides a systematic procedure for including plasma effects in the photon absorption coefficients. For mixtures, we do not follow an ideal gas mixing procedure for combining the various photon absorption coefficients from the different elements (Huebner 1986). Instead, coupled equations for the full mixture are solved at each density and temperature point.

The approach in the present work is based on the fact that many particle correlations are highly classical; consequently, it is restricted to regions where the de Broglie wavelength is less than the plasma screening length. We have, however, developed methods for systematically introducing quantum mechanics into the many-particle correlations. The first step is to obtain the grand canonical partition function in terms of an activity expansion (Rogers & DeWitt 1973). Following standard methods used for molecular gases, the activity is eliminated in favor of the density to obtain a virial expansion. It is well known that Coulomb systems always display collective behavior and do not approach a binary collision limit as the density is decreased. Thus, methods which assume an ideal gas environment governed by the Saha equation are built on a weak foundation. As a consequence of the long-ranged Coulomb potential the virial coefficients are individually divergent. Nevertheless, the Coulomb virial series can be obtained through a regrouping of the most divergent terms. In this process the Coulomb potential in the virial coefficients is replaced by a short-ranged Debye-Ḧuckel–like potential, except that some low-order diagrams which were already accounted for in introducing the screening are no longer present. These screened virial coefficients are known as Abe nodal functions (Abe 1959). Although the Abe nodal functions involve the weak coupling Debye potential, the complete set recovers both the weak and the strong coupling limits of the free energy (Rogers 1981).

Astrophysical plasmas are, in general, only partially ionized and cannot easily be treated by expansions in the density. In the region of partial ionization activity expansions are much more amenable to analysis. Consequently, the next step in the development is to convert the density expansion into a plasma activity expansion. This could have been accomplished directly through a diagrammatic resummation of the initial activity series, but it proves to be much easier to follow the procedure just described; that is, to remove first the long-ranged Coulomb divergences in the density expansion. The corresponding cluster coefficients that arise in the plasma activity expansion are for a Debye-like potential where again some low-order diagrams are missing since they are included through the screened interaction. At this point the plasma activity expansion views the system in terms of electrons and nuclei and is not properly ordered for the partially ionized regions of interest.

To overcome this shortcoming, the final step in the EOS theory is to define activities for composite particles (Rogers 1974) which are built up from products of electron and nucleus quantities. A renormalization of the electron-nucleus activity expansion leads to a new series in terms of an augmented set of activities. It is important to note that the composite particle activities actually employed in calculating the EOS are effective activities, since the Boltzmann factors are split into bound and continuous parts according the Planck-Larkin prescription (Pisano & McKellar 1989; Bolle 1987, 1989; Rogers 1977, 1979). This takes advantage of analytic properties of the trace for n-body configurations having bound states. For example, the bound state contribution to the two-body trace is

$$\mathbf{b}_{2,\text{bound}} = \sum_{j(\text{bound})} g_j[\exp(-E_j/kT) - 1 + E_j/kT] , \qquad (1)$$

with g_j the level degeneracy, E_j the level energy, and kT the temperature in energy units. The right hand side of equation (1) is the so-called Planck-Larkin partition function (PLPF). The fact that the PLPF is not a true partition function, but instead represents the two-body bound state contribution to the pressure, has led to some confusion. Note that the leading two terms in an expansion of the exponential in equation (1) are subtracted and the sum is convergent. This is due to the fact that the sum over scattering states analytically compensates for the divergent terms in the bound state sum (Rogers 1977). In other words, the divergence of the internal partition function is fictitious and is caused by an incomplete trace over bound states only. It is not present in the complete trace which also includes scattering states (for an exposition see Ebeling, Kraeft, & Kremp 1976). An important result of this final step is that the bound state energies are unaffected by the plasma except near the lowered continuum.

As a result of equation (1), the occupation numbers that arise in the EOS calculations are effective occupation numbers. However, the opacity calculations, which are the main interest in the present work, require the total state occupation numbers. The latter are obtained from a supplementary procedure subsequent to the EOS calculation (Rogers 1986, and references therein).

The EOS approach used in our work is quite distinct from the free energy minimization procedure of the Opacity Project. Their "chemical picture" is based on an occupation probability formalism which assumes that the bound state occupation can be separated into a part w_{ik}, the fraction of all particles of species k that can exist in state i with an electron bound to the atom or ion, and a part $(1 - w_{ik})$, the fraction of those states that are so perturbed by neighbors that the state is destroyed. Their cutoff procedure, based on Stark field ionization and finite size arguments, prevents the divergence of the internal partition function (Dappen, Anderson, & Mihalas 1987; Hummer & Mihalas 1988). The work is commonly referred to as the MHD equation of state. Even through the two EOS approaches are very different, the results for thermodynamic quantities in low-density astrophysical plasmas are nearly identical (Dappen, Lebreton, & Rogers 1990). A comparison of these two approaches to the EOS work by Eggleton, Faulkner, & Flannery (1973) produces small differences which lead to considerably better agreement between observed and predicted solar p-mode oscillation frequencies (Christensen-Dalsgaard, Dappen, & Lebreton 1988).

2.2. *Absorption Processes*

The OPAL code uses the method of detailed configuration accounting; that is, it considers ion stages and the electron configurations (including term structure) explicitly from the start. Such a treatment requires detailed atomic data which is computed using parametric potentials (Rogers 1981; Rogers et al. 1988). Briefly, the parametric potentials depend on the nuclear charge and the electron configuration. In order to incorporate the shell structure, a potential with one Yukawa term for each occupied shell was proposed,

$$V = -\frac{2}{r}\left[(Q + 1) + \sum_n N_n e^{-\alpha_n r}\right] \qquad (2)$$

(in rydbergs), where N_n is the number of electrons in a shell with principal quantum number n, and Q is the net ion charge. The screening parameters, α_n, for shell n were determined by iteratively solving a spin-averaged Dirac equation and matching the eigenvalues to the experimentally observed one-electron ionization energies. For isolated atoms and ions, the parametric potential approach produces energy levels, oscillator strengths, and photoionization cross sections comparable in accuracy to single-configuration, self-consistent field calculations with relativistic corrections (Rogers et al. 1988).

It is important to note that our atomic calculations have a reasonable degree of accuracy not only for valence electrons but also for photon absorptions involving inner core electrons as well as multiply excited ions. Both of these processes are necessary in determining the Rosseland mean opacity. For example, photon absorption by the inner shell electrons is important in stellar interiors (Iglesias & Rogers 1991a). It follows that OPAL does include autoionizing lines, but treats them simply as ordinary lines. That is, it ignores the possible interference effects between the final bound state and the continuum which requires configuration interaction calculations (e.g., Seaton 1987).

Photoionization processes are considered individually for every subshell in every electron configuration of the various ion stages. The calculation is done in the central field approxi-

mation for electrons with n greater than 4. For n less than 5, we include the configuration term splitting in the LS angular momentum coupling scheme. We also include the bound-free absorption from H^- (Wishart 1979), since it can dominate the absorption at low temperatures.

The bound-bound transitions are calculated for every subshell in each configuration of the various ion stages explicitly. The absorption-line energies and oscillator strengths are computed in the LS coupling scheme for transition electrons with both initial and final n less than 5. For jumping electrons with initial n greater than 4, configuration term splitting is neglected, and transitions are computed for the nl-subshell only. For electrons with initial n less than 5 but final n greater than 4, the lower configuration term splitting is included in the LS coupling scheme. Transitions to states with $n > 10$ are not explicitly included, but instead are approximately treated by extending the photoionization cross sections to lower photon energies.

Three additional approximations are made with regard to the angular momentum coupling. Due to memory and computer time constraints the number of lines in a single configuration-to-configuration transition array is restricted to 10,000. At present, if the actual number of lines is greater, the term splitting is ignored, and only a single, average line is considered. For similar reasons the term splitting is neglected for spectral lines with energies greater than $13.5\,kT$ (kT = temperature in energy units). At these higher photon energies the Rosseland mean weighting function is less than 1% of the peak value, and the details of the bound-bound transitions should not affect the Rosseland mean opacities. Finally, excited spectator electrons with n greater than 5 are included in the calculation of the configuration-averaged energies and wavefunctions, but are not included in the angular momentum coupling. This approximation reduces, in principle, the number of spectral lines in the calculation. However, these electrons reside in large orbits which do not couple strongly to the actual jumping electron. Furthermore, they usually belong to configurations of low abundance. Interestingly, due to the size constraint above, this last approximation can actually increase the total number of lines considered in the calculation for ions with partially filled M-shell configurations.

Except for some special cases, line shapes are assumed to be Voigts with Doppler broadening and the Lorentz width given by electron impact formulas from Dimitrijevic & Konjevic (1980, 1986, 1987). Their electron impact formulas require radial dipole integrals which are evaluated using the wavefunctions obtained from our parametric potentials. The exceptions are for the Lyman and Balmer series of hydrogenic systems for which we include fine structure and linear Stark effects due to ion electric microfields using subroutines generously provided by Lee (1988). Similar subroutines are used for the Lyman series of helium-like ions and transitions out of the $n = 2$ level in lithium-like ions. For one-electron systems we have modified the method by Griem (1960) in order to treat transitions from levels with n greater than 2. The modifications involve improved ion microfield distributions (Iglesias et al. 1985) and electron impact widths (Lee 1988).

Inverse bremsstrahlung is computed using the parametric potentials including plasma screening effects. Whenever possible approximate methods are used to evaluate the free-free Gaunt factors. We use an elastic scattering approximation for small photon energies and the Born-Elwert approximation at large photon energies (Johnson 1967). Otherwise, the brute force calculation of the dipole matrix element is done. In all cases the required thermal averages are done with the Dirac-Fermi distribution for the electrons, including the Pauli exclusion principle for final states (Huebner 1986). We do not consider inverse bremsstrahlung for neutral atoms except for H (Stilley & Callaway 1970) and He (Sommerville 1967). These calculations for the neutrals do not include plasma effects. However, if the absorption is dominated by the neutrals, then the charged particle density is relatively low, minimizing any screening effects.

The photon scattering from electrons is treated by a method described by Boercker (1987) modified to include relativistic corrections (Sampson 1959; Huebner 1986). In his approach,

TABLE 1

FRACTIONAL ABUNDANCES OF METALS NORMALIZED TO 1

			ANDERS-GREVESSE 1989[a]	
ELEMENT	COX-TABOR 1976	ROSS-ALLER 1976	14 Elements	16 Elements
C	0.19425	0.30279	0.22690	0.22690
N	0.05475	0.06326	0.07012	0.07012
O	0.43487	0.50249	0.53192	0.53192
NE	0.24503	0.02699	0.07688	0.07688
Na	0.00097	0.00138	0.00134	0.00134
Mg	0.01225	0.02892	0.02376	0.02376
Al	0.00081	0.00241	0.00184	0.00184
Si	0.01555	0.03250	0.02222	0.02222
S	0.0	0.01181	0.01038	0.01038
Ar	0.01628	0.00083	0.00236	0.00236
Ca	0.0	0.00177	0.00154	0.00143
Cr	0.0	0.0	0.0	0.00050
Fe	0.02522	0.02347	0.03073	0.02923
Ni	0.0	0.0	0.0	0.00111

[a] Abundances in solar photosphere.

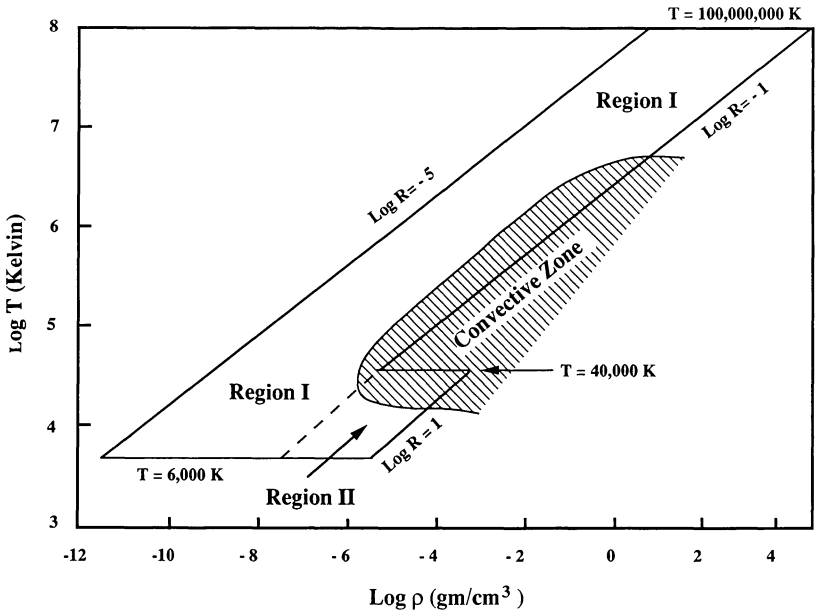

FIG. 1.—Schematic drawing showing the region in $\rho - T$ space covered by the opacity tables

Boercker treats electron correlations through the ring approximation plus first-order exchange terms. We also include Rayleigh scattering from neutral hydrogen and helium using the fits in Kurucz (1970):

$$\sigma^{\mathrm{Ray}}(\mathrm{H}) = 5.799 \times 10^{-13}\lambda^{-4} + 1.422 \times 10^{-6}\lambda^{-6} + 2.794\lambda^{-8}(\mathrm{cm}^2)\,, \quad (3)$$

$$\sigma^{\mathrm{Ray}}(\mathrm{He}) = 5.484 \times 10^{-14}\lambda^{-4}[1 + 2.44 \times 10^{-5}\lambda^{-2}](\mathrm{cm}^2)\,,$$

where λ is the wavelength in angstroms. These formulas are used for all λ, but the value of σ^{Ray} is never allowed to be greater than the Thomson scattering result.

The reader is reminded that only atomic photoabsorption processes are considered. Although H_2 and H_2^+ are included the EOS calculations (necessary for determining the H^- abundance), photoabsorption from molecules is neglected. In addition, the electron conduction opacity must be added to the radiative Rosseland mean values offered in the tables.

3. DESCRIPTION OF OPACITY TABLES

In constructing opacity tables several issues must be considered: (1) choice of metal abundances; (2) range of hydrogen mass fraction, X; (3) range of metal mass fraction, Z; (4) range of temperature and density; and (5) interpolation accuracy desired. Of course, a satisfactory answer to these issues depends on the intended use of the opacity tables. Our decisions on these points are based on previous tables and consultations with a number of users in the astrophysical community (see acknowledgements). Below we describe the choices for points (1)–(4) above, deferring the question of interpolation to the next section.

TABLE 2

COMPOSITION OF THE OPACITY TABLES GIVEN IN THE APPENDIX

Table Number	Metal Composition	X	Z
10	Anders-Grevesse	0.70	0.000
11	Anders-Grevesse	0.35	0.000
12	Anders-Grevesse	0.00	0.000
13	Anders-Grevesse	0.70	0.0001
14	Anders-Grevesse	0.35	0.0001
15	Anders-Grevesse	0.00	0.0001
16	Anders-Grevesse	0.70	0.0003
17	Anders-Grevesse	0.35	0.0003
18	Anders-Grevesse	0.00	0.0003
19	Anders-Grevesse	0.70	0.001
20	Anders-Grevesse	0.35	0.001
21	Anders-Grevesse	0.00	0.001
22	Anders-Grevesse	0.70	0.002
23	Anders-Grevesse	0.35	0.002
24	Anders-Grevesse	0.00	0.002
25	Anders-Grevesse	0.70	0.004
26	Anders-Grevesse	0.35	0.004
27	Anders-Grevesse	0.00	0.004
28	Anders-Grevesse	0.70	0.01
29	Anders-Grevesse	0.35	0.01
30	Anders-Grevesse	0.00	0.01
31	Anders-Grevesse	0.70	0.02
32	Anders-Grevesse	0.35	0.02
33	Anders-Grevesse	0.00	0.02
34	Anders-Grevesse	0.70	0.03
35	Anders-Grevesse	0.35	0.03
36	Anders-Grevesse	0.00	0.03
37	Cox-Tabor	0.70	0.001
38	Cox-Tabor	0.35	0.001
39	Cox-Tabor	0.00	0.001
40	Cox-Tabor	0.70	0.02
41	Cox-Tabor	0.35	0.02
42	Cox-Tabor	0.00	0.02
43	Ross-Aller	0.70	0.02
44	Ross-Aller	0.35	0.02
45	Ross-Aller	0.00	0.02

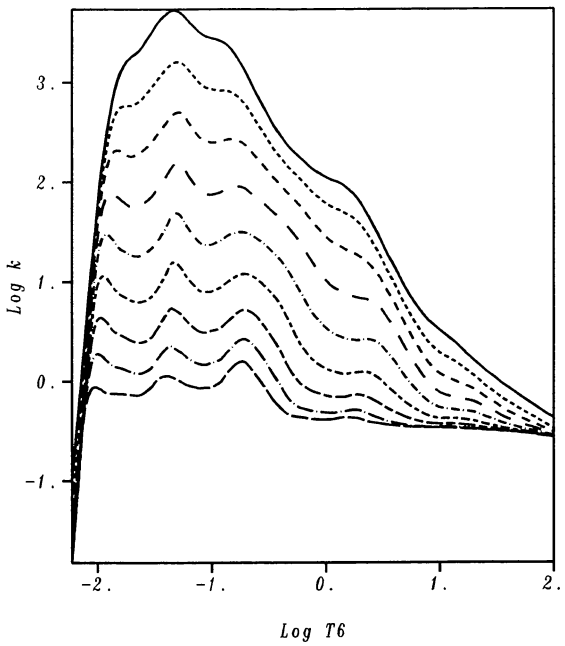

FIG. 2a

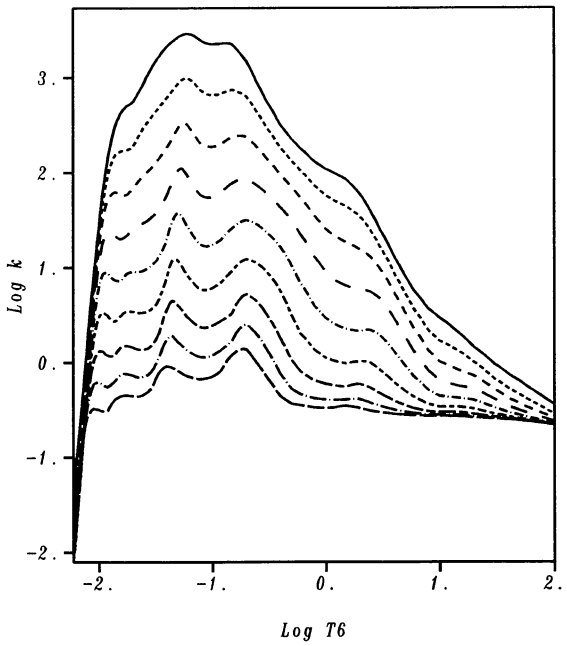

FIG. 2b

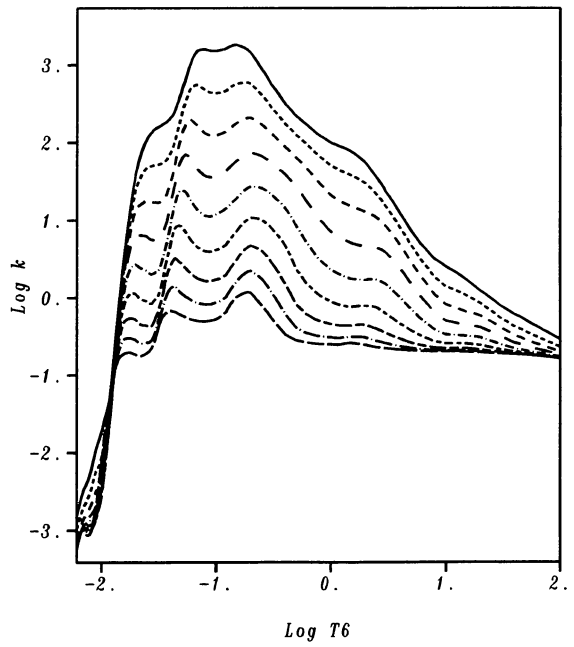

FIG. 2c

FIG. 2.—Rosseland mean opacity ($cm^2\ g^{-1}$) vs. temperature in Region I at constant R for the Anders-Grevesse composition and $Z = 0.02$: (*a*) $X = 0.7$, (*b*) $X = 0.35$, and (*c*) $X = 0$ with (*top to bottom*) log $R = -1, -1.5, -2, -2.5, -3, -3.5, -4, -4.5$, and -5.

We concluded that a single metal composition is sufficient for most purposes, and at present the Anders-Grevesse (1989) mixture seems an optimal choice. However, in order to estimate the opacity sensitivity to the metal abundances as well as to compare to previous work, we have included opacity results for the CT and Ross & Aller (1976) mixtures. The fractional metal abundances are given in Table 1, and since the total number of metals considered is limited to 12, elements of low relative abundances have been combined with their neighbors as described in Iglesias & Rogers (1991a). For the hydrogen mass fraction the range $0 < X < 0.8$ is sufficient for most purposes so that opacity results for $X = 0$, 0.35, and 0.7 each with nine values of metallicity covering the region from $Z = 0$ to 0.03 are tabulated.

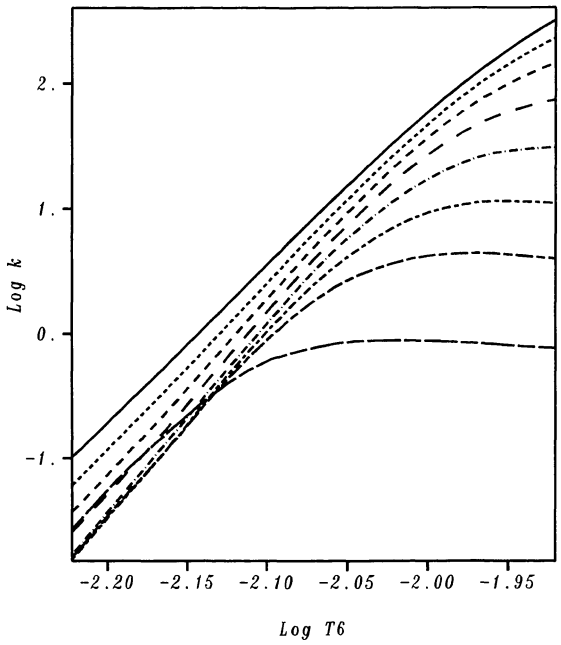

FIG. 3*a*

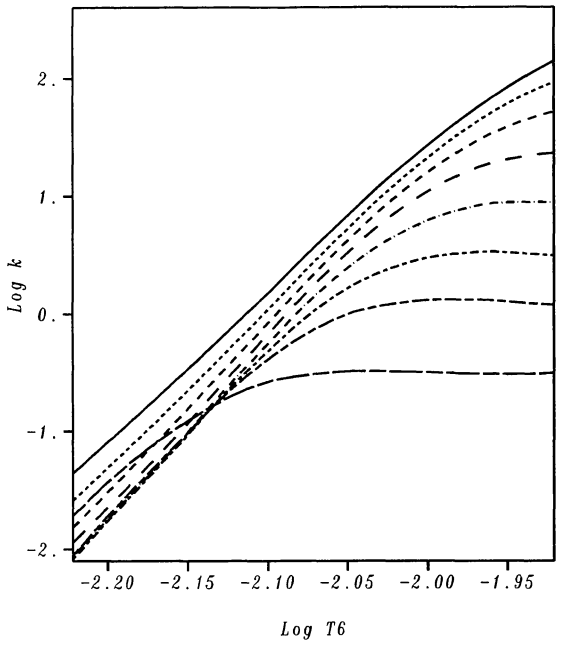

FIG. 3*b*

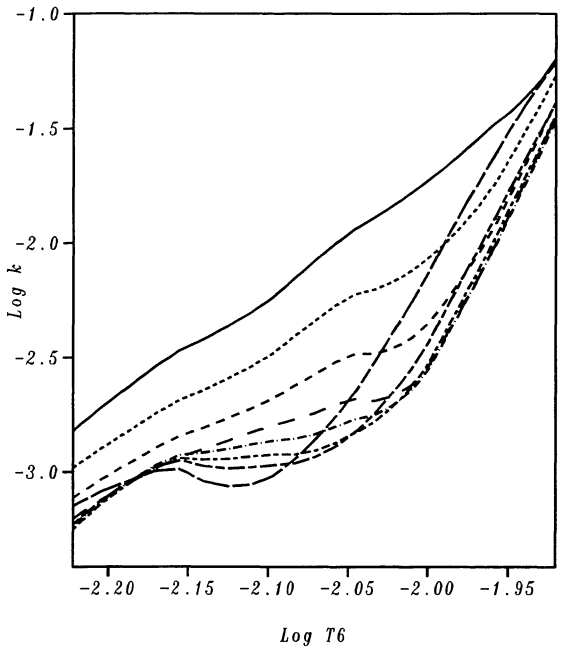

FIG. 3*c*

FIG. 3.—Same as Fig. 2 with an expanded temperature axis but excluding log $R = -4.5$.

The assumption of hydrostatic equilibrium is sufficient to establish that the density-temperature relation in the interior of stars approximately obeys $\rho \sim T^3$. Consequently, using a rectangular grid in $\rho - T$ space is not an efficient way to present opacity calculations. Instead, we follow Bahcall & Ulrich (1988) and provide opacity tables in $R - T_6$ space. Here, $R = \rho/T_6^3$ (cm^3 g^{-1}) with ρ the density in g cm^{-3} and T_6 the temperature in units of 10^6 K. The units in the definition of R and T_6 are such to make them dimensionless quantities. Previous researchers have also found advantages in using R and T as interpolation variables (Hejlesen 1980).

Figure 1 displays the region in $\rho - T$ space covered by our tables. For convenience in discussing the results we have conceptually separated the tables into two sections labeled Region I and Region II. Region I is bounded by lines of constant log $R = -5$ and log $R = -1$ including temperatures of up to

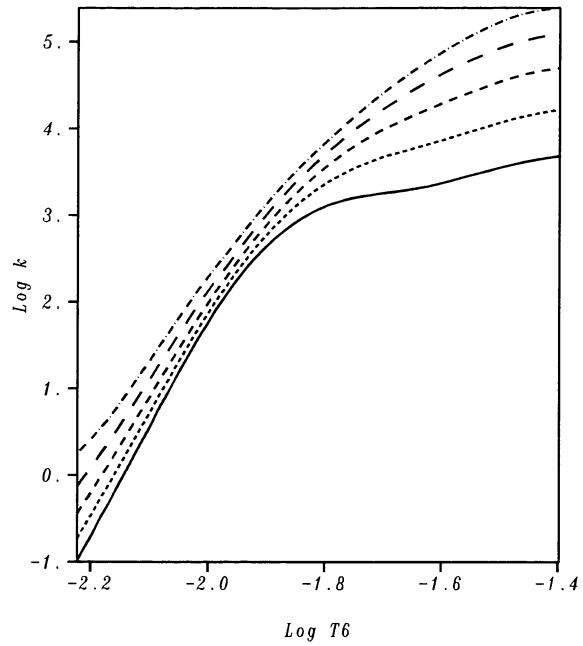

FIG. 4a

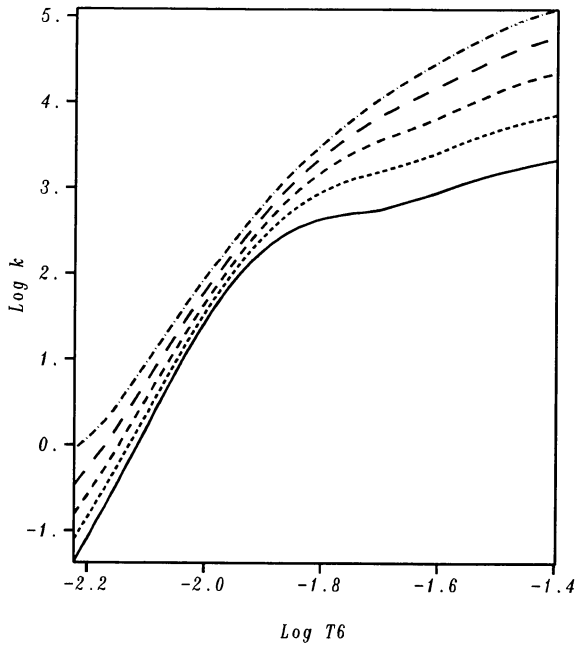

FIG. 4b

FIG. 4.—Rosseland mean opacity ($cm^2\ g^{-1}$) vs. temperature in Region II at constant R: (*a*) $X = 0.7$, and (*b*) $X = 0.35$ (*top to bottom*) $\log R = +1, +0.5, 0, -0.5$, and -1.

10^8 K. Region II is a high-density extension to $\log R = +1$, but with a much lower high-temperature cutoff of $T = 4 \times 10^4$ K. This extension is necessary because the $\rho \sim T^3$ relation behavior fails in the cooler regions of a star and the $\rho - T$ tracks tend toward relatively higher densities. Both Region I and II have a lower temperature limit of 6×10^3 K which is dictated by the omission of molecular opacity sources which are negligible at $T = 6 \times 10^3$ K but increase in importance for lower temperatures (Alexander, Johnson, & Rypma 1983). The transport of energy by radiation is not significant in the convective zone which is schematically shown in Figure 1. For this reason we have limited the calculations in Region II to lower temperatures.

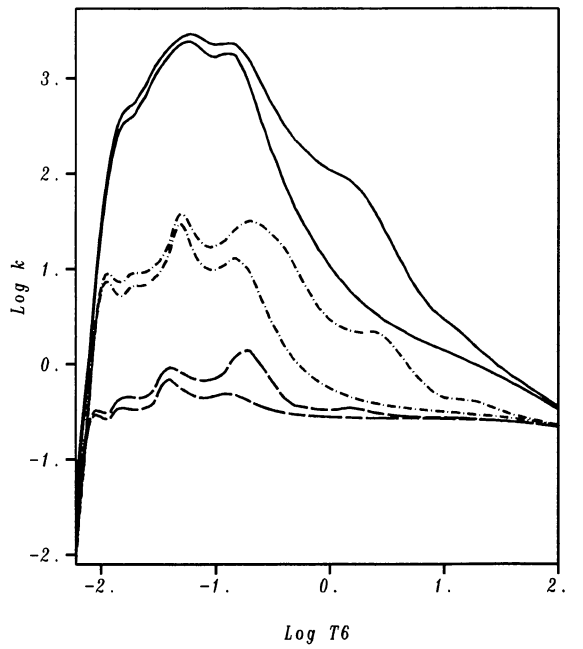

FIG. 5.—Effects of metallicity on opacity for the Anders-Grevesse composition and $X = 0.35$. Tracks of constant R: (*top to bottom*) $\log R = -1, -3$, and -5, where for a given pair of curves the lower is for $Z = 0$ and the higher for $Z = 0.02$.

The opacity tables have been collected in the Appendix, but in Table 2 we summarize their contents. Figures 2–18 provide a pictorial representation of the opacity tables in the Appendix. Figure 2 shows the Rosseland mean opacity, $\kappa(cm^2\ g^{-1})$, as a function of temperature at constant R for $Z = 0.02$. Panels (*a*), (*b*) and (*c*) of the figure show results for $X = 0.7$, 0.35, and 0, respectively; a pattern that is followed in latter figures. The plots are characterized by several bumps in κ and a sharp fall-off at low temperature. The fall-off is due to a decrease in absorption as the system becomes more neutral. The first few bumps in κ are due to H and He. The one near $T_6 \approx 0.01$ comes from H and is, of course, completely absent in Figure 2*c* with $X = 0$. Helium contributes to the bumps for $0.01 < T_6 < 0.1$. The strongest of these is near $\log T_6 = -1.3$ due to H, He, and He^+. The He^+ also produces a κ-bump at $\log T_6 \approx -0.8$ (see Fig. 5), but in Figure 2 it is masked due to photon absorption by the M-shell of Fe. The last κ-bump at $\log T_6 \approx 0.3$ is caused in part by photon absorption by the L-shell of Fe as well as photoionization from the K-shell of C, O, and Ne.

Figure 3 provides an expanded view of κ versus T_6 in Region I at low temperatures. Similar plots are provided in Figure 4 for Region II. Note that no results have been provided in the tables for $X = 0$ in Region II. The crossing of the constant R plots in Figure 3 is due to increased abundance of H^- (the dominant source of absorption) caused by higher ionization of the metals

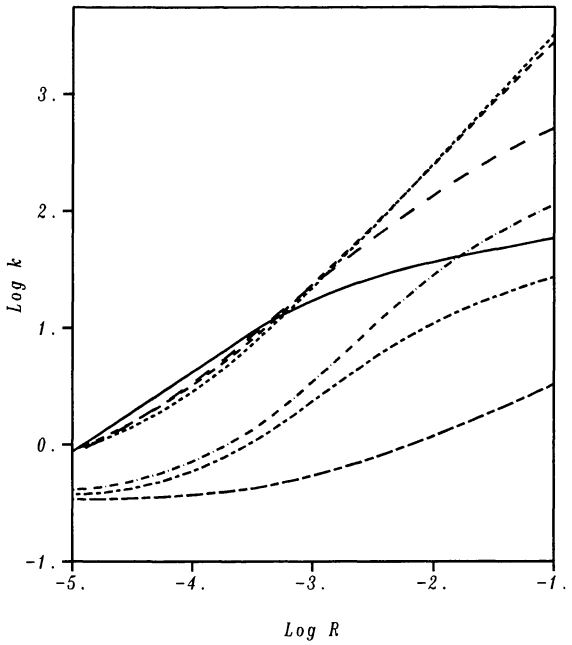

FIG. 6a

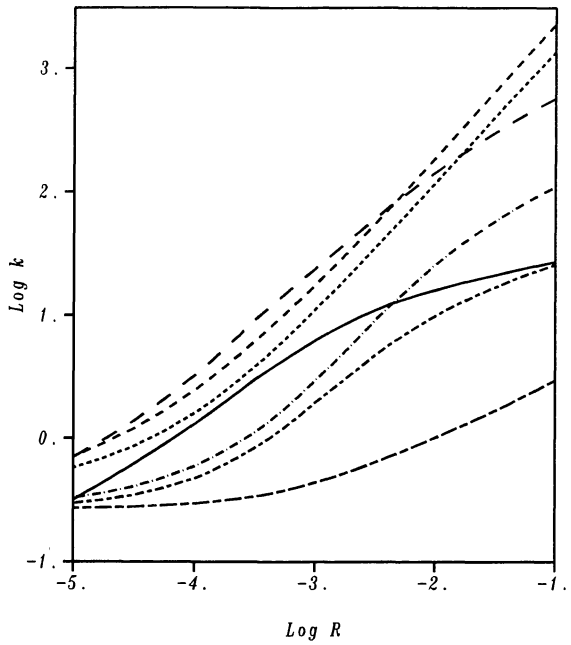

FIG. 6b

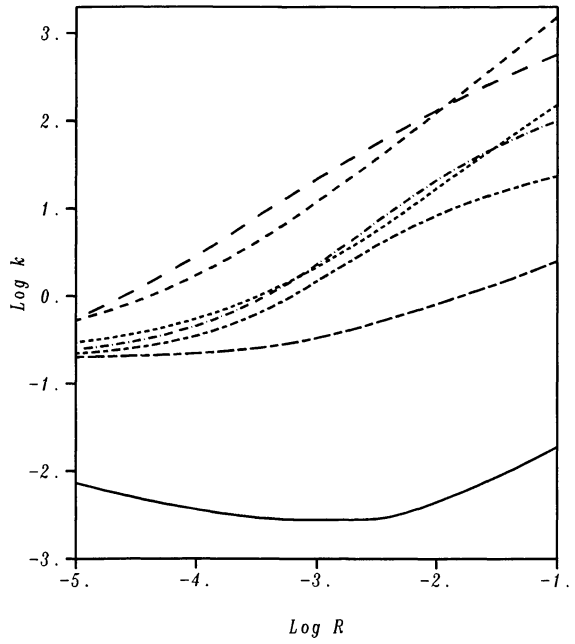

FIG. 6c

FIG. 6.—Rosseland mean opacity ($cm^2\ g^{-1}$) vs. R at constant temperature for Anders-Grevesse composition and $Z = 0.02$ (*a*) $X = 0.7$, (*b*) $X = 0.35$, and (*c*) $X = 0$ with (*solid line*) $T_6 = 0.01$; (*short-dash line*) $T_6 = 0.03$; (*medium-dash line*) $T_6 = 0.1$; (*long-dash line*) $T_6 = 0.3$; (*short-dash-dot line*) $T_6 = 1.0$; (*medium-dash-dot line*) $T_6 = 3.0$; and (*long-dash-dot line*) $T_6 = 10$.

at lower densities. To assess the overall importance of the metals, Figure 5 compares κ versus T_6 plots for $Z = 0$ and 0.02 at three values of R. Clearly, there are regions where the metals dominate the opacity. Even at low temperatures where the H and He bumps occur, the metals are not negligible. Only at the highest temperatures where the plasma is almost fully ionized and the opacity is mostly due to electron scattering do the effects of the metals on κ diminish.

Opacity isotherms (κ as a function of R at constant T) for Region I are shown in Figure 6. The behavior of each isotherm is monotonic except at very low temperature and $X = 0$. The isotherms cross at intermediate values of temperature and is a

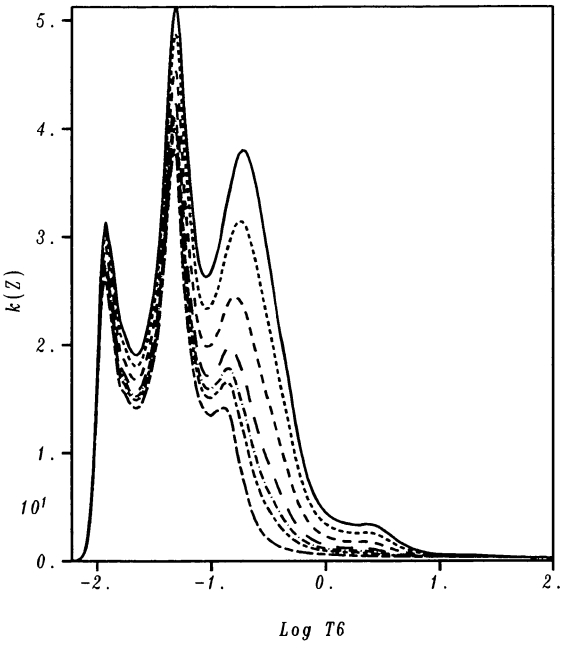

FIG. 7a

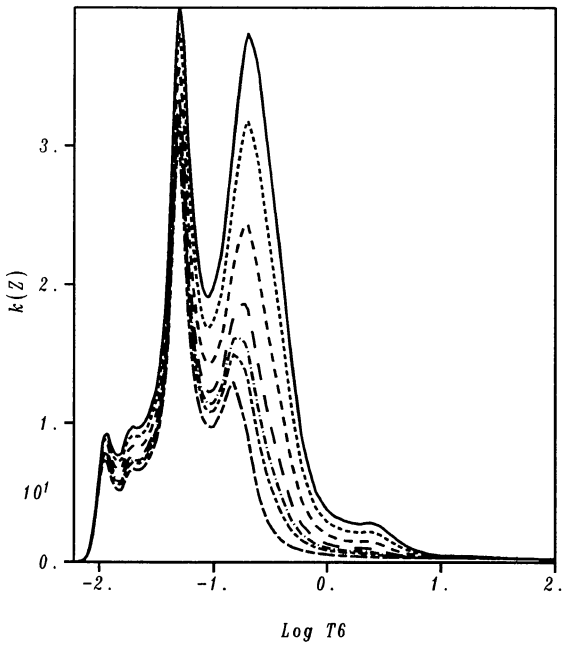

FIG. 7b

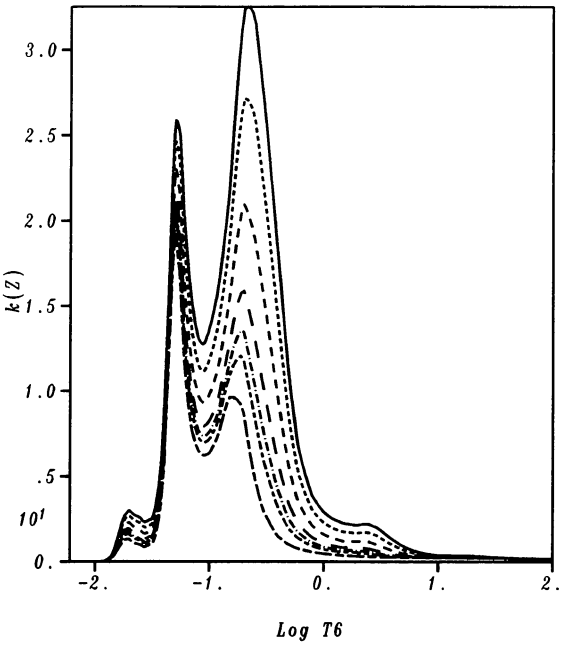

FIG. 7c

FIG. 7.—Rosseland mean opacity ($cm^2\ g^{-1}$) vs. temperature in Region I at log $R = -3$ for the Anders-Grevesse composition: (*a*) $X = 0.7$, (*b*) $X = 0.35$, and (*c*) $X = 0$ with (*top to bottom*) $Z = 0.03$, 0.02, 0.01, 0.004, 0.002, 0.001, and 0.

result of the opacity structure in Figure 2. Although the isotherms display somewhat different behavior with varying X and T_6, they are smooth functions of log R allowing for simple interpolation schemes.

The Z-dependence is presented in Figure 7 for log $R = -3$. The $Z = 0.02$ curve can be compared to the logarithmic plot of the same results in Figure 2. For clarity the $Z = 10^{-4}$ and 3×10^{-4} results are omitted. As expected, the regions near the H and He opacity bumps are weakly dependent on the metallicity while the M-shell Fe opacity bump (log $T_6 \approx -0.8$) grows dramatically with increasing Z. Figure 7 may be misleading in terms of the relative importance of the metals. In Figure 8 we present the same data, but now we plot log $[\kappa(Z)/\kappa(Z = 0)]$ versus log T_6. The dramatic increase in this quantity for $X = 0$

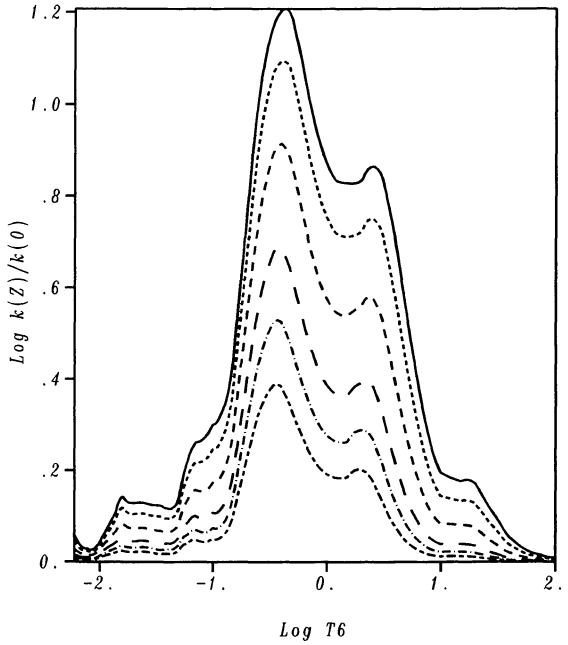

FIG. 8*a*

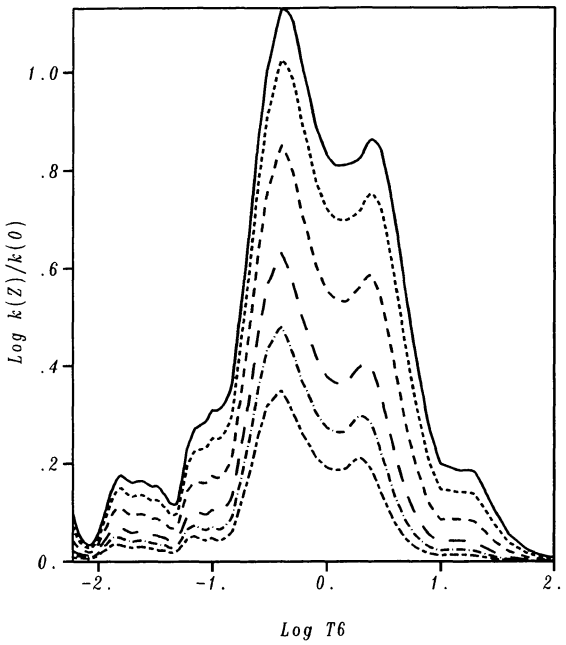

FIG. 8*b*

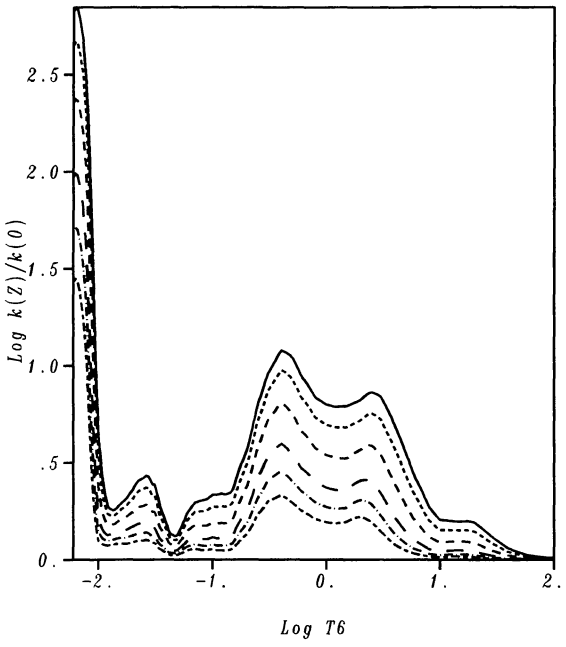

FIG. 8*c*

FIG. 8.—Log [$\kappa(Z)/\kappa(Z = 0)$] vs. log T_6: (*a*) $X = 0.7$, (*b*) $X = 0.35$, and (*c*) $X = 0$ with (*top to bottom*) $Z = 0.03$, 0.02, 0.01, 0.004, 0.002, and 0.001.

and low temperature in Figure 8*c* is due to the fact that neutral He makes a small contribution to the opacity (its bound-bound and bound-free transitions lie well beyond the peak of the Rosseland mean weighting functions), and the increased metallicity provides free electrons which can participate in inverse bremsstrahlung and Thomson scattering. The sensitivity to density is suggested in Figures 9 and 10 where plots similar to Figure 7 are shown for $X = 0.35$ at log $R = -5$ and -1, respectively.

The Z-dependence at fixed R and T is of interest. Figure 11 presents the plots of κ versus Z for log $R = -3$ and several temperatures. The curves are nearly linear for the large Z-values, but at temperatures near the M-shell Fe opacity bump the Z-dependence is strong. Figures 12 and 13 display

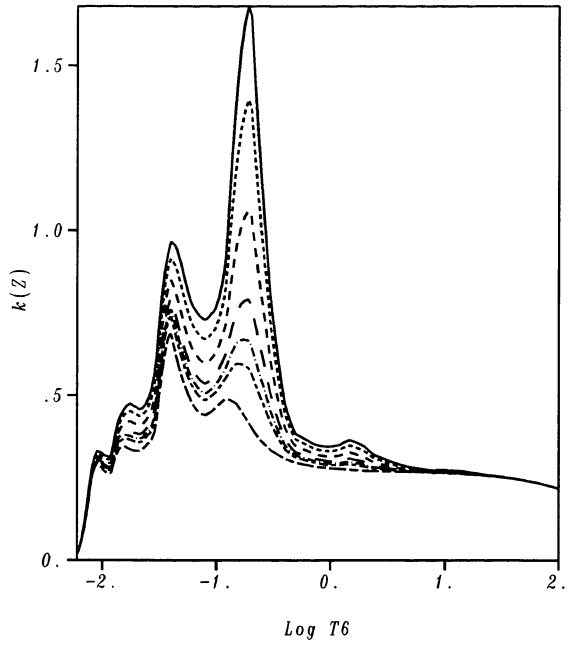

FIG. 9.—Same as Fig. 7*b* for log $R = -5$

the corresponding data for $X = 0.35$ at log $R = -5$ and log $R = -1$, respectively.

The opacity sensitivity to metal content in Region II is shown in Figure 14 for log $R = +1$. The dominant feature here is the strong dependence at low temperature. This is due to the enhanced H^- abundance as a result of electrons being donated by the metals. Similar results are plotted for $X = 0.35$ and log $R = 0$ in Figure 15 where due to the lower density leading to higher ionization of H, the relative enhancement of the H^- abundance is reduced with increasing metallicity.

Isotherms for Region II are plotted for representative values of temperatures in Figure 16. The Z-dependence for $X = 0.35$ at log $R = 0$ and log $R = +1$ for the same temperatures are given in Figures 17 and 18. Notice that the opacity dependence on Z is much weaker in Region II (compare to Fig. 11).

4. INTERPOLATION

The density of points for the temperature, R, and hydrogen mass fraction in the tables have been chosen so that simple interpolation schemes will yield small errors. In addition, we have included tables with nine values of metal mass fraction for the Anders-Grevesse composition ranging from $Z = 0$ to 0.03 in order to allow accurate interpolation in Z. In this section we illustrate the accuracy of the interpolations in these variables.

4.1. *Interpolation in T_6 and R*

One advantage in the present format for the tables is that the Rosseland mean opacity is less sensitive to changes in temperature at constant R than at constant density. This is because at constant R changes in ionization due to a temperature increase (decrease) are compensated by the corresponding increase (decrease) in density. Consequently, we expect that interpolation in temperature will be easier at constant R.

To test the interpolation in temperature, we recomputed existing points in the tables assuming the following form for the Rosseland mean opacity,

$$\log \kappa = \alpha + \beta \log(T_6) + \gamma[\log(T_6)]^2 . \quad (4)$$

Three neighboring opacity results at the same R-value were used in conjunction with equation (4) and, of course, no information about the point in question except the temperature. The interpolated opacities are compared to the actual value entered in the table, and the percent errors are presented in Table 3 for a representative sample. The errors in Table 3 are mostly a few percent or less. Furthermore, these errors should be an overestimate of the actual ones experienced in practice since in the exercise above an existing value in the table has been removed; in effect simulating a thinner temperature grid than is available. Nevertheless, further checks have been made in Table 3 in regions where there are large errors (labeled **A, B, C,** etc.). For these special cases intermediate temperature values not in the opacity tables were computed using equation (4). The interpolated results have been compared to calculations from the opacity code and the percent errors given in Table 4. Clearly, using the actual temperature grid in the opacity tables considerably reduces the simulated errors in interpolation given in Table 3. Consequently, we expect better than 2% errors using equation (4) with some infrequent excursions of as much as 5%.

A similar procedure was followed for interpolating in R (or density) at constant temperature assuming

$$\log \kappa = \alpha + \beta \log(R) + \gamma[\log(R)]^2 . \quad (5)$$

In this case, the results corresponding to Table 3 are smaller by more than a factor of 2. Accordingly, we again expect better

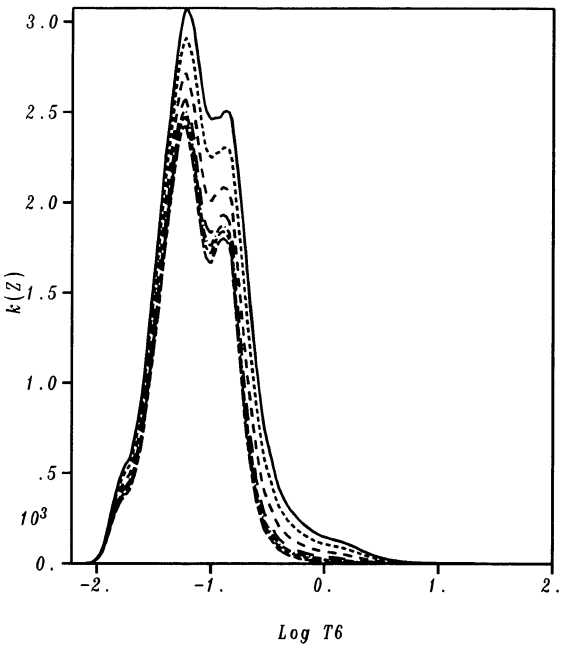

FIG. 10.—Same as Fig. 7*b* for log $R = -1$

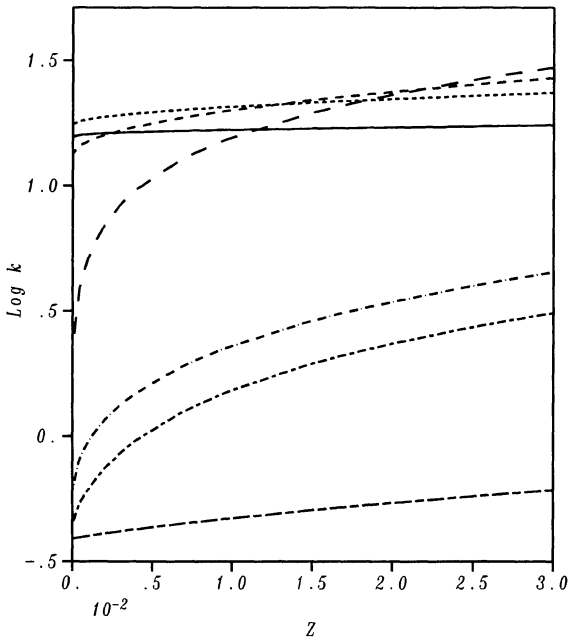

FIG. 11*a*

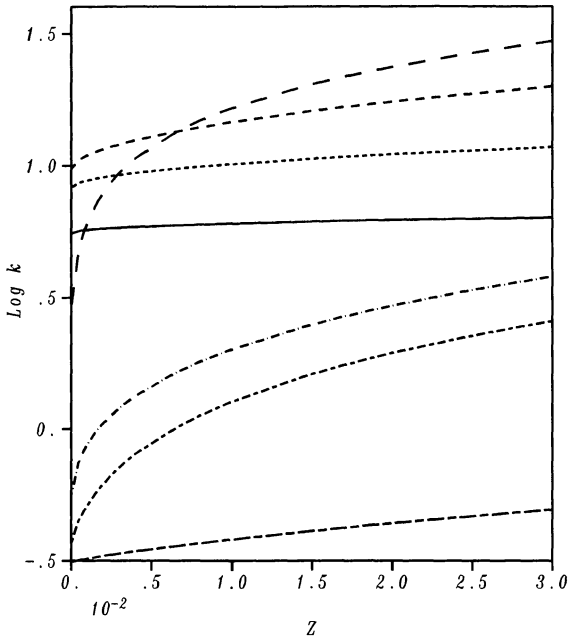

FIG. 11*b*

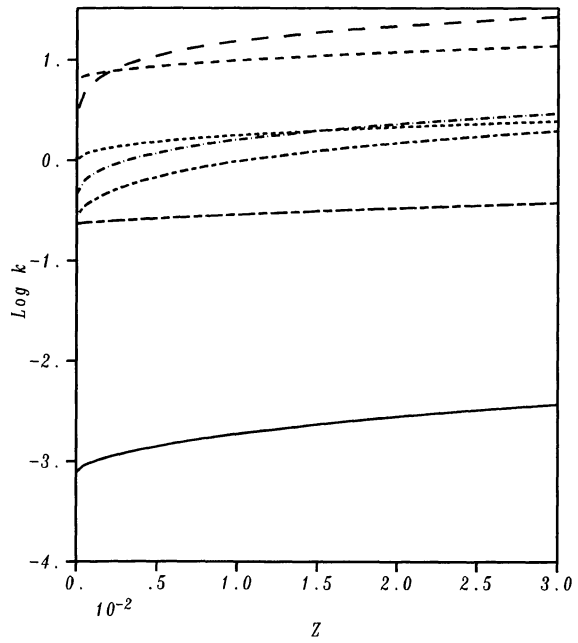

FIG. 11*c*

FIG. 11.—Rosseland mean opacity ($cm^2 g^{-1}$) vs. Z at constant log $R = -3$ for Anders-Grevesse composition: (*a*) $X = 0.7$, (*b*) $X = 0.35$, and (*c*) $X = 0$ with (*solid line*) $T_6 = 0.01$; (*short-dash line*) $T_6 = 0.03$; (*medium-dash line*) $T_6 = 0.1$; (*long-dash line*) $T_6 = 0.3$; (*short-dash-dot line*) $T_6 = 1.0$; (*medium-dash-dot line*) $T_6 = 3.0$; and (*long-dash-dot line*) $T_6 = 10$.

than 2% errors using equation (5) with perhaps some errors as large as 3%–4%.

4.2. *Interpolation in X*

Not surprisingly, the opacity tables are very much a linear function of X at high temperature. Somewhat less expectedly, the opacities are not far from linear in X everywhere except for the lowest temperatures and $X < 0.35$. In such cases, a quadratic dependence on X leads to a reasonable interpolation scheme.

In Tables 5 and 6 we compare the results of both linear and quadratic interpolation against the results from the opacity

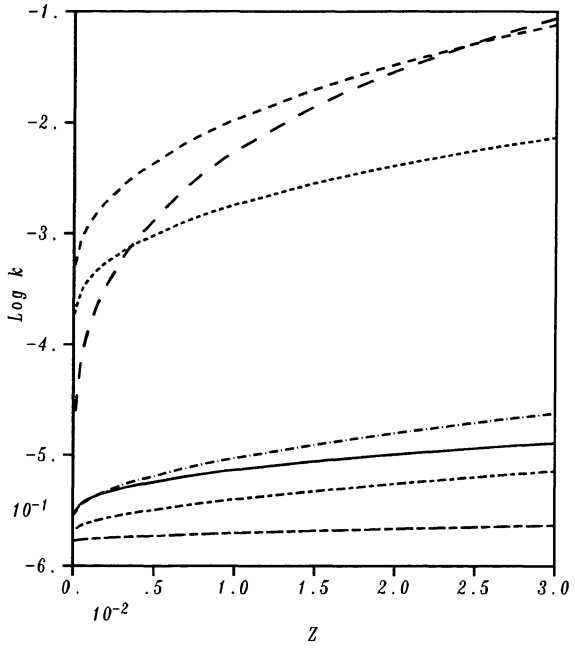

FIG. 12.—Same as Fig. 11*b* with log $R = -5$

code. These two tables show comparisons for two different values of R and Z. The values of R are representative of Regions I and II in the opacity tables. Note that there are no entries in the opacity tables for $X = 0$ in Region II (log $R > -1$); therefore, in doing the quadratic fit we have assumed that the $X = 0$ result is identically zero and only interpolate for $X > 0.35$. For the interpolation, this is a reasonable approximation since for $X > 0$ the dominant absorber is H^-; therefore, the value for $X = 0$ is much smaller than $X = 0.35$ and negligibly different from zero.

The tables clearly show that for $0.35 < X < 0.7$ the opacity is nearly linear in X for almost all temperatures. For $X < 0.35$, however, the situation is different, and now the quadratic fit does offer considerable improvement. It follows from these tables that the opacity for the lower Z mixtures are farther from the linear behavior in X than the higher metallicity ones. In particular, at the lowest temperature and high density even the quadratic fit fails for $Z = 0$.

In view of these results, using quadratic interpolation we can expect (except for the very lowest temperatures in Region II and small Z) better than a few percent error when interpolating for $X > 0.35$. For $X < 0.35$, the expected error is also few percent, but with excursions of about 10%–20% at very low temperatures.

4.3. *Interpolation in Z*

The opacity tables provide enough values of Z (for the Anders-Grevesse metal abundances) that quadratic interpolation provides reasonably accurate results. The testing procedure is identical to the one described above for the temperature and density interpolations. That is, a point on the table is removed, and the remainder of the table used to interpolate for the absent value. Assuming a quadratic fit

$$\kappa = \alpha + \beta Z + \gamma Z^2 , \qquad (6)$$

we check all entries in the Anders-Grevesse tables. Almost all the interpolated values (99% of all the test cases) had errors less than 5%, 92% had errors less than 2%, and none larger than 9% when compared to the entries in the tables. As in the case for the temperature and density, this procedure gives an overestimate of interpolation errors because it removes an existing entry in the tables. In practice, the larger errors should be reduced by better than a factor of 2 since then all the table entries would be used. Although the opacity is almost linear in the region $0.02 < Z < 0.03$, we caution against linear extrapolation for Z-values much larger than 0.03. We found that linear extrapolation to $Z = 0.04$ leads to modest errors of 7% or less, but the errors increase quickly for larger Z. For example, linear extrapolation to $Z = 0.05$ can lead to errors of as much as 15%.

The interpolation formulas used in this section do not necessarily represent an optimum choice. Rather, they are intended to illustrate the potential errors due to interpolation in several variables.

5. DISCUSSION

It is helpful to compare the new OPAL results with previous calculations since it allows the stellar modelers an opportunity to see if any significant differences occur which can affect their particular problem of interest. We begin our comparisons with the fits by Stellingwerf (1974, 1975) to the CT opacity calculations. These fits were developed for temperatures and densities which appear in typical Cepheid and RR Lyrae envelopes for mixtures with the CT metal abundances. In Figures 19 and 20 we plot OPAL results for the King I*a* ($X = 0.7$, $Z = 0.001$) and King IV *a* ($X = 0.7$, $Z = 0.02$) compositions for $R = 10^{-3}$ and $R = 10^{-4}$ along with the corresponding Stellingwerf fits. In Figure 21 we plot the ratio of OPAL opacities to the Stellingwerf fits. The most obvious feature is the opacity enhancement near log $T \approx 5.5$ which has been discussed previously (Iglesias et al. 1987, 1990; Iglesias & Rogers 1991b). This opacity en-

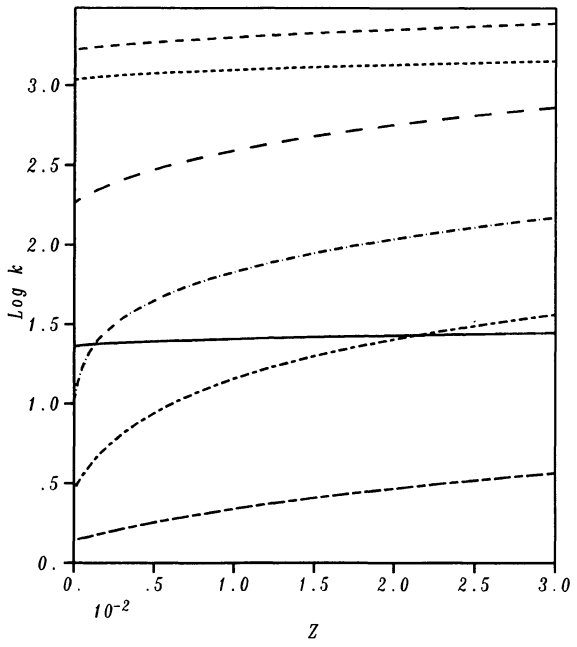

FIG. 13.—Same as Fig. 11*b* with log $R = -1$

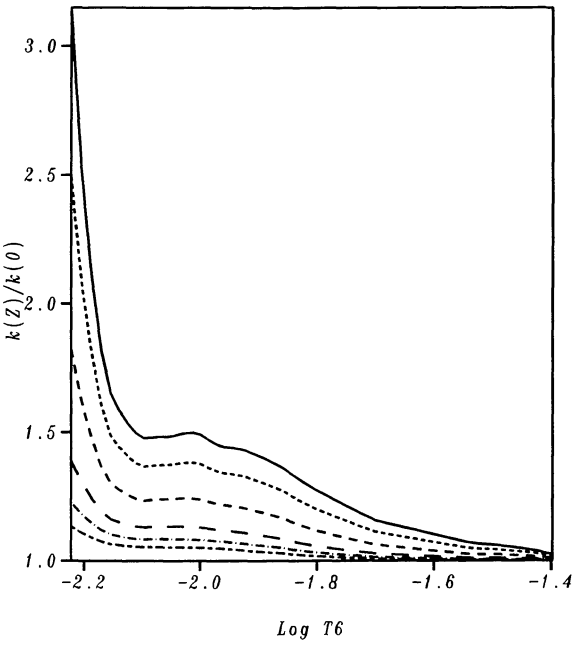

FIG. 14*a*

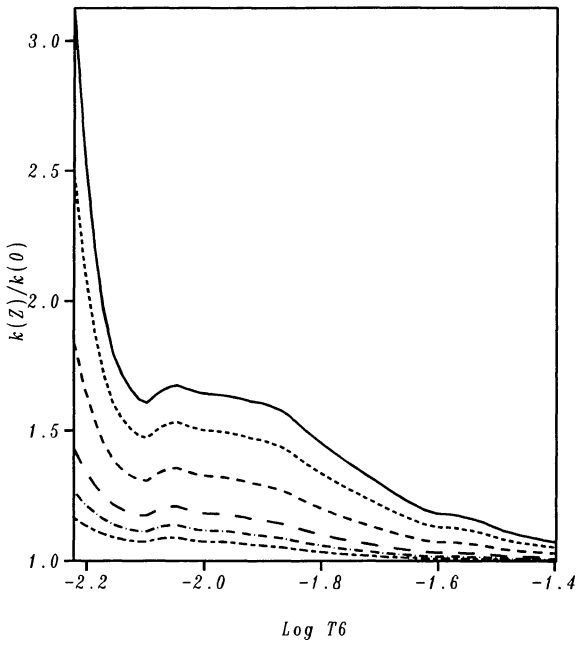

FIG. 14*b*

FIG. 14.—Same as Fig. 8*a* and 8*b* with log $R = +1$

hancement is due to improved atomic physics in OPAL. In particular, a better treatment of the bound-bound transitions. In Figure 22*a* we plot the Fe photon absorption coefficient as a function of photon energy in a mixture with $X = 0.7$ and $Z = 0.02$ at log $T = 5.4$ and log $R = -3.5$. For comparison, we plot in Figure 22*b* the Fe absorption under the same conditions but have not included the configuration term splitting. Clearly, the neglect of term splitting considerably underestimates the Fe absorption (the individual Fe Rosseland mean opacity is reduced by a factor of 33). In LAO not only was the term splitting almost completely neglected, but, in addition, they utilized hydrogenic oscillator strengths which are identically zero for the $\Delta n = 0$ transitions occurring around the 60 eV photon energy in Figure 22*a*. As can be seen in the figure, term splitting also affects the $\Delta n > 0$ transitions. Due to the small abundance of Fe in the mixtures, this large increase in the Fe opacity translates to the opacity increases in Figure 21.

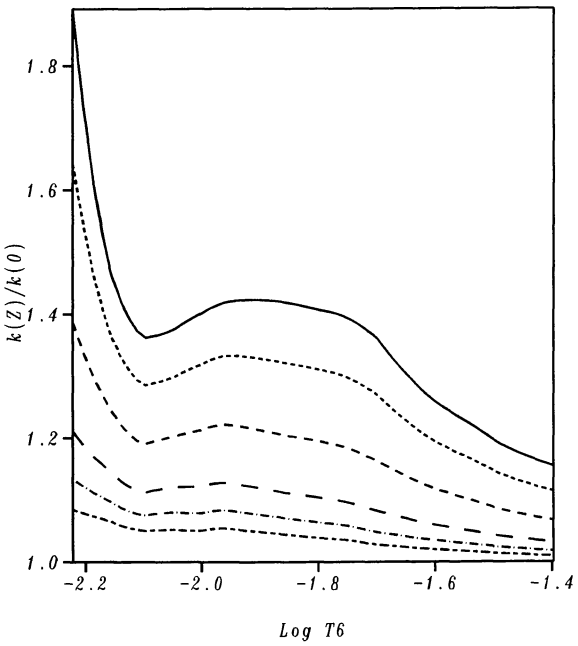

FIG. 15.—Same as Fig. 8*b* with log $R = 0$

A second region near log $T = 6.5$ in Figure 21 also shows substantial opacity increases over the Stellingwerf fits. In Figure 23 we repeat the calculations in Figure 22, but at log $T = 6.5$ and $R = 10^{-3}$. For these conditions it is transitions from principal quantum number $n = 2$ to $n = 3$ and above which mostly contribute to the Rosseland mean opacity (energies near 1000 eV in Fig. 23). It follows from the frequency dependent photoabsorption cross section that the term splitting in Fe is not as important as these higher temperatures, and, in fact, there is approximately a 30% increase in the individual Fe opacity due to the term splitting which seems too small to support the enhancement in Figure 21. Instead of comparing to the Stellingwerf fits, we made a direct comparison of OPAL to the CT tables at the same conditions and found a difference of only 8%. Our implementation of the Stellingwerf fit has been compared to other researchers (Iglesias et al. 1990), producing better than 10% agreement. Although the Stellingwerf fit may be artificially introducing this large disagreement near log $T \approx 6.5$, it is important to note that these fits are used extensively in stellar models.

In view of the discussion in the preceding paragraph, we compared the OPAL opacities along the $R = 10^{-3}$ and $R = 10^{-4}$ track directly to the CT tables, and the results are pre-

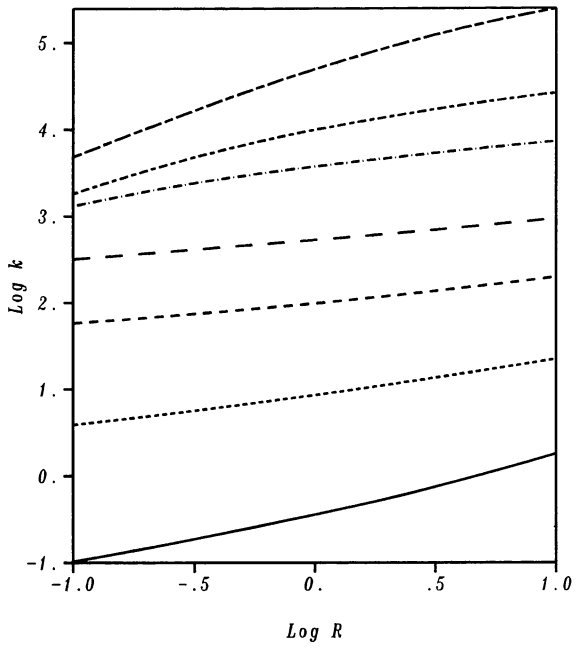

FIG. 16*a*

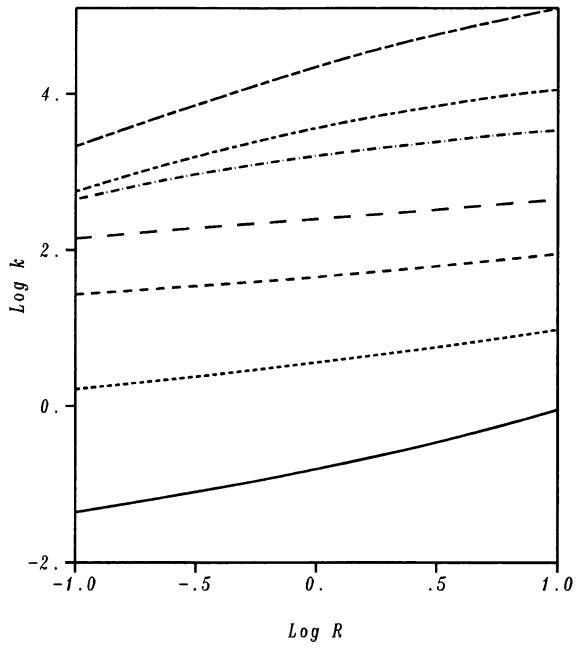

FIG. 16*b*

FIG. 16.—Rosseland mean opacity ($cm^2\ g^{-1}$) vs. R at constant temperature for Anders-Grevesse composition and $Z = 0.02$: (*a*) $X = 0.7$, (*b*) $X = 0.35$, and (*c*) $X = 0$ with (*solid line*) $T_6 = 0.006$; (*short-dash line*) $T_6 = 0.008$; (*medium-dash line*) $T_6 = 0.01$; (*long-dash line*) $T_6 = 0.012$; (*short-dash-dot line*) $T_6 = 0.14$; (*medium-dash-dot line*) $T_6 = 0.2$; and (*long-dash-dot line*) $T_6 = 0.4$.

sented in Figure 24. The large enhancement near log $T = 5.5$ remains, although modified, but not near log $T = 6.5$ which is now in the order of 10%–20%. These OPAL increases in opacity relatively to CT near log $T \approx 6.5$ and log $R \approx -3.5$ could be due to the improved atomic physics (see Fig. 23). However, at higher densities (log $R \approx -1$) similar opacity increases in OPAL are probably due to equation of state issues (Iglesias & Rogers 1991a).

A final comparison to the Stellingwerf fits is presented in Figure 25 for a very low metal abundance mixture. Here, $X =$

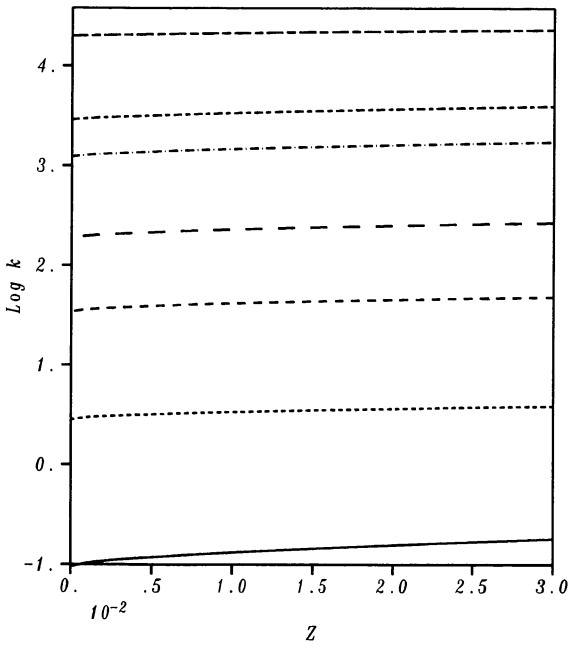

FIG. 17.—Same as Fig. 16*b* with log $R = 0$

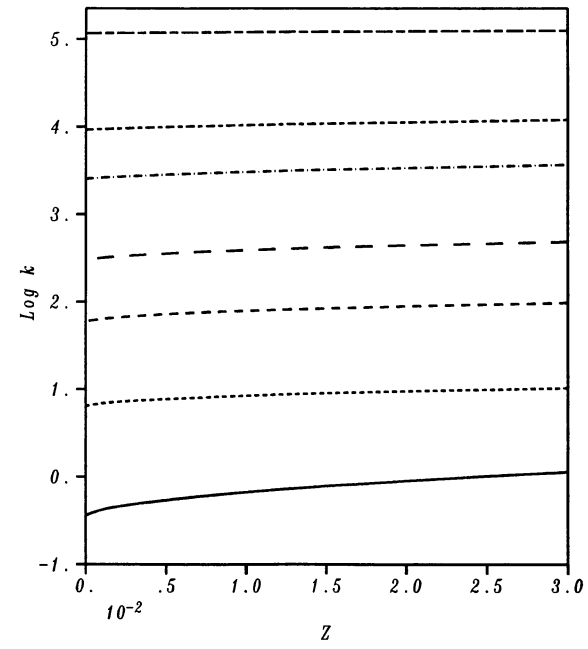

FIG. 18.—Same as Fig. 16*b* with log $R = +1$

TABLE 3

TEMPERATURE INTERPOLATION ERRORS IN PERCENT FOR $X = 0.35$ AND $Z = 0.02$

	log R						
T_6	−5	−4	−3	−2	−1	0	1
0.008	−4.8	−14.7	−12.5**G**	−5.7	−2.0	−4.9	−10.6**Q**
0.009	12.2	−1.4	−9.1	−6.3	−4.9**M**	−1.4	−1.8
0.010	4.8	8.1**D**	−0.5	−4.5	−2.8	−2.9	−2.9
0.011	2.3	3.8	1.9	−1.2	−1.3	0.3	2.3
0.012	2.5	7.4	9.9**H**	3.4	0.3	−0.8	−2.0
0.014	−13.3	−0.3	13.8	12.2**K**	2.8	0.4	−0.4
0.016	2.6	−10.5	0.7	8.3	3.9	1.2	1.8
0.018	0.5	2.9	−7.8	4.5	3.7	0.5	0.0
0.020	2.9	3.1	4.2**I**	−7.5	6.3	3.5**P**	0.5
0.025	3.4	5.4	7.2	−1.1	−8.0	7.5	2.6
0.030	1.8**A**	4.2	0.6	3.3	−4.1	−4.0	−0.2
0.035	−12.0	−0.3	2.7	−0.8	0.8	−2.8	−2.1
0.040	1.1	−11.9	−0.3	0.6	−0.7	...	...
0.050	0.8	8.6	−4.4	−3.8	−0.8	...	...
0.055	0.7	−0.5	4.2**J**	−2.2	−0.2	...	...
0.060	0.4	3.5	7.7	1.8	−0.6	...	...
0.070	−0.9	−1.9	−0.8	8.6	1.4	...	...
0.080	0.9	1.4	1.7	4.3	2.4	...	...
0.090	−0.7	−0.3	−0.4	−2.0	1.2	...	...
0.100	1.5	−1.3	−1.8	−0.3	−0.9	...	...
0.120	−0.2	−0.8	−0.3	−1.0	−3.4	...	...
0.150	−15.1**B**	3.0**E**	−8.4	−9.6**L**	−8.2**N**	...	...
0.200	−6.1**C**	23.3**F**	−5.2	−3.4	4.2**O**	...	...
0.250	10.6	8.2	3.1	5.1	5.6	...	...
0.300	2.5	3.4	2.2	1.9	2.0	...	...
0.400	6.0	1.6	−3.8	0.8	1.2	...	...
0.500	−0.5	7.9	1.7	−0.9	−0.6	...	...
0.600	−4.2	−1.0	5.8	−0.5	−1.3	...	...
0.800	0.9	−3.8	1.5	2.8	1.1	...	...
1.000	−0.1	−1.3	−0.6	2.2	0.2	...	...
1.200	0.0	−0.4	−0.9	−0.6	−2.0	...	...
1.500	−3.5	1.8	−0.5	−2.7	−3.9	...	...
2.000	2.0	−8.4	−0.7	−2.8	−0.8	...	...
2.500	1.7	2.1	−6.5	−3.0	1.5	...	...
3.000	−0.8	2.0	0.6	1.3	2.8	...	...
4.000	0.2	0.7	5.0	3.0	0.8	...	...
5.000	0.0	0.4	2.4	1.8	1.0	...	...
6.000	−0.3	−0.4	1.0	1.5	1.4	...	...
8.000	0.5	0.4	1.1	2.6	−0.2	...	...
10.00	−1.1	−1.0	−0.6	−1.0	−4.1	...	...
15.00	0.4	−2.8	−6.6	−7.0	−3.1	...	...
20.00	0.3	1.4	−2.8	−4.7	3.6	...	...
30.00	−0.1	0.5	4.0	4.6	−0.1	...	...
40.00	−0.2	−0.3	0.8	2.0	−0.6	...	...
60.00	−0.1	−0.5	−0.9	−1.6	−0.7	...	...
80.00	−0.2	0.3	−0.2	−0.8	0.0	...	...

0.7 and $Z = 0.0001$ where we have again assumed the metal abundances in CT. The figure shows not only about a 15% increase in opacity from OPAL centered at log $T \approx 5.5$, but also significant lower opacities (as much as 30%) for log $T \leq 5.3$. These opacity comparisons may be relevant to existing discrepancies in metal-poor pulsating stars (see a review by Renzini & Fusi-Pecci 1988). For example, Cox (1991) has shown that this combination of decrease and increase in opacity resolves the mass anomalies in RR Lyrae stars.

Recently Weiss et al. (1990) published opacity tables which include molecular effects at low temperatures. These tables are a compendium of results from the Los Alamos Astrophysical Library (Huebner et al. 1977). In Table 7 is a comparison to their opacities for the King IV *a* mixture ($X = 0.7$ and $Z = 0.02$ with CT metal abundances). We interpolated from our table to their published temperature and density grid and present the ratio of OPAL to their results. Again note the large increases in OPAL around log $T = 5.6$. Similar to the case with the CT tables, Table 7 shows OPAL with a 20% opacity enhancement near log $T = 6.3$ rather than the much larger differences observed in Figure 21.

Not all the differences between OPAL and the LAO calculations result in enhanced opacities. In the region log $T \leq 5$, the OPAL opacities can be smaller than those from LAO as well as the Stellingwerf fits (see Figs. 21, 24, 25 and Table 7). We suspect that the lower opacity in OPAL is due, in part, to the treatment of the spectral lines in hydrogen and neutral helium. As mentioned earlier, for these lines OPAL uses Stark broaden-

TABLE 4

TEMPERATURE INTERPOLATION ERRORS IN PERCENT FOR SPECIAL REGIONS OF TABLE 3

Label in Table 3	T_6	log R	κ(OPAL Code) (cm^2 g^{-1})	Percent Error
A	0.0325	−5	0.678	5.7
B	0.1750	−5	1.439	−4.0
C	0.2250	−5	1.174	−2.0
D	0.0105	−4	1.321	2.0
E	0.1750	−4	4.872	−3.6
F	0.2250	−4	5.023	−2.4
G	0.0085	−3	1.426	−0.6
H	0.0130	−3	8.184	−4.4
I	0.0225	−3	9.045	0.1
J	0.0570	−3	31.36	−0.7
K	0.0150	−2	60.85	−0.2
L	0.1350	−2	216.8	2.2
M	0.0085	−1	14.97	0.1
N	0.1350	−1	2333.	0.3
O	0.1750	−1	1901.	−2.1
P	0.0225	0	4993.	−1.2
Q	0.0085	+1	17.62	−0.5

ing codes developed by Lee (1988) which assume the asymptotic wing formula for the line shape,

$$I(\epsilon) \propto \epsilon^{-5/2} \times \begin{cases} 1, & \text{for neutral atoms} \\ e^{-\alpha\sqrt{\epsilon}}, & \text{for ions} , \end{cases} \quad (7)$$

where ϵ is the distance in energy from line center and α is a constant which depends on the ion charge. LAO uses a model developed by Griem (1960) which assumes the form

$$I(\epsilon) \propto \epsilon^{-2} \quad (8)$$

for the wing. Thus, even for neutrals their line shapes fall off slower, possibly leading to a higher opacity in this temperature region. In the far wing neither formula is likely to be correct; however, the ϵ^{-2} falloff in the LAO line shape comes from assuming that the electron impact width (valid for $\epsilon \cong 0$ with a constant value independent of ϵ) is valid in the line wing. In OPAL, the electron width decreases rapidly for ϵ/h greater than the electron plasma frequency eventually reaching the quasi-static limit form, equation (7) (Lee 1988; Seaton 1991).

To check our conjecture, we computed the opacity for the King IV a ($X = 0.7$ and $Z = 0.02$) mixture using Voigt profiles (with a ϵ^{-2} wing) for the hydrogen and helium lines at log T = 4.3 and log $\rho = -8$ giving an opacity increase of 16%. The same calculations were repeated at log $T = 4.84$ and log $\rho = -7$ now giving only a 0.4% increase in opacity. Although the temporary use of Voigt profiles for the hydrogen Lyman series in OPAL does not fully explain the differences in Table 7, it does bring the two opacity results closer together at the lower temperature. Just as important, this test demonstrates the uncertainties in opacity calculations due to line shapes.

Although the line shape codes by Lee (1988) have been extensively checked against experiment and other codes, here we present a test of their implementation in OPAL. In Figure 26, emission coefficients from OPAL are compared to the Balmer spectrum measured by Wiese, Kelleher, & Paquette (1972) in a high-current, wall-stabilized arc operated in hydrogen. In making the comparison it is important to remember that the experiment is probably not in thermal equilibrium (assumed in the OPAL calculation) and that the quoted temperature and electron density have experimental errors. Nevertheless, the OPAL result is in good agreement with the experiment which suggests that the line shape theory is reasonably correct, at least in the near wing (the far wing is obscured by the H^- absorption.

Unfortunately, the Wiese et al. experiment is not a sensitive test for EOS or occupation numbers, but rather it is an excellent test for Stark broadening of hydrogen spectral lines as originally intended by the authors. The reason is that a simple Saha-type EOS formulation with principal quantum number cutoff above the Inglis-Teller limit (Inglis & Teller 1939) will reproduce reasonably well the experimental data (Dappen et al. 1987). The difficulty is in reproducing the line spectra near threshold where a careful theory would need to Stark mix many states of different principal quantum numbers plus the continuum. Present line shape theories do not include this

TABLE 5

PERCENT ERRORS IN X INTERPOLATION FOR ANDERS-GREVESSE COMPOSITION AND log $R = -3$

	$Z = 0.00$				$Z = 0.02$			
	LINEAR FIT		QUADRATIC FIT		LINEAR FIT		QUADRATIC FIT	
T_6	$X = 0.2$	$X = 0.5$	$X = 0.2$	$X = 0.5$	$X = 0.2$	$X = 0.5$	$X = 0.2$	$X = 0.5$
0.006	−4.62	−5.41	−2.3	−4.74	−1.32	−3.80	−1.11	−3.71
0.008	−6.80	0.51	−2.72	1.96	−5.61	0.26	−2.20	1.49
0.010	−39.4	−2.08	−14.6	3.74	−35.6	−2.19	−13.8	3.18
0.014	−55.2	−13.7	5.90	−1.84	−46.4	−10.2	−0.26	−0.23
0.020	−2.51	−5.40	2.39	−3.13	−3.24	−4.99	1.50	−2.61
0.060	−1.74	1.08	−1.67	0.01	−1.35	−0.49	−1.57	−1.14
0.200	2.18	3.94	−1.61	−0.20	1.13	2.59	−1.28	0.32
0.600	1.16	1.27	−0.45	−0.28	0.01	1.04	−1.00	0.19
2.000	2.87	2.60	1.08	1.10	−0.75	−1.02	−1.22	−1.41
6.000	0.01	−0.17	−0.11	−0.27	0.20	0.16	0.02	0.01
20.00	0.08	−0.48	−0.20	−0.39	0.17	−0.32	0.17	−0.32
60.00	−0.17	−0.07	−0.32	−0.19	−0.14	−0.04	−0.30	−0.16

TABLE 6

PERCENT ERRORS IN X INTERPOLATION FOR ANDERS-GREVESSE COMPOSITION AND log R = +0.5

	Z = 0.00		Z = 0.02	
T_6	LINEAR FIT X = 0.5	QUADRATIC FIT[a] X = 0.5	LINEAR FIT X = 0.5	QUADRATIC FIT[a] X = 0.5
0.006	−36.0	−24.5	−1.67	−0.22
0.008	−4.84	−0.33	−2.33	0.62
0.010	−5.27	−3.30	−1.09	0.34
0.012	−2.91	−1.16	−0.62	0.06
0.016	−2.50	0.35	−0.67	0.55
0.020.....	−3.09	1.91	−2.34	0.77
0.025	−5.02	0.71	−3.96	0.75
0.040	−0.43	1.28	−2.09	0.86

[a] Assumed κ = 0 for X = 0.

coupling and therefore have unphysical broadening to regions far from line center leaving a spectral window near threshold. To avoid this problem, we have incorporated a phenomenological method (D'yachkov, Kobzev, & Pankratov 1988, and references therein) that mimics the line broadening of overlapping lines. Other authors (see, e.g., Ruzdjak & Vujnovic 1976; Dappen et al. 1987; Seaton 1991) have used similar schemes with reasonable success. All of these schemes, however, are in effect smoothing procedures which conserve oscillator strength and restrict the line radiation to the region near threshold.

We now return to Table 7 which shows that at log T = 3.84 and log ρ = −6 OPAL is almost half the Weiss et al. (1990) value. A comparison with CT for the same composition and matter conditions shows OPAL to be smaller by 20%. Since the OPAL opacity is dominated by the H^- photon absorption, we compare OPAL results to previous Z = 0 calculations. The comparison is presented in Table 8 and we find good agreement with the work by Lenzuni, Chernoff, & Salpeter (1991), but poor agreement with CT. Unfortunately, there are no Z = 0 tables in Weiss et al. for similar comparison. Of course, the abundance of H^- depends on the number of free electrons which at this low temperature is sensitive to the metal mass fraction. Consequently, the differences for Z = 0.02 could be in the equation of state treatment of the metals or the atomic physics.

As mentioned earlier, OPAL neglects molecular absorption so that the differences at the lowest temperature in Table 7 could be molecular opacity effects included in Weiss et al. (1990). However, according to Alexander et al. (1983), molecules are not important above 6×10^3 K. In Table 9 we compared the Alexander et al. opacities to the Weiss et al. results for the Cameron (1973) mixture in a limited density-temperature region. Some qualifications are necessary in these comparisons since the compositions are not identical (small differences in X and Z); nevertheless, the Alexander et al. opacities are considerably smaller. In fact, it is approximately half the Weiss

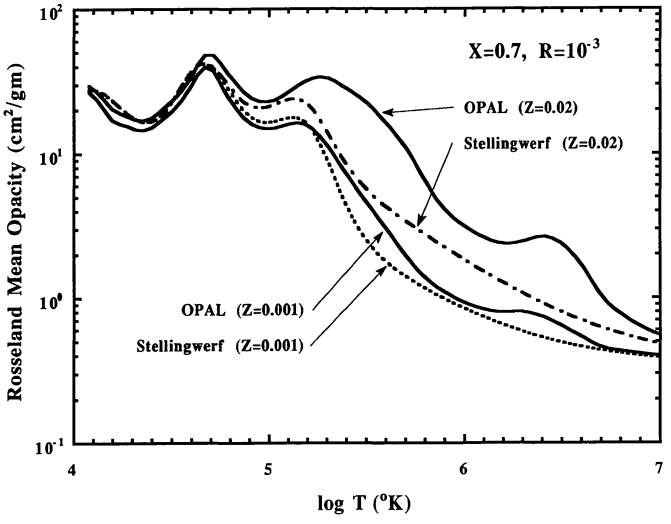

FIG. 19.—Rosseland mean opacity (cm^2 g^{-1}) vs. temperature for X = 0.7 at constant log R = −3 for CT composition from OPAL and Stellingwerf fits.

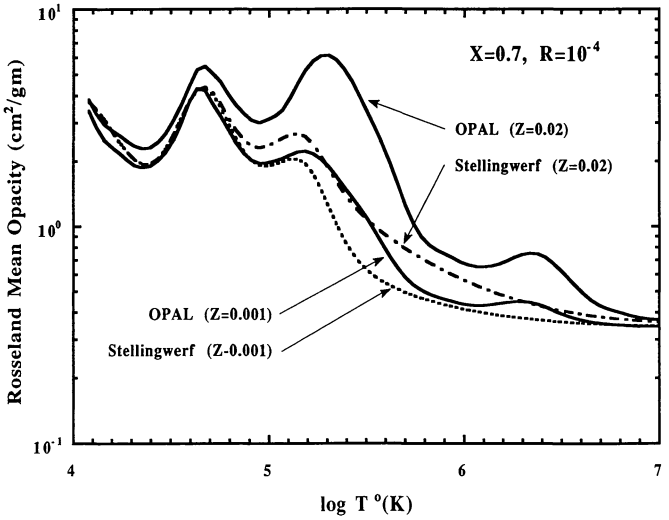

FIG. 20.—Same as Fig. 19 with log R = −4

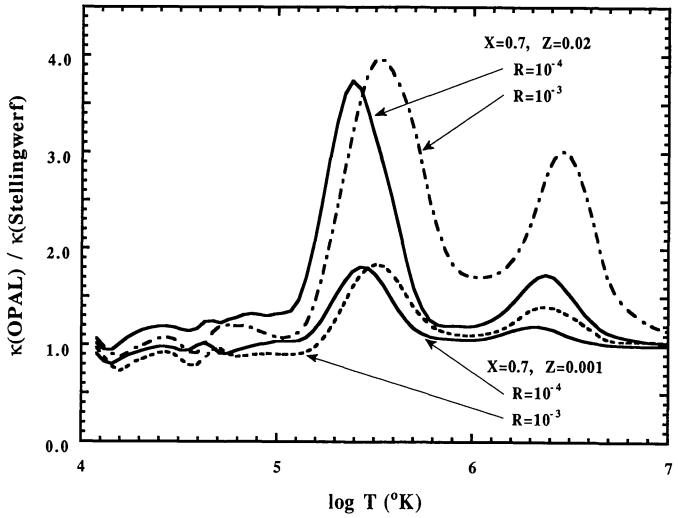

FIG. 21.—Ratio of OPAL to Stellingwerf fits vs. temperature at constant R for the same composition and matter conditions as in Figs. 19 and 20.

et al. value at log $T = 3.84$ and log $\rho = -6$ as was the case for OPAL with the CT mixture (see Table 7).

Uncertainties in opacities are not only due to approximations in the codes but also to the uncertainties in the chemical composition. It was shown in Iglesias & Rogers (1991a) that in the solar radiative interior opacity variations from commonly used metal abundances were comparable to those between the OPAL and LAO computer codes. Accordingly, we compare in Figure 27 the OPAL opacity for the Anders-Grevesse and CT metal abundances. There is as much as 17% difference between these two compositions for $Z = 0.02$ reducing to at most 5% for $Z = 0.0001$. It may seem paradoxical that the Anders-Grevesse composition almost always yields opacities which are larger than those from the CT mixture. The explanation is found in the distribution of metal abundances presented in Table 1. There, it can be seen that the fractional abundance of all the metals in the Anders-Grevesse composition are larger than those in the CT mixture except for two elements: Ne and Ar. Since the abundances in Table 1 are normalized to 1, it follows that when going from the CT metal composition to that of Anders-Grevesse the excess abundance of Ne and Ar is distributed over the remaining metallic elements. The result is an overall increase in opacity except in localized regions where Ne and Ar dominate the photon absorption. For example, the K-edge of highly ionized Ar is slightly above 4 KeV and, therefore, a strong absorber for T near 10^7 K (see Fig. 27).

A final point concerning the photon energy grid in OPAL. The calculations are done with 5000 uniformly distributed points in the range $0 < u \leq 20$, where u = (photon energy/kT). This is to be compared to the energy grid in LAO which consists of 3000 points for $0 < u \leq 30$. As a simple test we recomputed all the Rosseland mean opacities in the tables using 2500 points and the range $0 < u \leq 20$. These calculations were compared to the original results with 5000 points, and we found that for 92% of the cases the difference was less than 1%, 98% changed by less than 2%, and all cases had differences smaller than 5%. Although the test above is not definitive, it suggests that our energy grid is adequate.

6. UNCERTAINTIES IN METAL OPACITY

As mentioned earlier, the OPAL opacity increase over LAO in the temperature region 10^5 K $< T < 10^6$ K is mostly due to improved atomic physics of the Fe ions with partially filled M-shells. The extent to which Fe dominates the opacity in this region is shown in Figures 28 through 31 where calculations for the Anders-Grevesse mixture with and without the Fe contribution to the photon absorption are compared for various

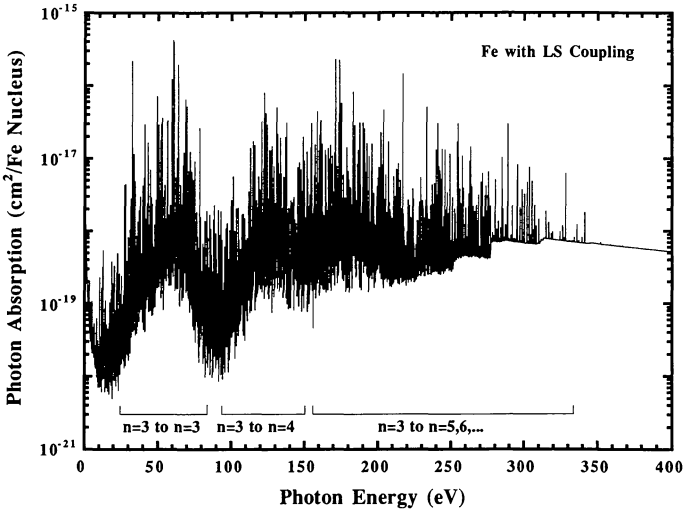

FIG. 22*a*

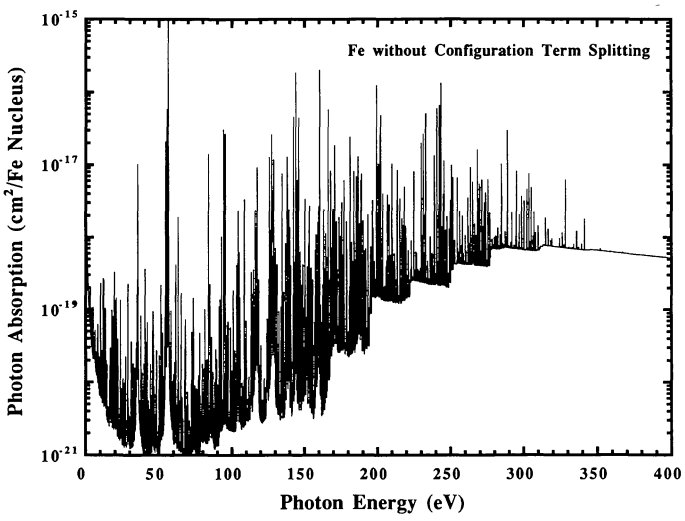

FIG. 22*b*

FIG. 22.—Iron frequency-dependent photon absorption for $X = 0.7$, $Z = 0.02$, and CT metal abundances at log $T = 5.4$ and log $R = -3.5$: (*a*) with and (*b*) without configuration term splitting. Initial and final principal quantum number for the optically active electron is denoted by n.

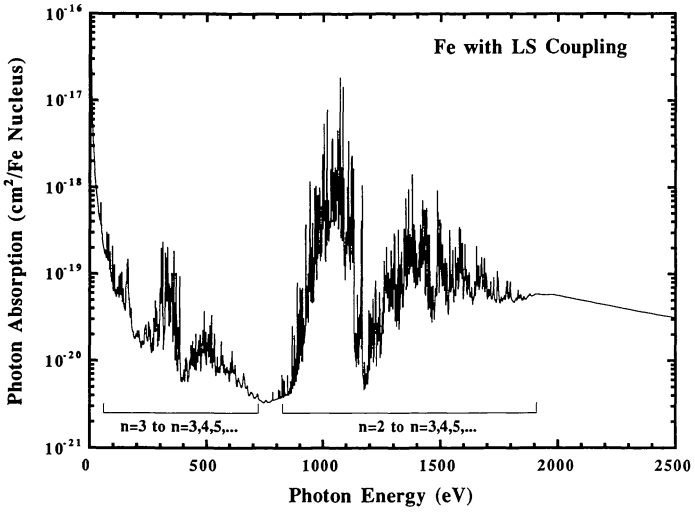

FIG. 23*a*

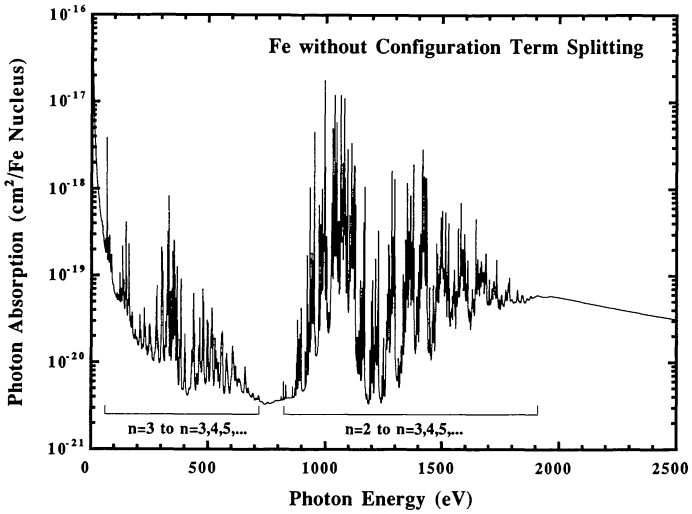

FIG. 23*b*

FIG. 23.—Same as Fig. 22 with log T = 6.5 and log R = −3

combinations of Z and R. In view of the importance of Fe to the opacity, we also compared compositions with the Fe abundance both enhanced and reduced by a factor of 2. Clearly, an accurate representation of the opacity for a given star will depend on the accuracy of the adopted Fe abundance.

The assumed Anders-Grevesse mixture in our calculations only considers 14 elements even though more than 14 are observed. The effect on the opacity is minimized by combining the missing element abundances with other elements nearby in atomic number present in the calculation. As a test, we computed opacities for a 16 element mixture adding Cr and Ni in the proportions given in Table 1. The results are compared in Figures 28–31 to the 14 element results where the explicit treatment of the 16 elements gives as much as 20% opacity increases for the higher metallicity mixture but shows only a few percent increase for the low-metallicity case. Note that the opacity sensitivity to the missing elements increases with decreasing density. Due to their extremely low abundances, it is generally assumed that elements with atomic number greater than 30 do not contribute significantly to astrophysical opacities. In view of the impact improved atomic physics had on the Fe photoabsorption coefficient and considering the results shown here for Cr and Ni, it is prudent that the contributions from the very heavy elements be assessed.

As described in § 2.2, in generating the atomic data pure LS-coupling is assumed. This is valid when the electrostatic interactions between electrons are much stronger than the interaction between the spin of an electron and its own orbital.

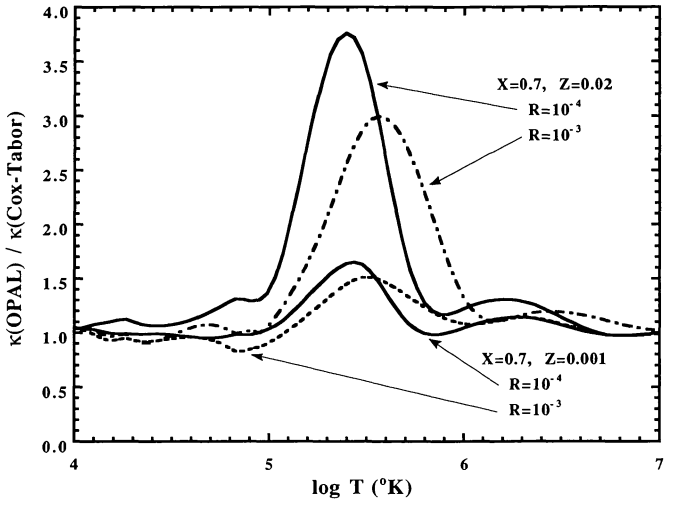

FIG. 24.—Ratio of OPAL to CT opacity tables vs. temperature at constant R.

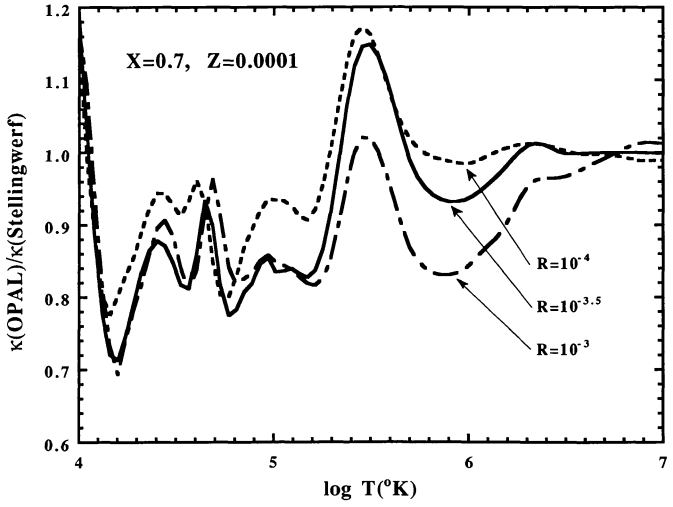

FIG. 25.—Ratio of OPAL to Stellingwerf fits for metal-poor CT composition.

TABLE 7

COMPARISON OF OPAL TO WEISS, KEADY, AND MAGEE (1990) FOR $X = 0.7$, $Z = 0.02$, AND COX-TABOR ABUNDANCES[a]

	log ρ (g cm^{-3})														
log t	−10	−9	−8	−7	−6	−5	−4	−3	−2	−1	0	+1	+2	+3	+4
3.843	1.08	0.99	0.73	0.61	0.54	...[b]	x[c]	...	x	x	x	x	x	x	x
3.988	1.00	0.95	0.89	0.80	0.71	...	x	...	x	x	x	x	x	x	x
4.065	1.09	1.02	0.93	0.86	0.81	0.73	x	...	x	x	x	x	x	x	x
4.079	0.89	0.92	0.91	0.82	0.79	0.78	x	x	x	x	x	x	x	x	x
4.114	0.88	0.88	0.86	0.76	0.76	0.78	x	x	x	x	x	x	x	x	x
4.176	0.88	0.80	0.84	0.85	0.81	0.78	...	x	x	x	x	x	x	x	x
4.204	0.90	0.79	0.84	0.89	0.85	0.79	...	x	x	x	x	x	x	x	x
4.255	0.90	0.80	0.85	0.86	0.86	0.82	...	...	x	x	x	x	x	x	x
4.301	0.92	0.79	0.81	0.83	0.87	0.85	...	...	x	x	x	x	x	x	x
4.602	...	1.12	1.03	0.96	0.99	...	...	...	x	x	x	x	x	x	x
4.778	...	...	0.99	0.92	0.96	1.12	...	...	x	x	x	x	x	x	x
4.903	...	...	1.05	0.89	0.91	0.87	...	...	x	x	x	x	x	x	x
5.000	...	...	1.15	1.08	1.01	0.90	...	...	x	x	x	x	x	x	x
5.301	...	...	...	2.47	2.38	1.83	1.38	...	...	x	x	x	x	x	x
5.602	...	...	...	...	1.20	2.14	2.44	1.44	...	...	x	x	x	x	x
5.778	...	...	...	...	...	1.09	1.72	1.77	1.26	...	...	x	x	x	x
5.903	x	...	...	...	...	1.03	1.22	1.57	1.26	...	...	x	x	x	x
6.000	x	...	...	...	...	1.02	1.10	1.33	1.32	...	...	x	x	x	x
6.301	x	...	...	...	...	...	1.09	1.20	1.16	1.14	...	x	x	x	x
6.602	x	x	...	...	...	...	...	1.00	1.07	1.16	1.10	...	x	x	x
6.778	x	x	...	...	...	...	...	...	0.98	1.03	1.01	1.08	...	x	x
6.903	x	x	...	...	...	...	...	...	0.99	1.00	1.00	1.00	...	x	x
7.000	x	x	...	...	...	...	...	...	1.00	1.00	1.00	1.00	...	x	x
7.301	x	x	x	...	...	...	...	...	...	1.00	1.01	1.05	1.06	...	x
7.602	x	x	x	...	...	...	...	...	...	...	1.00	1.00	1.00	0.97	...
7.778	x	x	x	...	...	...	...	...	...	...	...	1.00	0.99	0.96	0.82
7.903	x	x	x	x	...	...	...	...	...	...	...	0.99	0.99	0.96	0.84
8.000	x	x	x	x	...	...	...	...	...	...	...	0.99	0.99	0.97	0.85

[a] OPAL opacity divided by Weiss et al. 1990 result.
[b] Weiss et al. 1990 value outside range of OPAL tables.
[c] No entry in either table.

However, with increasing atomic number the spin-orbit interactions become more important and cannot be neglected. In such circumstances intermediate coupling calculations are necessary to properly predict the spectrum (Cowan 1981). To test the validity of the LS-coupling approximation for computing the opacity of astrophysical mixtures, calculations using intermediate coupling for the Fe are compared in Figures 28 through 31 to the pure LS results. The figures show that opacity increases due to the intermediate coupling are density dependent. For example, for a track at log $R = -2$ (not shown in

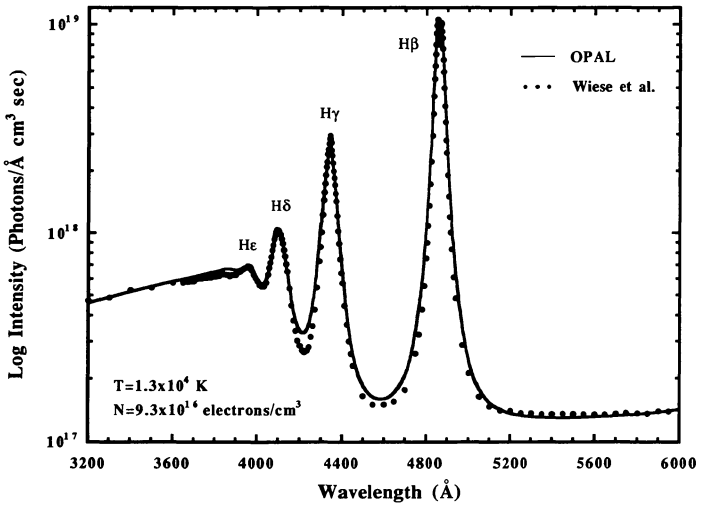

FIG. 26.—Comparison of OPAL to Wiese et al. (1972) hydrogen emission experiment.

TABLE 8

COMPARISON TO OTHER $Z = 0.00$ CALCULATIONS

T_6	ρ (g cm^{-3})	log (R)	Lenzuni et al.[a]	Cox-Tabor[b]
0.006	2.16×10^{-6}	+1.0	0.99	2.34
0.006	2.16×10^{-7}	0.0	0.94	2.21
0.006	2.16×10^{-8}	−1.0	0.94	2.21
0.006	2.16×10^{-9}	−2.0	1.04	2.42
0.006	2.16×10^{-10}	−3.0	0.97	2.04
0.006	2.16×10^{-11}	−4.0	1.05	1.83
0.006	2.16×10^{-12}	−5.0	1.03	1.58
0.007	3.43×10^{-6}	+1.0	0.92	1.99
0.007	3.43×10^{-7}	0.0	0.94	2.01
0.007	3.43×10^{-8}	−1.0	1.01	2.15
0.007	3.43×10^{-9}	−2.0	1.03	2.16
0.007	3.43×10^{-10}	−3.0	1.09	2.16
0.007	3.43×10^{-11}	−4.0	1.10	1.99
0.007	3.43×10^{-12}	−5.0	1.10	...

[a] OPAL divided by Lenzuni et al. 1991 with $X = 0.73$.
[b] OPAL divided by Cox & Tabor 1976 with $X = 0.7$.

TABLE 9

RATIO OF ALEXANDER ET AL.[a] TO WEISS ET AL.[b] OPACITIES FOR CAMERON MIXTURE

	log ρ (gm cm^{-3})		
log T	−8	−7	−6
3.764	0.58	0.51	0.50
3.843	0.47	0.42	0.43
3.968	0.82	0.77	0.73

[a] Alexander et al. 1983 with $X = 0.71$ and $Z = 0.02$.
[b] Weiss et al. 1990 with $X = 0.77$ and $Z = 0.018$.

the figures), the increases are at most a few percent since at these higher densities line broadening compensates for approximations in the term splitting calculations. At the lowest densities (log $R = -5$) the opacity increase due to intermediate coupling is comparable to doubling the Fe abundance as shown in Figures 29 and 31. Although in Figure 28 the mixture opacity increases by ~20% due to intermediate coupling, the Rosseland mean opacity for the individual Fe is more sensitive increasing by ~40%, while at the lower densities the individual Fe opacity increases by as much as ~55%.

The results above show that at the smaller densities the opacity is sensitive to the detailed treatment of the angular momentum coupling. The effect of the spin-orbit interaction is to increase the number of spectral lines. It further splits the LS-terms into total J-levels and is responsible for intercombination lines (transitions which change the total spin which are not allowed in pure LS). It seems that although in Fe the spin-orbit interaction is relatively small, the further splitting of the spectral lines is effective in further blocking the radiation. It is conceivable that the opacity may also be sensitive to higher multipoles (OPAL only considers electric dipole transitions). However, electric quadrupole and magnetic dipole transitions in partially filled M-shell ions of Fe are approximately 10^{-5}

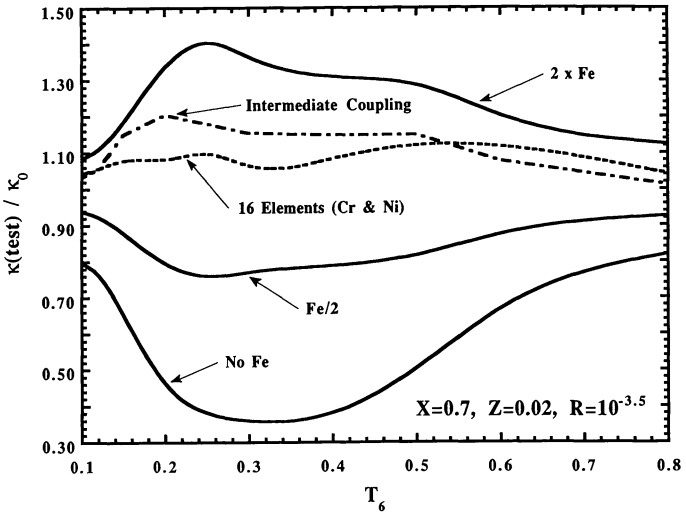

FIG. 28.—Ratio of modified opacity calculation, κ(test), to results in the tables, κ_0.

weaker than the dipole allowed lines. Consequently, it is reasonable to assume that the higher multipoles are negligible.

Another approximation in the angular momentum coupling, also described in § 2.2, is the neglect of term splitting for levels with principal quantum $n \geq 5$. We have done calculations for Fe with LS-coupling including principal quantum number $n \leq 6$, and have found small increases (less than 1%) to the mixture opacity and at most a few percent to the individual Fe opacity. Similar small increases in opacity are found when the limit on the number of lines in a configuration-to-configuration array described in § 2.2 is doubled to 20,000.

Hydrogen line shapes were shown earlier to affect the opacity at the lower temperatures. Here, we test the opacity sensitivity to line wings by replacing all the Voigt profiles in Fe by Gaussian line shapes, and we compare the results in Figures 32

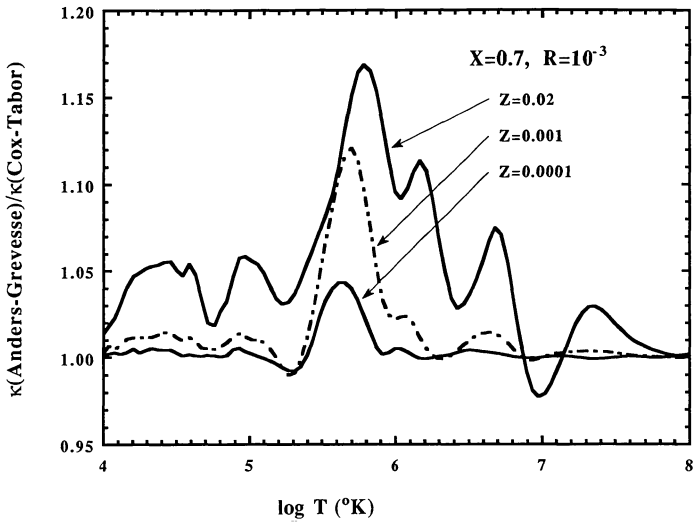

FIG. 27.—Ratio of OPAL results using Anders-Grevesse to CT metal abundances vs. temperature.

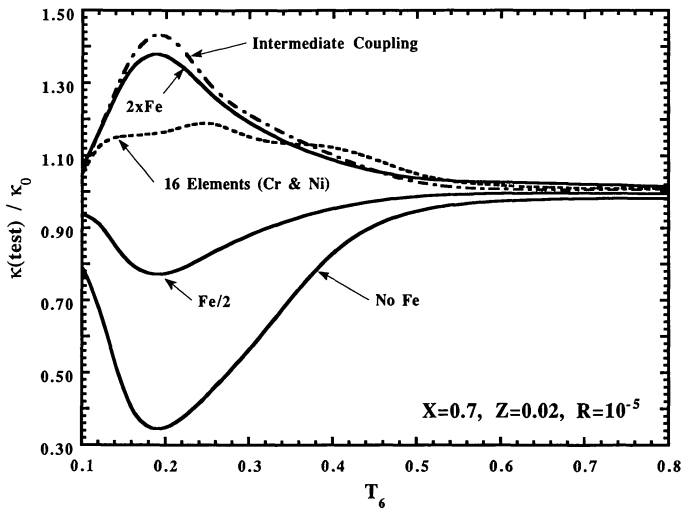

FIG. 29.—Ratio of modified opacity calculation, κ(test), to results in the tables, κ_0.

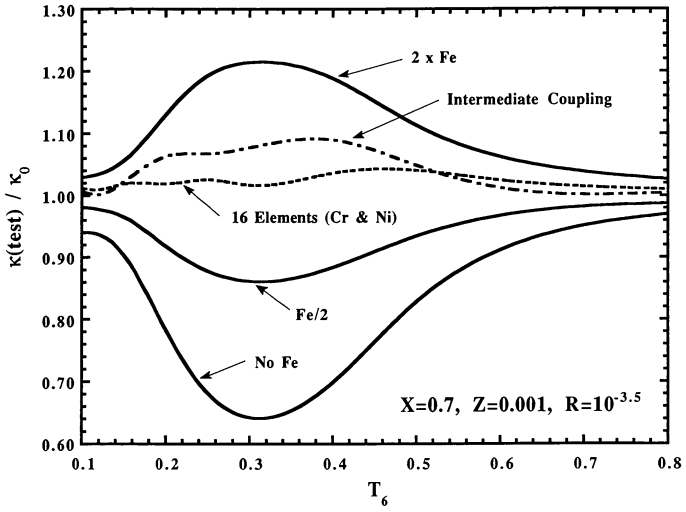

FIG. 30.—Ratio of modified opacity calculation, κ(test), to results in the tables, κ_0.

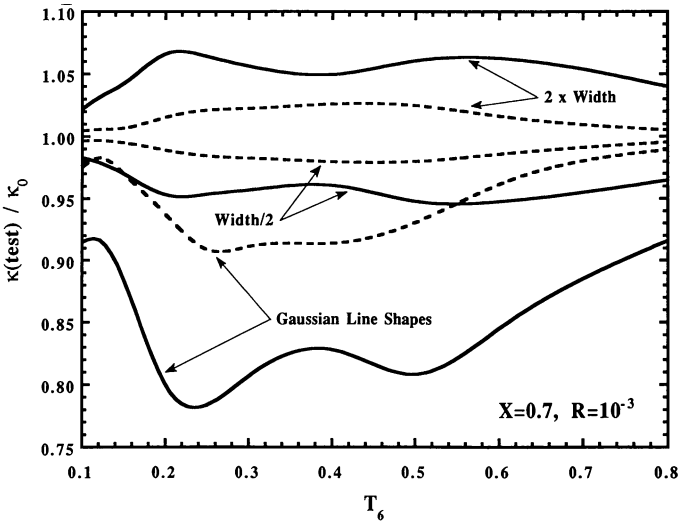

FIG. 32.—Ratio of modified opacity calculation, κ(test), to results in the tables, κ_0. Two metallicities are shown: (*solid lines*) Z = 0.02 and (*dashed lines*) Z = 0.001.

and 33. The width of a Gaussian is chosen so as to have the same full width at half-maximum as the Voigt profile it replaces. Again, the opacity is most sensitive at the lowest densities and higher metallicity decreasing by as much as 65% for Z = 0.02 and $R = 10^{-5}$ which is comparable to removing the Fe contribution. More moderate reductions in opacity are found for the lower metallicity and higher density cases in Figures 32 and 33. We emphasize that the use of Gaussian line shapes is an extreme test of line wing effects. Nevertheless, it demonstrates the possible uncertainties in opacity calculations due to line shapes.

The large number of spectral lines involved in the opacity calculations requires simplifying approximations for the line widths. Not only are the electron impact widths approximate (see § 2.2), but the broadening due to the ions is ignored (except for the linear Stark cases). The ions only make a small contribution near line center since ion impact widths are smaller than those from the electrons. However, the ions shift lines and modify the line wings through the quadratic Stark effect (Griem 1974). To test the sensitivity of the opacity to the impact widths, calculations where the line widths of all the Fe lines are multiplied by factors of $\frac{1}{2}$ and 2 are compared in Figures 32 and 33. Clearly, the mixture opacity is not as sensitive to the line widths as it is to the treatment of the line wings, but note that increasing the line widths has a larger effect on the opacity than the comparable reduction in line width.

7. CONCLUSION

Radiative Rosseland mean opacity tables have been tabulated using the OPAL code for various compositions over a

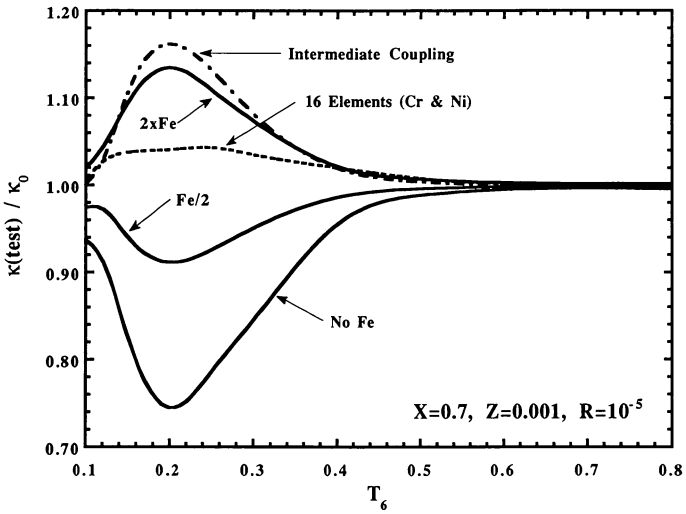

FIG. 31.—Ratio of modified opacity calculation, κ(test), to results in the tables, κ_0.

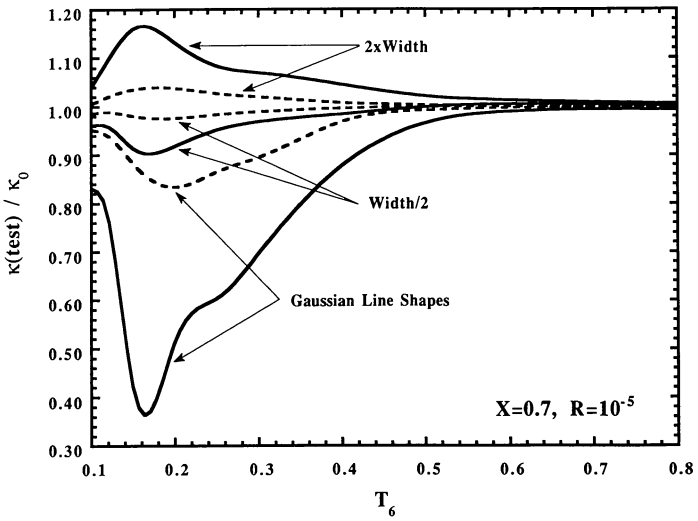

FIG. 33.—Ratio of modified opacity calculation, κ(test), to results in the tables, κ_0. Two metallicities are shown: (*solid lines*) Z = 0.02 and (*dashed lines*) Z = 0.001.

range of densities and temperatures typical of stellar conditions. The OPAL code removes several approximations made in previous calculations. The EOS approach avoids the ad hoc cutoffs and intuitive arguments present in free energy minimization schemes. The parametric potential model offers reasonably accurate atomic data (for example, a few percent error in configuration-averaged energies compared to experiment). Furthermore, OPAL includes configuration term splitting (in the LS-coupling scheme) which considerably increases the number of spectral lines (as much as factors of 10^3 over LAO for some cases), thus, filling in spurious "windows" in the absorption coefficient and restricting the flow of photons.

It was shown that the opacity is sensitive to H line shapes and possibly He for the temperature range $10^4\ \mathrm{K} < T < 10^5\ \mathrm{K}$ where OPAL predicts smaller opacities. Although not considered here, the shapes of autoionizing lines may also be a source of uncertainty. The latter could be most important at low densities and temperatures in pure metal mixtures ($Z = 1$) where the autoionizing widths can be much larger than those from Stark broadening and the continuum absorption from H and He would not overwhelm the metal line opacity.

The improvements in atomic physics lead to a large opacity enhancement over past calculations at $T \approx 3 \times 10^5$ K. Since this opacity bump depends on the metals (in particular Fe), it has a strong dependence on Z not present in the H and He bumps or earlier opacity calculations. Hence, the instabilities associated with it should display sensitivity to the metallicity absent in previous stellar models and possibly subject to stellar observations.

There can be no doubt that the OPAL opacity enhancement due to the metals near $T \approx 3 \times 10^5$ K is real. However, due to the very complex nature of the atomic physics and line broadening theories involved in the photon absorption calculation of ions with partially filled M-shells, the precise magnitude of the enhancement must be regarded as somewhat uncertain. Although the sensitivity tests in § 6 are neither exhaustive nor do they reflect any possible (but presently unknown) errors in the EOS calculations or the atomic data generation, the comparisons suggests errors of the order of 20% due to the treatment of lines widths and to the reduction of the mixture to 14 elements. At the lowest densities the better treatment of the angular momentum coupling for Fe ions using intermediate coupling does result in opacity increases comparable to doubling the Fe abundance. The largest uncertainties are found for the smallest R-value and highest metallicity. In any case, we feel it unjustified to include the computationally difficult intermediate coupling calculations in the present tables since other uncertainties such as line broadening and the Fe abundance, which for many stars is not well known, are comparable in size. Such calculations are reserved for the future. It should be noted that both intermediate coupling and including more elements in the mixture increase the opacity.

At higher temperatures, $T \approx 3 \times 10^6$ K, modest opacity enhancements of 10%–30% are noted which can affect helioseismology as well as lithium depletion. For low densities, these larger opacities at the hotter temperatures are probably due to improved atomic physics. At higher densities the enhancement is due to equation of state issues.

The opacity tables extend to low enough temperatures ($T = 6 \times 10^3$ K) to allow a smooth transition into other tables which include molecular absorption coefficients. For $Z = 0$ at these low temperatures, we obtained excellent agreement with the work by Lenzuni et al. (1991), but poor agreement (OPAL is smaller by as much as a factor of 2) for $Z = 0.02$ with LAO codes that include molecular opacities. Note that comparisons of the Alexander et al. (1983) results (which includes molecules) to the LAO calculations also show similar factors of 2 discrepancies.

The density and temperature covered by the tables should be sufficient for a broad range of astrophysical applications. However, a number of important issues cannot be addressed. For example, the opacity tables in the Appendix allow for changes in metallicity, Z, but not for changes in the relative metal abundances (except for the few tables with CT and Ross-Aller mixtures). Requests for compositions with different metal abundances can easily be satisfied for $X = 0$, 0.35, or 0.7 and $0 < Z < 0.03$. The reason is that we can take advantage of the fact that the EOS is dominated by H and He so that occupation numbers are insensitive to changes in the abundance of an individual metal. Therefore, we can remix the individual element frequency-dependent photon absorption coefficients computed assuming the Anders-Grevesse composition to obtain the Rosseland mean opacity of a new mixture with different relative metal abundances but fixed X and Z.

We are indebted to Brian G. Wilson for developing the angular momentum coupling subroutines in the atomic physics calculations and to Richard W. Lee for his line broadening codes, support, and encouragement. We recognize Kem H. Cook, Fritz J. Swenson, Marc H. Pinnsoneault, and, in particular, David Dearborn for valuable discussions in the construction and shape of the opacity tables. In addition, extra thanks are due to Kem H. Cook for help in the preliminary calculation of the tables. We thank Norm H. Magee for pointing out a numerical problem with our linear Stark line shapes. Special thanks are due to A. N. Cox, whose insatiable appetite for results and preliminary use of those results was a source of encouragement. We recognize valuable discussions at an Opacity Workshop hosted by the Opacity Project and IBM in Caracas, Venezuela during June 1991 which led to some of the tests performed in § 6. Finally, we thank H. Graboske for suggesting as well as supporting the development of the OPAL code. Work was performed under the auspices of the Department of Energy by Lawrence Livermore National Laboratory under contract W-7405-Eng-48.

APPENDIX

The radiative Rosseland mean opacities for the various compositions are collected in Tables 10 through 45. A summary of their contents is given in Table 2. In these tables we tabulate the decadic logarithm of the opacity, $\kappa(\mathrm{cm}^2\,\mathrm{g}^{-1})$, for columns at integer and half-integer values of $\log R$, where $R = \rho/T_6^3$ with T_6 the temperature in units of 10^6 K and ρ the matter density in g cm^{-3}. In Region I (see Fig. 1) we have tabulated opacities for 50 values of T_6 at each R, while in Region II only 15 temperatures are given. Note that no results are provided for $X = 0$ in Region II. Region I's of Tables 37 and 40 have already appeared in Iglesias & Rogers (1991b), except for the new values at $T_6 = 0.011$. However, they are reproduced here not only for completeness, but also because a small numerical error was found by N. H. Magee (1991, private communication) in the linear Stark broadening codes. The error leads to changes of several percent in the opacity for $0.012 < T_6 < 0.2$ at the higher densities. As mentioned earlier, note that the tables do not include electron conduction and neglect molecular photoabsorption.

TABLE 10

ANDERS-GREVESSE ABUNDANCES FOR $X = 0.70$ AND $Z = 0.00$

	Log R												
T6	-5.0	-4.5	-4.0	-3.5	-3.0	-2.5	-2.0	-1.5	-1.0	-0.5	0.0	0.5	1.0
0.006	-1.588	-1.739	-1.825	-1.846	-1.815	-1.629	-1.470	-1.263	-1.094	-0.869	-0.640	-0.401	-0.143
0.007	-0.723	-0.796	-0.830	-0.827	-0.769	-0.670	-0.547	-0.382	-0.205	-0.030	0.165	0.378	0.601
0.008	-0.224	-0.120	-0.033	0.037	0.098	0.189	0.286	0.402	0.538	0.684	0.842	1.019	1.213
0.009	-0.096	0.191	0.434	0.632	0.785	0.893	0.987	1.084	1.181	1.290	1.410	1.556	1.721
0.010	-0.107	0.234	0.579	0.929	1.196	1.392	1.527	1.624	1.708	1.799	1.901	2.020	2.156
0.011	-0.145	0.193	0.572	0.991	1.388	1.681	1.885	2.026	2.118	2.202	2.294	2.391	2.521
0.012	-0.180	0.139	0.519	0.960	1.415	1.810	2.106	2.297	2.437	2.537	2.632	2.733	2.848
0.014	-0.205	0.048	0.391	0.825	1.314	1.806	2.241	2.585	2.837	3.012	3.139	3.259	3.378
0.016	-0.229	0.018	0.341	0.741	1.205	1.726	2.218	2.671	3.041	3.307	3.499	3.651	3.786
0.018	-0.251	-0.024	0.296	0.709	1.186	1.679	2.175	2.681	3.135	3.490	3.755	3.949	4.110
0.020	-0.258	-0.054	0.260	0.684	1.160	1.657	2.170	2.685	3.182	3.612	3.939	4.180	4.375
0.025	-0.229	-0.046	0.255	0.676	1.166	1.695	2.231	2.765	3.300	3.808	4.238	4.582	4.836
0.030	-0.168	0.014	0.318	0.743	1.245	1.772	2.317	2.869	3.440	3.971	4.442	4.832	5.138
0.035	-0.078	0.124	0.432	0.845	1.341	1.874	2.420	2.977	3.552	4.100	4.589	4.995	5.312
0.040	-0.064	0.221	0.571	0.985	1.461	1.980	2.516	3.068	3.631	4.175	4.666	5.073	5.384
0.045	-0.101	0.211	0.606	1.084	1.565	2.065	2.583	3.120	3.664				
0.050	-0.138	0.149	0.541	1.038	1.568	2.091	2.604	3.125	3.649				
0.055	-0.170	0.099	0.469	0.941	1.476	2.030	2.570	3.091	3.603				
0.060	-0.198	0.059	0.409	0.854	1.376	1.925	2.489	3.032	3.540				
0.070	-0.230	-0.011	0.311	0.736	1.242	1.761	2.329	2.895	3.431				
0.080	-0.242	-0.044	0.260	0.670	1.169	1.685	2.239	2.799	3.354				
0.090	-0.240	-0.055	0.241	0.649	1.140	1.655	2.202	2.758	3.316				
0.100	-0.240	-0.050	0.243	0.639	1.128	1.652	2.196	2.749	3.305				
0.120	-0.246	-0.045	0.258	0.661	1.145	1.672	2.210	2.754	3.292				
0.150	-0.286	-0.078	0.229	0.634	1.112	1.621	2.135	2.646	3.141				
0.200	-0.350	-0.196	0.054	0.400	0.818	1.280	1.758	2.236	2.700				
0.250	-0.387	-0.281	-0.090	0.184	0.539	0.957	1.413	1.881	2.340				
0.300	-0.409	-0.332	-0.182	0.041	0.347	0.729	1.163	1.620	2.077				
0.400	-0.431	-0.384	-0.280	-0.118	0.123	0.446	0.839	1.275	1.724				
0.500	-0.442	-0.409	-0.329	-0.200	0.000	0.282	0.641	1.055	1.493				
0.600	-0.449	-0.424	-0.357	-0.249	-0.074	0.179	0.511	0.905	1.333				
0.800	-0.456	-0.439	-0.389	-0.305	-0.164	0.049	0.341	0.704	1.115				
1.000	-0.460	-0.447	-0.405	-0.335	-0.213	-0.026	0.238	0.577	0.972				
1.200	-0.462	-0.452	-0.416	-0.354	-0.245	-0.076	0.168	0.489	0.870				
1.500	-0.464	-0.456	-0.426	-0.374	-0.284	-0.129	0.092	0.392	0.753				
2.000	-0.468	-0.461	-0.436	-0.393	-0.313	-0.182	0.017	0.291	0.628				
2.500	-0.469	-0.464	-0.442	-0.404	-0.334	-0.214	-0.028	0.228	0.553				
3.000	-0.470	-0.466	-0.447	-0.413	-0.349	-0.240	-0.068	0.171	0.492				
4.000	-0.471	-0.468	-0.452	-0.423	-0.366	-0.269	-0.115	0.105	0.427				
5.000	-0.473	-0.469	-0.455	-0.430	-0.378	-0.290	-0.149	0.064	0.367				
6.000	-0.474	-0.472	-0.459	-0.436	-0.388	-0.306	-0.177	0.033	0.322				
8.000	-0.476	-0.475	-0.464	-0.444	-0.401	-0.330	-0.211	-0.012	0.256				
10.000	-0.478	-0.476	-0.467	-0.450	-0.411	-0.349	-0.227	-0.050	0.208				
15.000	-0.484	-0.483	-0.476	-0.460	-0.428	-0.376	-0.272	-0.112	0.115				
20.000	-0.489	-0.487	-0.480	-0.470	-0.440	-0.392	-0.303	-0.159	0.047				
30.000	-0.498	-0.498	-0.494	-0.485	-0.459	-0.419	-0.345	-0.229	-0.055				
40.000	-0.508	-0.508	-0.505	-0.497	-0.476	-0.441	-0.380	-0.284	-0.132				
60.000	-0.526	-0.525	-0.522	-0.519	-0.504	-0.478	-0.438	-0.371	-0.249				
80.000	-0.544	-0.547	-0.545	-0.538	-0.527	-0.512	-0.487	-0.441	-0.335				
100.000	-0.563	-0.562	-0.561	-0.560	-0.551	-0.543	-0.532	-0.502	-0.403				

TABLE 11

ANDERS-GREVESSE ABUNDANCES FOR $X = 0.35$ AND $Z = 0.00$

	Log R												
T6	-5.0	-4.5	-4.0	-3.5	-3.0	-2.5	-2.0	-1.5	-1.0	-0.5	0.0	0.5	1.0
0.006	-1.745	-1.969	-2.104	-2.148	-2.132	-2.014	-1.902	-1.679	-1.474	-1.251	-1.021	-0.747	-0.443
0.007	-0.978	-1.058	-1.110	-1.136	-1.125	-1.052	-0.936	-0.785	-0.613	-0.434	-0.245	-0.030	0.196
0.008	-0.596	-0.478	-0.380	-0.304	-0.240	-0.162	-0.077	0.024	0.150	0.285	0.451	0.617	0.807
0.009	-0.535	-0.269	-0.018	0.219	0.401	0.533	0.634	0.725	0.821	0.922	1.035	1.157	1.309
0.010	-0.554	-0.270	0.057	0.425	0.744	0.992	1.152	1.267	1.360	1.452	1.535	1.644	1.773
0.011	-0.578	-0.317	0.022	0.438	0.863	1.219	1.464	1.655	1.764	1.849	1.939	2.034	2.144
0.012	-0.573	-0.344	-0.025	0.386	0.845	1.279	1.642	1.888	2.058	2.175	2.275	2.371	2.477
0.014	-0.473	-0.300	-0.044	0.294	0.728	1.200	1.693	2.089	2.397	2.614	2.768	2.890	3.006
0.016	-0.464	-0.246	0.025	0.348	0.724	1.168	1.644	2.105	2.534	2.856	3.091	3.264	3.405
0.018	-0.476	-0.275	0.012	0.387	0.805	1.215	1.641	2.111	2.583	2.994	3.310	3.540	3.718
0.020	-0.479	-0.301	-0.016	0.376	0.828	1.293	1.723	2.162	2.628	3.078	3.462	3.748	3.966
0.025	-0.452	-0.293	-0.019	0.370	0.838	1.357	1.871	2.370	2.843	3.311	3.740	4.112	4.409
0.030	-0.375	-0.223	0.047	0.434	0.918	1.429	1.963	2.498	3.033	3.541	3.992	4.385	4.706
0.035	-0.204	-0.042	0.214	0.563	1.028	1.534	2.064	2.604	3.158	3.697	4.184	4.594	4.929
0.040	-0.164	0.135	0.456	0.799	1.202	1.663	2.171	2.701	3.250	3.795	4.299	4.726	5.066
0.045	-0.213	0.134	0.532	0.980	1.400	1.819	2.280	2.786	3.316				
0.050	-0.257	0.038	0.439	0.945	1.476	1.935	2.378	2.853	3.358				
0.055	-0.291	-0.028	0.342	0.820	1.383	1.925	2.424	2.896	3.380				
0.060	-0.318	-0.080	0.264	0.712	1.244	1.818	2.389	2.899	3.383				
0.070	-0.347	-0.142	0.170	0.586	1.091	1.631	2.223	2.807	3.338				
0.080	-0.356	-0.174	0.119	0.525	1.015	1.543	2.115	2.701	3.270				
0.090	-0.346	-0.181	0.104	0.510	0.991	1.514	2.075	2.650	3.230				
0.100	-0.333	-0.171	0.111	0.514	0.990	1.518	2.074	2.641	3.222				
0.120	-0.311	-0.128	0.164	0.563	1.044	1.573	2.121	2.687	3.253				
0.150	-0.325	-0.198	0.118	0.624	1.112	1.631	2.162	2.704	3.231				
0.200	-0.393	-0.196	0.101	0.496	0.955	1.434	1.928	2.420	2.894				
0.250	-0.445	-0.311	-0.071	0.273	0.680	1.126	1.598	2.075	2.538				
0.300	-0.477	-0.374	-0.181	0.103	0.463	0.878	1.335	1.803	2.264				
0.400	-0.512	-0.450	-0.312	-0.097	0.189	0.553	0.978	1.431	1.887				
0.500	-0.529	-0.480	-0.375	-0.212	0.032	0.356	0.749	1.187	1.637				
0.600	-0.539	-0.502	-0.416	-0.279	-0.066	0.225	0.592	1.012	1.454				
0.800	-0.549	-0.525	-0.461	-0.356	-0.184	0.063	0.389	0.778	1.203				
1.000	-0.555	-0.537	-0.485	-0.398	-0.252	-0.036	0.257	0.620	1.029				
1.200	-0.558	-0.544	-0.499	-0.425	-0.297	-0.103	0.167	0.509	0.906				
1.500	-0.561	-0.550	-0.514	-0.451	-0.344	-0.172	0.072	0.391	0.771				
2.000	-0.567	-0.557	-0.527	-0.477	-0.388	-0.241	-0.025	0.268	0.624				
2.500	-0.568	-0.561	-0.535	-0.492	-0.412	-0.280	-0.080	0.195	0.537				
3.000	-0.569	-0.563	-0.541	-0.504	-0.433	-0.313	-0.129	0.128	0.459				
4.000	-0.570	-0.566	-0.548	-0.516	-0.454	-0.348	-0.182	0.056	0.374				
5.000	-0.572	-0.570	-0.554	-0.524	-0.468	-0.372	-0.214	0.006	0.306				
6.000	-0.573	-0.571	-0.557	-0.531	-0.480	-0.391	-0.244	-0.035	0.254				
8.000	-0.575	-0.573	-0.561	-0.540	-0.495	-0.414	-0.288	-0.089	0.189				
10.000	-0.577	-0.575	-0.565	-0.546	-0.505	-0.435	-0.311	-0.128	0.141				
15.000	-0.583	-0.581	-0.572	-0.558	-0.523	-0.466	-0.361	-0.190	0.046				
20.000	-0.588	-0.586	-0.579	-0.567	-0.539	-0.486	-0.391	-0.237	-0.023				
30.000	-0.597	-0.596	-0.590	-0.581	-0.555	-0.514	-0.431	-0.306	-0.125				
40.000	-0.607	-0.605	-0.601	-0.594	-0.572	-0.534	-0.466	-0.360	-0.202				
60.000	-0.625	-0.624	-0.621	-0.617	-0.599	-0.570	-0.522	-0.445	-0.319				
80.000	-0.644	-0.644	-0.642	-0.637	-0.625	-0.602	-0.569	-0.513	-0.407				
100.000	-0.662	-0.660	-0.658	-0.657	-0.647	-0.633	-0.611	-0.572	-0.477				

TABLE 12

ANDERS-GREVESSE ABUNDANCES FOR $X = 0.00$ AND $Z = 0.000$

	Log R								
T6	-5.0	-4.5	-4.0	-3.5	-3.0	-2.5	-2.0	-1.5	-1.0
0.006	-6.225	-6.153	-6.074	-5.988	-5.886	-5.774	-5.663	-5.573	-5.478
0.007	-5.330	-5.534	-5.617	-5.582	-5.497	-5.406	-5.305	-5.188	-5.062
0.008	-4.014	-4.348	-4.635	-4.876	-5.018	-5.020	-4.939	-4.838	-4.727
0.009	-2.962	-3.239	-3.523	-3.813	-4.071	-4.343	-4.438	-4.421	-4.342
0.010	-2.264	-2.493	-2.712	-2.919	-3.107	-3.375	-3.532	-3.610	-3.607
0.011	-1.717	-1.907	-2.077	-2.227	-2.337	-2.441	-2.491	-2.509	-2.506
0.012	-1.301	-1.428	-1.539	-1.633	-1.703	-1.747	-1.767	-1.771	-1.756
0.014	-0.900	-0.827	-0.767	-0.722	-0.694	-0.683	-0.665	-0.651	-0.634
0.016	-0.866	-0.696	-0.501	-0.283	-0.110	0.008	0.086	0.139	0.179
0.018	-0.883	-0.733	-0.508	-0.207	0.108	0.372	0.563	0.676	0.751
0.020	-0.899	-0.774	-0.559	-0.255	0.117	0.495	0.809	1.026	1.167
0.025	-0.907	-0.820	-0.644	-0.379	-0.014	0.429	0.896	1.288	1.633
0.030	-0.713	-0.658	-0.523	-0.306	0.003	0.391	0.857	1.298	1.762
0.035	-0.372	-0.258	-0.109	0.074	0.312	0.594	0.953	1.348	1.826
0.040	-0.310	-0.002	0.281	0.539	0.767	0.994	1.227	1.535	1.952
0.045	-0.366	-0.012	0.379	0.806	1.148	1.404	1.613	1.840	2.164
0.050	-0.411	-0.143	0.254	0.780	1.283	1.671	1.947	2.171	2.433
0.055	-0.445	-0.221	0.138	0.633	1.204	1.733	2.141	2.436	2.698
0.060	-0.471	-0.257	0.073	0.520	1.057	1.647	2.179	2.589	2.905
0.070	-0.496	-0.313	-0.019	0.384	0.886	1.433	2.038	2.612	3.084
0.080	-0.500	-0.338	-0.061	0.329	0.813	1.336	1.918	2.514	3.074
0.090	-0.488	-0.340	-0.076	0.304	0.795	1.313	1.879	2.463	3.047
0.100	-0.469	-0.316	-0.062	0.296	0.804	1.329	1.890	2.453	3.042
0.120	-0.431	-0.276	-0.004	0.384	0.873	1.395	1.949	2.520	3.096
0.150	-0.422	-0.218	0.086	0.488	0.983	1.509	2.050	2.608	3.155
0.200	-0.481	-0.268	0.047	0.462	0.937	1.435	1.940	2.442	2.924
0.250	-0.541	-0.366	-0.098	0.262	0.693	1.154	1.635	2.117	2.585
0.300	-0.581	-0.446	-0.224	0.085	0.469	0.905	1.372	1.846	2.311
0.400	-0.625	-0.539	-0.379	-0.146	0.172	0.562	1.002	1.464	1.926
0.500	-0.647	-0.586	-0.462	-0.274	-0.004	0.350	0.764	1.213	1.664
0.600	-0.659	-0.614	-0.512	-0.354	-0.117	0.202	0.591	1.024	1.473
0.800	-0.673	-0.643	-0.567	-0.445	-0.253	0.020	0.368	0.774	1.209
1.000	-0.679	-0.657	-0.596	-0.496	-0.333	-0.095	0.219	0.599	1.019
1.200	-0.693	-0.669	-0.615	-0.529	-0.386	-0.173	0.116	0.475	0.883
1.500	-0.688	-0.675	-0.632	-0.561	-0.441	-0.253	0.008	0.343	0.736
2.000	-0.692	-0.682	-0.649	-0.593	-0.493	-0.335	-0.104	0.203	0.575
2.500	-0.694	-0.687	-0.659	-0.610	-0.522	-0.379	-0.167	0.124	0.481
3.000	-0.696	-0.690	-0.666	-0.624	-0.547	-0.418	-0.223	0.050	0.391
4.000	-0.698	-0.694	-0.674	-0.639	-0.572	-0.458	-0.281	-0.028	0.289
5.000	-0.700	-0.699	-0.681	-0.648	-0.588	-0.484	-0.319	-0.083	0.214
6.000	-0.701	-0.699	-0.683	-0.656	-0.602	-0.506	-0.353	-0.133	0.155
8.000	-0.704	-0.702	-0.689	-0.665	-0.618	-0.532	-0.394	-0.196	0.089
10.000	-0.706	-0.705	-0.693	-0.672	-0.630	-0.550	-0.426	-0.238	0.043
15.000	-0.711	-0.711	-0.702	-0.685	-0.648	-0.585	-0.480	-0.300	-0.052
20.000	-0.716	-0.716	-0.708	-0.692	-0.662	-0.608	-0.509	-0.344	-0.120
30.000	-0.726	-0.726	-0.720	-0.708	-0.685	-0.639	-0.547	-0.413	-0.221
40.000	-0.736	-0.736	-0.731	-0.720	-0.703	-0.658	-0.581	-0.465	-0.297
60.000	-0.754	-0.753	-0.749	-0.744	-0.729	-0.691	-0.634	-0.546	-0.412
80.000	-0.772	-0.770	-0.768	-0.766	-0.749	-0.722	-0.679	-0.611	-0.501
100.000	-0.791	-0.789	-0.788	-0.786	-0.771	-0.751	-0.720	-0.668	-0.574

TABLE 13

ANDERS-GREVESSE ABUNDANCES FOR $X = 0.70$ AND $Z = 0.0001$

	Log R												
T6	-5.0	-4.5	-4.0	-3.5	-3.0	-2.5	-2.0	-1.5	-1.0	-0.5	0.0	0.5	1.0
0.006	-1.587	-1.738	-1.824	-1.845	-1.813	-1.627	-1.469	-1.261	-1.090	-0.865	-0.635	-0.394	-0.133
0.007	-0.722	-0.794	-0.829	-0.825	-0.767	-0.668	-0.544	-0.379	-0.202	-0.026	0.171	0.384	0.608
0.008	-0.222	-0.119	-0.032	0.038	0.100	0.191	0.288	0.405	0.541	0.688	0.846	1.024	1.219
0.009	-0.093	0.193	0.435	0.634	0.787	0.895	0.989	1.086	1.183	1.292	1.414	1.560	1.726
0.010	-0.103	0.238	0.583	0.932	1.199	1.395	1.529	1.626	1.711	1.801	1.903	2.022	2.161
0.011	-0.140	0.199	0.578	0.997	1.393	1.685	1.888	2.029	2.121	2.206	2.298	2.394	2.524
0.012	-0.175	0.144	0.525	0.965	1.420	1.813	2.108	2.299	2.439	2.539	2.635	2.735	2.850
0.014	-0.198	0.056	0.400	0.833	1.320	1.810	2.244	2.588	2.840	3.014	3.141	3.261	3.379
0.016	-0.220	0.028	0.351	0.750	1.213	1.731	2.221	2.673	3.043	3.309	3.501	3.652	3.786
0.018	-0.239	-0.012	0.307	0.718	1.192	1.684	2.179	2.684	3.137	3.492	3.756	3.950	4.110
0.020	-0.246	-0.040	0.274	0.694	1.167	1.662	2.175	2.689	3.185	3.614	3.940	4.181	4.375
0.025	-0.220	-0.036	0.266	0.684	1.173	1.701	2.235	2.768	3.302	3.809	4.238	4.583	4.836
0.030	-0.159	0.024	0.327	0.749	1.250	1.775	2.320	2.872	3.441	3.972	4.442	4.833	5.138
0.035	-0.069	0.134	0.441	0.851	1.345	1.878	2.424	2.981	3.554	4.100	4.590	4.995	5.312
0.040	-0.054	0.230	0.579	0.990	1.465	1.984	2.519	3.071	3.633	4.176	4.667	5.073	5.384
0.045	-0.090	0.221	0.615	1.090	1.568	2.067	2.585	3.121	3.664				
0.050	-0.124	0.164	0.555	1.048	1.575	2.096	2.606	3.127	3.650				
0.055	-0.157	0.115	0.486	0.955	1.486	2.037	2.574	3.094	3.604				
0.060	-0.185	0.074	0.426	0.869	1.386	1.933	2.494	3.034	3.542				
0.070	-0.215	0.008	0.331	0.755	1.256	1.773	2.336	2.898	3.432				
0.080	-0.230	-0.029	0.276	0.684	1.180	1.695	2.246	2.803	3.356				
0.090	-0.226	-0.039	0.258	0.665	1.153	1.665	2.209	2.762	3.318				
0.100	-0.229	-0.035	0.258	0.653	1.141	1.662	2.203	2.753	3.307				
0.120	-0.228	-0.026	0.275	0.677	1.159	1.681	2.215	2.756	3.294				
0.150	-0.259	-0.049	0.257	0.661	1.135	1.637	2.144	2.652	3.145				
0.200	-0.309	-0.147	0.110	0.461	0.876	1.321	1.781	2.248	2.705				
0.250	-0.354	-0.231	-0.024	0.267	0.622	1.020	1.449	1.898	2.347				
0.300	-0.381	-0.284	-0.113	0.132	0.443	0.805	1.209	1.644	2.088				
0.400	-0.420	-0.362	-0.236	-0.042	0.218	0.535	0.904	1.313	1.744				
0.500	-0.436	-0.398	-0.302	-0.150	0.078	0.371	0.717	1.107	1.522				
0.600	-0.444	-0.416	-0.339	-0.212	-0.009	0.261	0.592	0.968	1.374				
0.800	-0.452	-0.433	-0.375	-0.279	-0.114	0.126	0.435	0.790	1.175				
1.000	-0.457	-0.443	-0.395	-0.314	-0.168	0.055	0.349	0.683	1.042				
1.200	-0.457	-0.446	-0.405	-0.334	-0.203	0.005	0.284	0.597	0.938				
1.500	-0.458	-0.447	-0.412	-0.351	-0.241	-0.052	0.198	0.484	0.810				
2.000	-0.463	-0.454	-0.421	-0.366	-0.269	-0.117	0.091	0.352	0.666				
2.500	-0.466	-0.459	-0.431	-0.385	-0.300	-0.166	0.021	0.268	0.578				
3.000	-0.468	-0.462	-0.439	-0.400	-0.325	-0.207	-0.034	0.199	0.511				
4.000	-0.471	-0.467	-0.449	-0.417	-0.355	-0.252	-0.096	0.121	0.437				
5.000	-0.472	-0.469	-0.454	-0.427	-0.372	-0.280	-0.137	0.074	0.374				
6.000	-0.474	-0.472	-0.458	-0.434	-0.384	-0.300	-0.169	0.039	0.326				
8.000	-0.476	-0.475	-0.464	-0.443	-0.399	-0.327	-0.207	-0.009	0.259				
10.000	-0.478	-0.476	-0.466	-0.449	-0.411	-0.346	-0.224	-0.047	0.211				
15.000	-0.483	-0.483	-0.475	-0.459	-0.426	-0.374	-0.269	-0.110	0.117				
20.000	-0.489	-0.487	-0.480	-0.469	-0.439	-0.390	-0.301	-0.157	0.048				
30.000	-0.498	-0.498	-0.493	-0.484	-0.459	-0.418	-0.344	-0.228	-0.055				
40.000	-0.508	-0.508	-0.505	-0.497	-0.475	-0.440	-0.380	-0.284	-0.132				
60.000	-0.526	-0.525	-0.522	-0.519	-0.504	-0.478	-0.438	-0.371	-0.248				
80.000	-0.544	-0.547	-0.545	-0.538	-0.527	-0.512	-0.487	-0.441	-0.335				
100.000	-0.563	-0.562	-0.561	-0.560	-0.551	-0.543	-0.531	-0.502	-0.402				

TABLE 14

ANDERS-GREVESSE ABUNDANCES FOR $X = 0.35$ AND $Z = 0.0001$

	Log R												
T6	-5.0	-4.5	-4.0	-3.5	-3.0	-2.5	-2.0	-1.5	-1.0	-0.5	0.0	0.5	1.0
0.006	-1.744	-1.968	-2.102	-2.146	-2.130	-2.012	-1.900	-1.676	-1.470	-1.245	-1.013	-0.737	-0.429
0.007	-0.976	-1.056	-1.108	-1.134	-1.123	-1.049	-0.933	-0.781	-0.609	-0.428	-0.238	-0.022	0.205
0.008	-0.594	-0.476	-0.379	-0.303	-0.238	-0.160	-0.074	0.027	0.154	0.290	0.456	0.624	0.815
0.009	-0.531	-0.266	-0.015	0.221	0.403	0.536	0.636	0.728	0.824	0.926	1.039	1.164	1.317
0.010	-0.549	-0.264	0.062	0.429	0.748	0.996	1.156	1.271	1.364	1.456	1.540	1.651	1.780
0.011	-0.572	-0.309	0.030	0.446	0.870	1.224	1.471	1.659	1.768	1.855	1.945	2.040	2.151
0.012	-0.568	-0.337	-0.016	0.395	0.853	1.285	1.646	1.892	2.062	2.179	2.280	2.376	2.482
0.014	-0.464	-0.289	-0.032	0.306	0.739	1.209	1.699	2.094	2.402	2.618	2.772	2.894	3.009
0.016	-0.453	-0.234	0.038	0.361	0.735	1.177	1.651	2.111	2.538	2.859	3.094	3.267	3.407
0.018	-0.464	-0.260	0.027	0.399	0.814	1.222	1.648	2.116	2.587	2.997	3.312	3.542	3.719
0.020	-0.467	-0.285	0.001	0.390	0.837	1.300	1.729	2.167	2.633	3.081	3.464	3.749	3.967
0.025	-0.442	-0.281	-0.007	0.382	0.847	1.364	1.877	2.375	2.846	3.313	3.741	4.112	4.409
0.030	-0.364	-0.211	0.058	0.443	0.924	1.434	1.967	2.502	3.036	3.543	3.993	4.386	4.706
0.035	-0.194	-0.030	0.225	0.571	1.034	1.539	2.070	2.609	3.161	3.698	4.184	4.595	4.929
0.040	-0.154	0.144	0.464	0.806	1.207	1.668	2.175	2.705	3.253	3.797	4.300	4.727	5.066
0.045	-0.201	0.144	0.540	0.986	1.404	1.823	2.283	2.787	3.317				
0.050	-0.242	0.055	0.453	0.954	1.482	1.939	2.381	2.855	3.360				
0.055	-0.276	-0.010	0.360	0.834	1.392	1.931	2.428	2.898	3.382				
0.060	-0.304	-0.063	0.281	0.729	1.256	1.826	2.393	2.901	3.385				
0.070	-0.332	-0.121	0.191	0.606	1.106	1.643	2.230	2.810	3.340				
0.080	-0.343	-0.159	0.135	0.540	1.027	1.553	2.122	2.705	3.272				
0.090	-0.332	-0.163	0.123	0.527	1.004	1.524	2.081	2.654	3.232				
0.100	-0.322	-0.157	0.127	0.529	1.002	1.528	2.080	2.645	3.224				
0.120	-0.295	-0.111	0.180	0.579	1.054	1.581	2.126	2.690	3.255				
0.150	-0.299	-0.171	0.143	0.643	1.125	1.639	2.166	2.706	3.233				
0.200	-0.351	-0.146	0.152	0.544	0.993	1.459	1.941	2.431	2.904				
0.250	-0.410	-0.257	-0.004	0.346	0.745	1.170	1.621	2.086	2.543				
0.300	-0.448	-0.322	-0.110	0.189	0.544	0.937	1.367	1.819	2.271				
0.400	-0.501	-0.427	-0.267	-0.021	0.275	0.629	1.028	1.458	1.900				
0.500	-0.522	-0.468	-0.347	-0.162	0.106	0.435	0.812	1.226	1.658				
0.600	-0.533	-0.493	-0.396	-0.243	-0.004	0.302	0.663	1.064	1.485				
0.800	-0.545	-0.519	-0.447	-0.328	-0.133	0.139	0.478	0.856	1.254				
1.000	-0.552	-0.533	-0.474	-0.376	-0.205	0.047	0.368	0.721	1.092				
1.200	-0.552	-0.538	-0.488	-0.404	-0.252	-0.019	0.283	0.614	0.969				
1.500	-0.554	-0.541	-0.498	-0.426	-0.298	-0.091	0.178	0.482	0.825				
2.000	-0.561	-0.549	-0.512	-0.449	-0.341	-0.172	0.051	0.329	0.661				
2.500	-0.565	-0.555	-0.524	-0.471	-0.376	-0.230	-0.029	0.235	0.562				
3.000	-0.567	-0.560	-0.534	-0.490	-0.408	-0.279	-0.093	0.158	0.478				
4.000	-0.570	-0.565	-0.545	-0.510	-0.442	-0.331	-0.162	0.072	0.385				
5.000	-0.571	-0.569	-0.552	-0.521	-0.461	-0.362	-0.202	0.016	0.313				
6.000	-0.573	-0.570	-0.556	-0.529	-0.476	-0.384	-0.236	-0.028	0.259				
8.000	-0.575	-0.573	-0.561	-0.539	-0.492	-0.410	-0.283	-0.085	0.192				
10.000	-0.577	-0.575	-0.564	-0.545	-0.503	-0.432	-0.308	-0.124	0.144				
15.000	-0.583	-0.581	-0.572	-0.556	-0.521	-0.463	-0.358	-0.188	0.048				
20.000	-0.588	-0.586	-0.579	-0.566	-0.537	-0.483	-0.388	-0.235	-0.022				
30.000	-0.597	-0.596	-0.590	-0.581	-0.555	-0.513	-0.430	-0.306	-0.124				
40.000	-0.607	-0.605	-0.601	-0.594	-0.571	-0.534	-0.465	-0.360	-0.202				
60.000	-0.625	-0.624	-0.621	-0.617	-0.599	-0.570	-0.522	-0.445	-0.318				
80.000	-0.644	-0.644	-0.642	-0.637	-0.625	-0.602	-0.569	-0.513	-0.407				
100.000	-0.662	-0.660	-0.658	-0.657	-0.647	-0.632	-0.611	-0.572	-0.477				

TABLE 15

ANDERS-GREVESSE ABUNDANCES FOR $X = 0.00$ AND $Z = 0.0001$

	Log R								
T6	-5.0	-4.5	-4.0	-3.5	-3.0	-2.5	-2.0	-1.5	-1.0
0.006	-5.098	-5.135	-5.162	-5.180	-5.167	-5.136	-5.063	-4.964	-4.840
0.007	-4.870	-4.886	-4.892	-4.889	-4.873	-4.865	-4.780	-4.653	-4.486
0.008	-3.988	-4.299	-4.521	-4.655	-4.684	-4.648	-4.551	-4.409	-4.234
0.009	-2.953	-3.226	-3.502	-3.779	-4.013	-4.230	-4.238	-4.119	-3.938
0.010	-2.255	-2.482	-2.696	-2.898	-3.078	-3.339	-3.472	-3.501	-3.413
0.011	-1.707	-1.895	-2.061	-2.206	-2.310	-2.406	-2.444	-2.447	-2.423
0.012	-1.293	-1.417	-1.524	-1.614	-1.677	-1.714	-1.725	-1.713	-1.686
0.014	-0.890	-0.813	-0.749	-0.700	-0.667	-0.648	-0.623	-0.597	-0.564
0.016	-0.851	-0.678	-0.480	-0.259	-0.084	0.037	0.120	0.179	0.228
0.018	-0.865	-0.711	-0.484	-0.183	0.132	0.395	0.587	0.704	0.786
0.020	-0.882	-0.749	-0.530	-0.225	0.144	0.519	0.831	1.048	1.192
0.025	-0.889	-0.797	-0.616	-0.347	0.019	0.458	0.918	1.311	1.655
0.030	-0.697	-0.639	-0.500	-0.280	0.030	0.418	0.881	1.321	1.781
0.035	-0.359	-0.243	-0.093	0.090	0.329	0.614	0.973	1.369	1.844
0.040	-0.299	0.008	0.290	0.547	0.775	1.006	1.242	1.552	1.967
0.045	-0.352	0.000	0.388	0.813	1.153	1.410	1.620	1.850	2.175
0.050	-0.394	-0.123	0.272	0.791	1.290	1.677	1.953	2.178	2.440
0.055	-0.429	-0.189	0.171	0.649	1.214	1.739	2.145	2.440	2.702
0.060	-0.455	-0.238	0.093	0.538	1.070	1.654	2.184	2.593	2.908
0.070	-0.480	-0.291	0.004	0.406	0.903	1.446	2.045	2.615	3.087
0.080	-0.487	-0.321	-0.044	0.345	0.826	1.347	1.926	2.519	3.076
0.090	-0.473	-0.321	-0.056	0.322	0.809	1.324	1.886	2.467	3.049
0.100	-0.457	-0.306	-0.044	0.329	0.818	1.339	1.897	2.458	3.044
0.120	-0.414	-0.258	0.015	0.405	0.885	1.404	1.954	2.522	3.098
0.150	-0.394	-0.193	0.109	0.512	0.995	1.516	2.053	2.610	3.156
0.200	-0.435	-0.216	0.099	0.508	0.968	1.454	1.950	2.447	2.927
0.250	-0.503	-0.308	-0.029	0.333	0.752	1.192	1.654	2.126	2.589
0.300	-0.550	-0.389	-0.148	0.172	0.547	0.958	1.400	1.859	2.317
0.400	-0.614	-0.514	-0.333	-0.072	0.258	0.634	1.049	1.489	1.937
0.500	-0.640	-0.570	-0.434	-0.234	0.070	0.427	0.824	1.249	1.684
0.600	-0.655	-0.605	-0.492	-0.316	-0.055	0.279	0.660	1.073	1.502
0.800	-0.669	-0.636	-0.552	-0.415	-0.200	0.099	0.459	0.852	1.258
1.000	-0.676	-0.653	-0.586	-0.472	-0.284	-0.008	0.334	0.702	1.082
1.200	-0.678	-0.660	-0.603	-0.507	-0.339	-0.085	0.236	0.583	0.948
1.500	-0.680	-0.664	-0.615	-0.533	-0.390	-0.168	0.119	0.438	0.792
2.000	-0.686	-0.674	-0.633	-0.562	-0.442	-0.260	-0.022	0.268	0.615
2.500	-0.691	-0.682	-0.647	-0.588	-0.484	-0.325	-0.111	0.167	0.509
3.000	-0.694	-0.687	-0.659	-0.610	-0.522	-0.381	-0.183	0.082	0.412
4.000	-0.698	-0.693	-0.671	-0.632	-0.560	-0.439	-0.259	-0.009	0.301
5.000	-0.700	-0.698	-0.680	-0.644	-0.581	-0.474	-0.306	-0.072	0.222
6.000	-0.701	-0.698	-0.682	-0.653	-0.598	-0.499	-0.344	-0.125	0.161
8.000	-0.704	-0.702	-0.688	-0.664	-0.616	-0.528	-0.389	-0.191	0.093
10.000	-0.706	-0.704	-0.692	-0.671	-0.628	-0.547	-0.421	-0.234	0.046
15.000	-0.711	-0.710	-0.701	-0.683	-0.646	-0.582	-0.476	-0.296	-0.050
20.000	-0.716	-0.716	-0.708	-0.691	-0.660	-0.606	-0.506	-0.342	-0.119
30.000	-0.726	-0.726	-0.720	-0.707	-0.684	-0.638	-0.546	-0.412	-0.221
40.000	-0.736	-0.736	-0.731	-0.720	-0.702	-0.658	-0.580	-0.464	-0.297
60.000	-0.754	-0.753	-0.749	-0.744	-0.728	-0.691	-0.634	-0.546	-0.412
80.000	-0.772	-0.770	-0.768	-0.766	-0.749	-0.722	-0.679	-0.611	-0.501
100.000	-0.791	-0.789	-0.788	-0.786	-0.771	-0.751	-0.720	-0.668	-0.573

TABLE 16

ANDERS-GREVESSE ABUNDANCES FOR $X = 0.70$ AND $Z = 0.0003$

	Log R												
T6	-5.0	-4.5	-4.0	-3.5	-3.0	-2.5	-2.0	-1.5	-1.0	-0.5	0.0	0.5	1.0
0.006	-1.586	-1.737	-1.823	-1.844	-1.812	-1.626	-1.467	-1.269	-1.087	-0.861	-0.629	-0.386	-0.120
0.007	-0.721	-0.793	-0.828	-0.824	-0.766	-0.666	-0.542	-0.377	-0.206	-0.022	0.175	0.389	0.614
0.008	-0.221	-0.118	-0.031	0.039	0.101	0.192	0.289	0.406	0.541	0.691	0.850	1.028	1.224
0.009	-0.091	0.194	0.436	0.635	0.788	0.896	0.991	1.088	1.185	1.295	1.418	1.564	1.731
0.010	-0.101	0.240	0.585	0.935	1.201	1.397	1.531	1.628	1.713	1.804	1.906	2.026	2.166
0.011	-0.137	0.202	0.581	1.001	1.396	1.688	1.891	2.031	2.124	2.209	2.301	2.399	2.528
0.012	-0.172	0.149	0.529	0.970	1.424	1.815	2.111	2.302	2.442	2.543	2.638	2.739	2.854
0.014	-0.193	0.062	0.406	0.839	1.325	1.814	2.248	2.591	2.842	3.017	3.144	3.264	3.382
0.016	-0.213	0.035	0.358	0.756	1.218	1.736	2.226	2.677	3.046	3.312	3.503	3.654	3.788
0.018	-0.231	-0.003	0.316	0.725	1.197	1.688	2.183	2.688	3.139	3.494	3.758	3.951	4.111
0.020	-0.239	-0.031	0.282	0.700	1.172	1.667	2.178	2.692	3.187	3.615	3.941	4.182	4.376
0.025	-0.214	-0.028	0.274	0.691	1.178	1.705	2.238	2.772	3.304	3.810	4.239	4.583	4.836
0.030	-0.151	0.033	0.335	0.756	1.254	1.779	2.323	2.875	3.444	3.973	4.443	4.833	5.138
0.035	-0.061	0.143	0.449	0.856	1.349	1.882	2.428	2.984	3.556	4.102	4.591	4.996	5.312
0.040	-0.047	0.237	0.585	0.996	1.469	1.987	2.522	3.074	3.635	4.177	4.667	5.073	5.384
0.045	-0.082	0.230	0.623	1.096	1.573	2.071	2.588	3.123	3.666				
0.050	-0.116	0.174	0.564	1.056	1.581	2.101	2.610	3.130	3.652				
0.055	-0.148	0.126	0.497	0.966	1.495	2.043	2.578	3.097	3.606				
0.060	-0.175	0.082	0.434	0.881	1.396	1.941	2.500	3.038	3.544				
0.070	-0.205	0.020	0.344	0.768	1.268	1.785	2.345	2.904	3.435				
0.080	-0.221	-0.018	0.288	0.696	1.191	1.706	2.255	2.809	3.359				
0.090	-0.216	-0.027	0.270	0.676	1.163	1.674	2.216	2.768	3.321				
0.100	-0.219	-0.023	0.272	0.666	1.154	1.672	2.211	2.759	3.310				
0.120	-0.215	-0.011	0.290	0.691	1.172	1.691	2.221	2.761	3.296				
0.150	-0.234	-0.023	0.284	0.687	1.160	1.656	2.156	2.659	3.149				
0.200	-0.273	-0.103	0.161	0.519	0.936	1.373	1.817	2.267	2.714				
0.250	-0.323	-0.185	0.037	0.345	0.708	1.097	1.502	1.928	2.362				
0.300	-0.359	-0.244	-0.053	0.217	0.541	0.898	1.276	1.683	2.107				
0.400	-0.410	-0.344	-0.197	0.032	0.320	0.641	0.989	1.369	1.775				
0.500	-0.430	-0.388	-0.277	-0.098	0.165	0.477	0.814	1.178	1.565				
0.600	-0.439	-0.409	-0.320	-0.173	0.064	0.361	0.691	1.047	1.426				
0.800	-0.448	-0.427	-0.361	-0.250	-0.059	0.211	0.534	0.882	1.247				
1.000	-0.453	-0.438	-0.383	-0.289	-0.118	0.136	0.455	0.794	1.132				
1.200	-0.453	-0.440	-0.393	-0.311	-0.155	0.090	0.401	0.722	1.034				
1.500	-0.451	-0.439	-0.397	-0.325	-0.193	0.034	0.319	0.608	0.899				
2.000	-0.457	-0.446	-0.405	-0.337	-0.217	-0.034	0.196	0.447	0.731				
2.500	-0.463	-0.454	-0.420	-0.361	-0.255	-0.098	0.099	0.335	0.624				
3.000	-0.466	-0.459	-0.431	-0.384	-0.292	-0.155	0.024	0.249	0.544				
4.000	-0.470	-0.466	-0.445	-0.409	-0.338	-0.224	-0.063	0.151	0.455				
5.000	-0.472	-0.468	-0.452	-0.422	-0.362	-0.263	-0.117	0.092	0.386				
6.000	-0.473	-0.471	-0.457	-0.431	-0.378	-0.289	-0.155	0.052	0.335				
8.000	-0.476	-0.474	-0.463	-0.441	-0.396	-0.321	-0.199	-0.001	0.265				
10.000	-0.478	-0.475	-0.465	-0.447	2.541	-0.342	-0.218	-0.041	0.215				
15.000	-0.483	-0.483	-0.474	-0.457	-0.423	-0.370	-0.264	-0.105	0.120				
20.000	-0.489	-0.486	-0.479	-0.468	-0.436	-0.387	-0.297	-0.154	0.050				
30.000	-0.498	-0.498	-0.493	-0.484	-0.458	-0.417	-0.342	-0.227	-0.054				
40.000	-0.508	-0.508	-0.505	-0.497	-0.475	-0.440	-0.379	-0.283	-0.131				
60.000	-0.526	-0.525	-0.522	-0.519	-0.504	-0.478	-0.438	-0.370	-0.248				
80.000	-0.544	-0.547	-0.545	-0.538	-0.527	-0.511	-0.487	-0.441	-0.334				
100.000	-0.563	-0.562	-0.561	-0.560	-0.551	-0.543	-0.531	-0.502	-0.402				

TABLE 17

ANDERS-GREVESSE ABUNDANCES FOR $X = 0.35$ AND $Z = 0.0003$

	Log R												
T6	-5.0	-4.5	-4.0	-3.5	-3.0	-2.5	-2.0	-1.5	-1.0	-0.5	0.0	0.5	1.0
0.006	-1.742	-1.966	-2.100	-2.144	-2.128	-2.010	-1.897	-1.673	-1.466	-1.240	-1.005	-0.726	-0.413
0.007	-0.975	-1.055	-1.107	-1.133	-1.121	-1.048	-0.931	-0.778	-0.605	-0.423	-0.231	-0.015	0.214
0.008	-0.592	-0.474	-0.377	-0.301	-0.236	-0.158	-0.072	0.030	0.157	0.295	0.461	0.630	0.822
0.009	-0.528	-0.264	-0.014	0.223	0.405	0.538	0.638	0.730	0.827	0.930	1.045	1.172	1.326
0.010	-0.546	-0.260	0.066	0.432	0.751	0.999	1.158	1.273	1.367	1.460	1.545	1.657	1.788
0.011	-0.568	-0.304	0.036	0.451	0.875	1.228	1.476	1.662	1.772	1.859	1.950	2.046	2.158
0.012	-0.563	-0.332	-0.010	0.402	0.859	1.290	1.650	1.896	2.066	2.184	2.285	2.381	2.489
0.014	-0.459	-0.282	-0.024	0.314	0.748	1.217	1.704	2.099	2.406	2.622	2.776	2.899	3.014
0.016	-0.445	-0.225	0.046	0.369	0.742	1.184	1.658	2.117	2.543	2.864	3.098	3.271	3.410
0.018	-0.455	-0.250	0.037	0.408	0.821	1.229	1.654	2.121	2.592	3.001	3.316	3.545	3.721
0.020	-0.460	-0.275	0.011	0.398	0.844	1.305	1.734	2.172	2.637	3.085	3.467	3.751	3.969
0.025	-0.435	-0.273	0.003	0.391	0.854	1.369	1.882	2.379	2.850	3.316	3.743	4.114	4.410
0.030	-0.356	-0.201	0.068	0.452	0.931	1.439	1.972	2.506	3.039	3.545	3.995	4.387	4.707
0.035	-0.186	-0.021	0.234	0.579	1.040	1.543	2.074	2.613	3.165	3.700	4.185	4.596	4.930
0.040	-0.147	0.151	0.470	0.811	1.212	1.673	2.178	2.708	3.255	3.799	4.301	4.727	5.066
0.045	-0.192	0.153	0.548	0.992	1.408	1.827	2.286	2.790	3.319				
0.050	-0.233	0.065	0.463	0.962	1.488	1.943	2.385	2.858	3.362				
0.055	-0.267	0.001	0.372	0.845	1.401	1.936	2.432	2.901	3.384				
0.060	-0.293	-0.050	0.295	0.741	1.267	1.833	2.397	2.904	3.387				
0.070	-0.322	-0.108	0.205	0.620	1.118	1.654	2.237	2.814	3.342				
0.080	-0.333	-0.147	0.148	0.551	1.038	1.564	2.130	2.710	3.275				
0.090	-0.322	-0.151	0.136	0.539	1.014	1.533	2.088	2.659	3.235				
0.100	-0.311	-0.144	0.141	0.543	1.014	1.538	2.089	2.651	3.227				
0.120	-0.282	-0.097	0.194	0.593	1.064	1.589	2.131	2.694	3.257				
0.150	-0.274	-0.145	0.167	0.662	1.141	1.650	2.172	2.710	3.235				
0.200	-0.315	-0.103	0.199	0.591	1.036	1.492	1.962	2.442	2.909				
0.250	-0.378	-0.208	0.057	0.415	0.814	1.226	1.657	2.104	2.551				
0.300	-0.425	-0.280	-0.049	0.270	0.629	1.010	1.415	1.845	2.284				
0.400	-0.492	-0.408	-0.228	0.049	0.368	0.719	1.095	1.500	1.922				
0.500	-0.517	-0.457	-0.322	-0.111	0.187	0.529	0.894	1.282	1.690				
0.600	-0.528	-0.485	-0.378	-0.204	0.065	0.393	0.750	1.130	1.528				
0.800	-0.541	-0.513	-0.432	-0.299	-0.079	0.220	0.569	0.939	1.318				
1.000	-0.548	-0.528	-0.462	-0.350	-0.155	0.127	0.470	0.826	1.176				
1.200	-0.548	-0.532	-0.476	-0.380	-0.203	0.066	0.399	0.734	1.060				
1.500	-0.547	-0.532	-0.483	-0.399	-0.248	-0.004	0.299	0.602	0.910				
2.000	-0.556	-0.541	-0.495	-0.418	-0.286	-0.085	0.157	0.424	0.725				
2.500	-0.562	-0.551	-0.512	-0.446	-0.330	-0.159	0.051	0.303	0.608				
3.000	-0.565	-0.557	-0.526	-0.474	-0.374	-0.225	-0.033	0.209	0.512				
4.000	-0.569	-0.564	-0.541	-0.501	-0.424	-0.301	-0.127	0.103	0.405				
5.000	-0.571	-0.568	-0.550	-0.516	-0.451	-0.344	-0.180	0.036	0.326				
6.000	-0.572	-0.570	-0.554	-0.526	-0.469	-0.373	-0.221	-0.015	0.269				
8.000	-0.575	-0.572	-0.560	-0.537	-0.489	-0.404	-0.275	-0.077	0.198				
10.000	-0.577	-0.574	-0.563	-0.544	-0.501	-0.427	-0.301	-0.118	0.149				
15.000	-0.583	-0.580	-0.571	-0.554	-0.518	-0.459	-0.352	-0.182	0.052				
20.000	-0.588	-0.586	-0.578	-0.564	-0.535	-0.479	-0.384	-0.231	-0.019				
30.000	-0.597	-0.596	-0.590	-0.581	-0.554	-0.511	-0.428	-0.304	-0.123				
40.000	-0.607	-0.605	-0.601	-0.594	-0.571	-0.533	-0.464	-0.359	-0.201				
60.000	-0.625	-0.624	-0.621	-0.617	-0.599	-0.569	-0.521	-0.444	-0.318				
80.000	-0.644	-0.644	-0.642	-0.637	-0.625	-0.602	-0.568	-0.513	-0.406				
100.000	-0.662	-0.660	-0.658	-0.657	-0.646	-0.632	-0.611	-0.572	-0.477				

TABLE 18

ANDERS-GREVESSE ABUNDANCES FOR $X = 0.00$ AND $Z = 0.0003$

	Log R								
T6	-5.0	-4.5	-4.0	-3.5	-3.0	-2.5	-2.0	-1.5	-1.0
0.006	-4.776	-4.816	-4.846	-4.867	-4.855	-4.828	-4.752	-4.643	-4.505
0.007	-4.580	-4.579	-4.577	-4.574	-4.562	-4.563	-4.479	-4.342	-4.156
0.008	-3.950	-4.210	-4.372	-4.436	-4.426	-4.381	-4.279	-4.118	-3.917
0.009	-2.944	-3.214	-3.479	-3.739	-3.938	-4.090	-4.028	-3.853	-3.628
0.010	-2.250	-2.474	-2.685	-2.883	-3.056	-3.305	-3.407	-3.376	-3.212
0.011	-1.702	-1.888	-2.051	-2.192	-2.292	-2.382	-2.413	-2.405	-2.362
0.012	-1.287	-1.410	-1.514	-1.600	-1.660	-1.692	-1.697	-1.679	-1.646
0.014	-0.882	-0.803	-0.738	-0.685	-0.648	-0.624	-0.593	-0.561	-0.521
0.016	-0.841	-0.665	-0.466	-0.243	-0.064	0.060	0.147	0.212	0.268
0.018	-0.853	-0.697	-0.467	-0.164	0.151	0.416	0.608	0.731	0.820
0.020	-0.870	-0.733	-0.511	-0.204	0.165	0.539	0.850	1.070	1.219
0.025	-0.876	-0.781	-0.597	-0.325	0.042	0.480	0.938	1.332	1.677
0.030	-0.685	-0.625	-0.484	-0.262	0.050	0.438	0.900	1.342	1.800
0.035	-0.351	-0.233	-0.082	0.102	0.342	0.629	0.991	1.389	1.864
0.040	-0.290	0.016	0.297	0.554	0.783	1.015	1.254	1.567	1.983
0.045	-0.342	0.009	0.396	0.819	1.159	1.416	1.628	1.860	2.187
0.050	-0.384	-0.110	0.284	0.799	1.296	1.682	1.959	2.185	2.448
0.055	-0.418	-0.175	0.185	0.662	1.223	1.744	2.150	2.445	2.707
0.060	-0.443	-0.224	0.108	0.552	1.081	1.661	2.188	2.597	2.912
0.070	-0.468	-0.277	0.020	0.421	0.916	1.458	2.053	2.620	3.090
0.080	-0.476	-0.307	-0.029	0.358	0.837	1.358	1.934	2.525	3.079
0.090	-0.462	-0.307	-0.041	0.335	0.820	1.334	1.894	2.473	3.053
0.100	-0.446	-0.292	-0.029	0.345	0.831	1.350	1.906	2.464	3.047
0.120	-0.401	-0.242	0.031	0.419	0.895	1.412	1.960	2.527	3.100
0.150	-0.367	-0.167	0.133	0.532	1.009	1.526	2.059	2.613	3.158
0.200	-0.396	-0.170	0.146	0.551	1.003	1.480	1.967	2.456	2.931
0.250	-0.470	-0.257	0.032	0.399	0.813	1.241	1.684	2.142	2.597
0.300	-0.527	-0.345	-0.086	0.249	0.626	1.024	1.442	1.882	2.328
0.400	-0.605	-0.495	-0.295	-0.005	0.346	0.719	1.110	1.526	1.957
0.500	-0.634	-0.557	-0.410	-0.193	0.147	0.516	0.899	1.301	1.713
0.600	-0.650	-0.598	-0.474	-0.278	0.012	0.366	0.742	1.135	1.541
0.800	-0.665	-0.630	-0.537	-0.386	-0.146	0.177	0.547	0.931	1.319
1.000	-0.673	-0.648	-0.572	-0.446	-0.233	0.072	0.434	0.806	1.165
1.200	-0.673	-0.653	-0.590	-0.482	-0.290	0.001	0.352	0.704	1.040
1.500	-0.673	-0.655	-0.598	-0.505	-0.339	-0.078	0.242	0.561	0.880
2.000	-0.681	-0.666	-0.616	-0.530	-0.384	-0.168	0.089	0.368	0.682
2.500	-0.688	-0.677	-0.635	-0.562	-0.435	-0.249	-0.025	0.240	0.557
3.000	-0.692	-0.684	-0.651	-0.594	-0.487	-0.324	-0.118	0.137	0.450
4.000	-0.697	-0.692	-0.667	-0.624	-0.542	-0.408	-0.221	0.024	0.324
5.000	-0.699	-0.697	-0.678	-0.639	-0.570	-0.455	-0.282	-0.050	0.237
6.000	-0.701	-0.698	-0.681	-0.650	-0.591	-0.487	-0.328	-0.110	0.172
8.000	-0.704	-0.701	-0.688	-0.662	-0.612	-0.522	-0.380	-0.181	0.100
10.000	-0.705	-0.704	-0.692	-0.669	-0.625	-0.542	-0.414	-0.226	0.053
15.000	-0.711	-0.710	-0.700	-0.681	-0.642	-0.576	-0.469	-0.290	-0.045
20.000	-0.716	-0.716	-0.707	-0.690	-0.657	-0.601	-0.501	-0.338	-0.116
30.000	-0.726	-0.726	-0.720	-0.707	-0.683	-0.636	-0.544	-0.410	-0.219
40.000	-0.736	-0.736	-0.731	-0.720	-0.702	-0.657	-0.579	-0.463	-0.296
60.000	-0.754	-0.753	-0.749	-0.744	-0.728	-0.690	-0.634	-0.545	-0.412
80.000	-0.772	-0.770	-0.768	-0.766	-0.749	-0.722	-0.679	-0.611	-0.500
100.000	-0.791	-0.789	-0.788	-0.786	-0.771	-0.751	-0.719	-0.668	-0.573

TABLE 19

ANDERS-GREVESSE ABUNDANCES FOR $X = 0.70$ AND $Z = 0.001$

	Log R												
T6	-5.0	-4.5	-4.0	-3.5	-3.0	-2.5	-2.0	-1.5	-1.0	-0.5	0.0	0.5	1.0
0.006	-1.584	-1.735	-1.821	-1.841	-1.808	-1.622	-1.463	-1.254	-1.079	-0.850	-0.614	-0.365	-0.089
0.007	-0.719	-0.792	-0.826	-0.822	-0.764	-0.664	-0.539	-0.373	-0.193	-0.014	0.185	0.401	0.629
0.008	-0.219	-0.116	-0.029	0.041	0.103	0.195	0.292	0.410	0.548	0.697	0.859	1.039	1.236
0.009	-0.088	0.197	0.439	0.637	0.790	0.899	0.994	1.091	1.190	1.301	1.426	1.575	1.744
0.010	-0.096	0.245	0.590	0.939	1.205	1.400	1.535	1.632	1.718	1.811	1.916	2.038	2.178
0.011	-0.131	0.209	0.589	1.009	1.402	1.693	1.895	2.036	2.130	2.216	2.310	2.409	2.541
0.012	-0.165	0.156	0.538	0.979	1.431	1.821	2.116	2.308	2.448	2.550	2.646	2.749	2.865
0.014	-0.184	0.074	0.418	0.850	1.335	1.822	2.254	2.597	2.848	3.023	3.151	3.272	3.390
0.016	-0.201	0.048	0.371	0.769	1.229	1.746	2.235	2.685	3.053	3.318	3.508	3.659	3.793
0.018	-0.217	0.013	0.331	0.738	1.208	1.698	2.192	2.695	3.146	3.500	3.763	3.955	4.115
0.020	-0.226	-0.015	0.298	0.713	1.182	1.676	2.186	2.698	3.193	3.620	3.945	4.185	4.378
0.025	-0.202	-0.013	0.289	0.705	1.189	1.713	2.246	2.779	3.310	3.814	4.242	4.585	4.838
0.030	-0.137	0.048	0.350	0.768	1.265	1.788	2.331	2.882	3.449	3.976	4.446	4.835	5.139
0.035	-0.048	0.158	0.464	0.868	1.358	1.891	2.436	2.992	3.562	4.105	4.593	4.997	5.313
0.040	-0.034	0.249	0.596	1.008	1.479	1.996	2.529	3.079	3.639	4.180	4.669	5.074	5.384
0.045	-0.066	0.247	0.638	1.109	1.583	2.079	2.595	3.128	3.670				
0.050	-0.099	0.192	0.583	1.072	1.594	2.112	2.619	3.136	3.656				
0.055	-0.131	0.146	0.519	0.987	1.514	2.058	2.589	3.104	3.611				
0.060	-0.157	0.107	0.461	0.904	1.417	1.960	2.514	3.048	3.551				
0.070	-0.186	0.042	0.368	0.793	1.292	1.809	2.364	2.918	3.444				
0.080	-0.202	0.004	0.311	0.720	1.213	1.728	2.274	2.825	3.369				
0.090	-0.198	-0.004	0.295	0.700	1.184	1.695	2.235	2.783	3.331				
0.100	-0.198	0.004	0.301	0.693	1.179	1.694	2.230	2.774	3.319				
0.120	-0.188	0.018	0.321	0.720	1.200	1.712	2.237	2.772	3.303				
0.150	-0.184	0.028	0.334	0.736	1.208	1.698	2.188	2.678	3.157				
0.200	-0.204	-0.021	0.254	0.621	1.043	1.475	1.901	2.323	2.742				
0.250	-0.264	-0.100	0.148	0.479	0.856	1.243	1.625	2.011	2.406				
0.300	-0.317	-0.172	0.055	0.365	0.714	1.073	1.424	1.785	2.164				
0.400	-0.391	-0.308	-0.121	0.168	0.507	0.843	1.165	1.497	1.854				
0.500	-0.420	-0.369	-0.228	0.003	0.331	0.680	1.004	1.328	1.666				
0.600	-0.429	-0.394	-0.283	-0.095	0.206	0.553	0.887	1.211	1.544				
0.800	-0.439	-0.414	-0.331	-0.192	0.054	0.379	0.722	1.055	1.387				
1.000	-0.446	-0.425	-0.355	-0.237	-0.021	0.287	0.637	0.979	1.300				
1.200	-0.444	-0.427	-0.367	-0.262	-0.061	0.239	0.591	0.928	1.225				
1.500	-0.440	-0.422	-0.367	-0.272	-0.099	0.189	0.528	0.836	1.096				
2.000	-0.447	-0.429	-0.371	-0.275	-0.111	0.130	0.406	0.659	0.897				
2.500	-0.457	-0.444	-0.394	-0.306	-0.155	0.056	0.282	0.505	0.752				
3.000	-0.462	-0.453	-0.413	-0.344	-0.211	-0.028	0.172	0.384	0.643				
4.000	-0.468	-0.462	-0.435	-0.387	-0.290	-0.145	0.031	0.237	0.515				
5.000	-0.471	-0.466	-0.446	-0.409	-0.333	-0.213	-0.053	0.150	0.426				
6.000	-0.473	-0.470	-0.453	-0.422	-0.358	-0.255	-0.111	0.092	0.363				
8.000	-0.475	-0.474	-0.460	-0.436	-0.385	-0.302	-0.174	0.023	0.284				
10.000	-0.477	-0.474	-0.463	-0.443	-0.398	-0.329	-0.200	-0.021	0.232				
15.000	-0.482	-0.481	-0.471	-0.453	-0.415	-0.358	-0.249	-0.090	0.131				
20.000	-0.488	-0.486	-0.478	-0.464	-0.429	-0.376	-0.285	-0.144	0.057				
30.000	-0.498	-0.498	-0.493	-0.482	-0.454	-0.411	-0.336	-0.222	-0.050				
40.000	-0.508	-0.508	-0.504	-0.496	-0.473	-0.437	-0.376	-0.280	-0.129				
60.000	-0.526	-0.525	-0.522	-0.518	-0.503	-0.477	-0.436	-0.369	-0.248				
80.000	-0.544	-0.547	-0.545	-0.538	-0.527	-0.511	-0.486	-0.439	-0.333				
100.000	-0.563	-0.562	-0.561	-0.560	-0.551	-0.542	-0.531	-0.501	-0.401				

TABLE 20

ANDERS-GREVESSE ABUNDANCES FOR $X = 0.35$ AND $Z = 0.001$

	Log R												
T6	-5.0	-4.5	-4.0	-3.5	-3.0	-2.5	-2.0	-1.5	-1.0	-0.5	0.0	0.5	1.0
0.006	-1.740	-1.963	-2.097	-2.140	-2.123	-2.005	-1.891	-1.666	-1.456	-1.227	-0.986	-0.701	-0.377
0.007	-0.973	-1.053	-1.105	-1.130	-1.118	-1.044	-0.926	-0.772	-0.598	-0.413	-0.218	0.001	0.234
0.008	-0.588	-0.471	-0.375	-0.299	-0.234	-0.155	-0.068	0.036	0.163	0.304	0.472	0.644	0.838
0.009	-0.523	-0.260	-0.010	0.226	0.408	0.541	0.641	0.735	0.833	0.938	1.056	1.188	1.346
0.010	-0.540	-0.253	0.073	0.438	0.757	1.003	1.163	1.279	1.373	1.467	1.556	1.671	1.804
0.011	-0.561	-0.294	0.047	0.462	0.884	1.236	1.485	1.669	1.780	1.869	1.962	2.060	2.174
0.012	-0.556	-0.322	0.002	0.415	0.871	1.300	1.658	1.904	2.074	2.194	2.297	2.395	2.504
0.014	-0.449	-0.269	-0.010	0.330	0.764	1.233	1.715	2.109	2.415	2.632	2.787	2.910	3.027
0.016	-0.432	-0.211	0.062	0.386	0.758	1.198	1.671	2.130	2.555	2.874	3.108	3.280	3.419
0.018	-0.439	-0.232	0.056	0.425	0.835	1.242	1.667	2.134	2.603	3.011	3.324	3.553	3.728
0.020	-0.445	-0.256	0.031	0.415	0.857	1.315	1.745	2.182	2.647	3.094	3.474	3.758	3.974
0.025	-0.421	-0.256	0.021	0.409	0.868	1.381	1.892	2.389	2.859	3.324	3.749	4.118	4.412
0.030	-0.340	-0.183	0.086	0.468	0.944	1.451	1.981	2.516	3.048	3.551	3.999	4.390	4.709
0.035	-0.173	-0.005	0.251	0.595	1.051	1.553	2.084	2.623	3.173	3.706	4.189	4.598	4.931
0.040	-0.132	0.164	0.482	0.823	1.223	1.683	2.188	2.715	3.261	3.803	4.303	4.729	5.068
0.045	-0.175	0.169	0.562	1.004	1.419	1.836	2.294	2.797	3.324				
0.050	-0.215	0.085	0.482	0.977	1.499	1.953	2.394	2.865	3.366				
0.055	-0.248	0.024	0.396	0.867	1.417	1.948	2.440	2.907	3.389				
0.060	-0.274	-0.027	0.319	0.765	1.289	1.849	2.409	2.913	3.392				
0.070	-0.301	-0.084	0.232	0.645	1.142	1.676	2.255	2.826	3.349				
0.080	-0.313	-0.123	0.174	0.576	1.061	1.586	2.148	2.724	3.283				
0.090	-0.303	-0.125	0.163	0.563	1.035	1.554	2.107	2.674	3.245				
0.100	-0.290	-0.116	0.170	0.570	1.038	1.559	2.107	2.666	3.236				
0.120	-0.256	-0.069	0.224	0.623	1.087	1.607	2.146	2.704	3.263				
0.150	-0.224	-0.093	0.216	0.702	1.175	1.676	2.191	2.721	3.240				
0.200	-0.245	-0.022	0.285	0.677	1.116	1.564	2.016	2.472	2.919				
0.250	-0.318	-0.120	0.165	0.537	0.938	1.341	1.745	2.159	2.579				
0.300	-0.383	-0.206	0.059	0.410	0.781	1.155	1.528	1.917	2.322				
0.400	-0.474	-0.373	-0.156	0.177	0.537	0.894	1.239	1.600	1.981				
0.500	-0.506	-0.438	-0.275	-0.017	0.338	0.710	1.058	1.407	1.770				
0.600	-0.518	-0.470	-0.341	-0.129	0.197	0.567	0.922	1.270	1.625				
0.800	-0.532	-0.500	-0.403	-0.241	0.028	0.376	0.740	1.093	1.442				
1.000	-0.540	-0.515	-0.435	-0.298	-0.060	0.270	0.640	0.999	1.332				
1.200	-0.539	-0.518	-0.449	-0.331	-0.110	0.210	0.582	0.934	1.241				
1.500	-0.535	-0.527	-0.463	-0.346	-0.154	0.149	0.505	0.826	1.099				
2.000	-0.547	-0.525	-0.461	-0.355	-0.178	0.081	0.369	0.635	0.888				
2.500	-0.556	-0.542	-0.487	-0.391	-0.227	0.000	0.238	0.474	0.735				
3.000	-0.561	-0.550	-0.508	-0.435	-0.292	-0.094	0.120	0.347	0.613				
4.000	-0.567	-0.560	-0.531	-0.479	-0.376	-0.220	-0.029	0.192	0.468				
5.000	-0.570	-0.566	-0.544	-0.503	-0.422	-0.292	-0.115	0.096	0.369				
6.000	-0.572	-0.569	-0.551	-0.517	-0.450	-0.337	-0.176	0.028	0.300				
8.000	-0.574	-0.572	-0.557	-0.532	-0.478	-0.385	-0.249	-0.050	0.220				
10.000	-0.576	-0.573	-0.561	-0.539	-0.492	-0.414	-0.282	-0.096	0.167				
15.000	-0.582	-0.579	-0.568	-0.549	-0.509	-0.446	-0.335	-0.165	0.064				
20.000	-0.587	-0.585	-0.576	-0.560	-0.527	-0.467	-0.370	-0.220	-0.012				
30.000	-0.597	-0.596	-0.590	-0.579	-0.550	-0.505	-0.422	-0.299	-0.119				
40.000	-0.607	-0.605	-0.601	-0.593	-0.569	-0.530	-0.461	-0.356	-0.198				
60.000	-0.625	-0.624	-0.621	-0.617	-0.599	-0.568	-0.520	-0.442	-0.316				
80.000	-0.644	-0.644	-0.642	-0.637	-0.625	-0.601	-0.567	-0.511	-0.405				
100.000	-0.662	-0.660	-0.658	-0.657	-0.646	-0.632	-0.610	-0.571	-0.475				

TABLE 21

ANDERS-GREVESSE ABUNDANCES FOR $X = 0.00$ AND $Z = 0.001$

	Log R								
T6	-5.0	-4.5	-4.0	-3.5	-3.0	-2.5	-2.0	-1.5	-1.0
0.006	-4.366	-4.409	-4.441	-4.463	-4.451	-4.423	-4.340	-4.220	-4.068
0.007	-4.189	-4.178	-4.169	-4.164	-4.152	-4.158	-4.071	-3.923	-3.720
0.008	-3.844	-4.005	-4.087	-4.091	-4.054	-4.000	-3.890	-3.710	-3.485
0.009	-2.924	-3.184	-3.421	-3.635	-3.759	-3.809	-3.676	-3.454	-3.193
0.010	-2.238	-2.458	-2.662	-2.850	-3.009	-3.222	-3.252	-3.122	-2.875
0.011	-1.691	-1.874	-2.032	-2.167	-2.259	-2.338	-2.355	-2.322	-2.239
0.012	-1.277	-1.396	-1.496	-1.576	-1.630	-1.655	-1.653	-1.624	-1.580
0.014	-0.869	-0.786	-0.716	-0.659	-0.615	-0.584	-0.547	-0.508	-0.460
0.016	-0.823	-0.643	-0.440	-0.213	-0.028	0.102	0.196	0.270	0.336
0.018	-0.831	-0.670	-0.436	-0.129	0.190	0.457	0.652	0.784	0.885
0.020	-0.849	-0.704	-0.476	-0.165	0.205	0.579	0.891	1.117	1.274
0.025	-0.853	-0.752	-0.562	-0.285	0.085	0.522	0.978	1.378	1.725
0.030	-0.663	-0.599	-0.454	-0.227	0.088	0.478	0.941	1.388	1.845
0.035	-0.335	-0.215	-0.061	0.125	0.367	0.658	1.026	1.433	1.908
0.040	-0.274	0.031	0.311	0.568	0.799	1.034	1.280	1.601	2.019
0.045	-0.321	0.027	0.411	0.832	1.170	1.429	1.644	1.884	2.213
0.050	-0.363	-0.086	0.306	0.815	1.308	1.693	1.970	2.200	2.467
0.055	-0.398	-0.158	0.203	0.685	1.240	1.756	2.160	2.456	2.720
0.060	-0.422	-0.198	0.135	0.578	1.103	1.677	2.199	2.606	2.922
0.070	-0.446	-0.250	0.049	0.449	0.942	1.481	2.070	2.631	3.098
0.080	-0.454	-0.280	-0.001	0.385	0.862	1.381	1.953	2.539	3.088
0.090	-0.442	-0.280	-0.011	0.363	0.843	1.356	1.913	2.489	3.063
0.100	-0.424	-0.259	0.004	0.364	0.856	1.373	1.924	2.479	3.058
0.120	-0.373	-0.209	0.063	0.444	0.920	1.433	1.976	2.537	3.108
0.150	-0.314	-0.114	0.180	0.569	1.039	1.549	2.075	2.623	3.164
0.200	-0.323	-0.084	0.232	0.627	1.072	1.538	2.009	2.483	2.945
0.250	-0.409	-0.168	0.139	0.514	0.925	1.342	1.760	2.187	2.620
0.300	-0.486	-0.269	0.021	0.383	0.769	1.155	1.542	1.944	2.361
0.400	-0.589	-0.460	-0.226	0.115	0.503	0.881	1.243	1.617	2.010
0.500	-0.624	-0.536	-0.365	-0.113	0.287	0.684	1.052	1.416	1.786
0.600	-0.642	-0.584	-0.438	-0.207	0.136	0.529	0.904	1.267	1.632
0.800	-0.657	-0.618	-0.508	-0.329	-0.043	0.324	0.708	1.077	1.437
1.000	-0.665	-0.636	-0.546	-0.393	-0.140	0.209	0.596	0.973	1.318
1.200	-0.673	-0.642	-0.562	-0.433	-0.200	0.142	0.529	0.899	1.220
1.500	-0.661	-0.637	-0.567	-0.450	-0.246	0.072	0.444	0.784	1.071
2.000	-0.672	-0.649	-0.581	-0.467	-0.273	0.002	0.305	0.584	0.850
2.500	-0.683	-0.669	-0.610	-0.507	-0.330	-0.085	0.169	0.418	0.690
3.000	-0.688	-0.678	-0.633	-0.555	-0.403	-0.187	0.043	0.283	0.557
4.000	-0.695	-0.688	-0.657	-0.602	-0.494	-0.323	-0.116	0.120	0.394
5.000	-0.698	-0.696	-0.672	-0.626	-0.540	-0.401	-0.212	0.016	0.285
6.000	-0.700	-0.697	-0.677	-0.641	-0.571	-0.450	-0.278	-0.062	0.208
8.000	-0.703	-0.701	-0.685	-0.657	-0.601	-0.502	-0.353	-0.152	0.125
10.000	-0.704	-0.702	-0.689	-0.665	-0.617	-0.528	-0.394	-0.202	0.074
15.000	-0.710	-0.708	-0.697	-0.675	-0.632	-0.561	-0.449	-0.270	-0.031
20.000	-0.716	-0.716	-0.706	-0.686	-0.649	-0.587	-0.485	-0.324	-0.107
30.000	-0.726	-0.726	-0.719	-0.705	-0.679	-0.630	-0.536	-0.404	-0.215
40.000	-0.735	-0.736	-0.730	-0.719	-0.700	-0.654	-0.575	-0.460	-0.293
60.000	-0.754	-0.753	-0.749	-0.743	-0.728	-0.689	-0.632	-0.543	-0.410
80.000	-0.772	-0.770	-0.768	-0.766	-0.749	-0.721	-0.678	-0.609	-0.499
100.000	-0.791	-0.789	-0.788	-0.786	-0.771	-0.751	-0.719	-0.667	-0.572

TABLE 22

ANDERS-GREVESSE ABUNDANCES FOR $X = 0.70$ AND $Z = 0.002$

	Log R												
T6	-5.0	-4.5	-4.0	-3.5	-3.0	-2.5	-2.0	-1.5	-1.0	-0.5	0.0	0.5	1.0
0.006	-1.582	-1.733	-1.818	-1.838	-1.805	-1.619	-1.460	-1.250	-1.070	-0.838	-0.598	-0.342	-0.054
0.007	-0.718	-0.790	-0.825	-0.820	-0.762	-0.661	-0.536	-0.368	-0.187	-0.006	0.195	0.413	0.644
0.008	-0.217	-0.114	-0.028	0.043	0.105	0.197	0.295	0.414	0.553	0.703	0.867	1.049	1.248
0.009	-0.085	0.199	0.440	0.639	0.792	0.901	0.996	1.095	1.194	1.308	1.435	1.586	1.757
0.010	-0.091	0.249	0.594	0.942	1.209	1.404	1.538	1.636	1.723	1.817	1.924	2.049	2.190
0.011	-0.125	0.216	0.596	1.015	1.407	1.698	1.900	2.041	2.136	2.224	2.319	2.420	2.552
0.012	-0.159	0.164	0.546	0.987	1.438	1.826	2.121	2.313	2.454	2.557	2.655	2.758	2.875
0.014	-0.176	0.084	0.429	0.861	1.344	1.829	2.261	2.603	2.854	3.030	3.159	3.280	3.399
0.016	-0.191	0.059	0.383	0.781	1.240	1.755	2.244	2.693	3.060	3.324	3.515	3.665	3.799
0.018	-0.205	0.026	0.345	0.750	1.218	1.707	2.200	2.703	3.153	3.506	3.768	3.960	4.119
0.020	-0.214	0.000	0.313	0.724	1.191	1.684	2.194	2.706	3.200	3.626	3.950	4.188	4.381
0.025	-0.191	0.000	0.303	0.717	1.199	1.721	2.254	2.785	3.316	3.819	4.246	4.588	4.840
0.030	-0.125	0.062	0.363	0.780	1.274	1.796	2.340	2.890	3.455	3.980	4.449	4.837	5.140
0.035	-0.037	0.171	0.477	0.879	1.367	1.899	2.444	2.999	3.568	4.108	4.596	4.998	5.314
0.040	-0.022	0.260	0.607	1.018	1.489	2.004	2.536	3.084	3.643	4.183	4.671	5.075	5.385
0.045	-0.051	0.261	0.652	1.120	1.593	2.087	2.602	3.133	3.674				
0.050	-0.084	0.208	0.599	1.087	1.606	2.122	2.628	3.143	3.661				
0.055	-0.116	0.164	0.538	1.006	1.530	2.073	2.600	3.113	3.618				
0.060	-0.141	0.125	0.480	0.924	1.436	1.978	2.529	3.059	3.558				
0.070	-0.169	0.062	0.390	0.815	1.313	1.831	2.383	2.933	3.454				
0.080	-0.185	0.025	0.334	0.742	1.233	1.750	2.293	2.842	3.380				
0.090	-0.181	0.018	0.319	0.723	1.205	1.716	2.255	2.800	3.342				
0.100	-0.179	0.028	0.327	0.718	1.202	1.715	2.249	2.790	3.330				
0.120	-0.164	0.045	0.349	0.748	1.226	1.733	2.254	2.786	3.312				
0.150	-0.140	0.071	0.377	0.777	1.247	1.735	2.220	2.703	3.172				
0.200	-0.144	0.048	0.329	0.699	1.123	1.557	1.978	2.383	2.778				
0.250	-0.214	-0.031	0.234	0.580	0.966	1.355	1.733	2.096	2.458				
0.300	-0.281	-0.112	0.140	0.474	0.842	1.208	1.552	1.886	2.228				
0.400	-0.375	-0.274	-0.057	0.277	0.648	0.999	1.312	1.617	1.936				
0.500	-0.410	-0.351	-0.185	0.090	0.465	0.840	1.159	1.459	1.762				
0.600	-0.421	-0.380	-0.249	-0.027	0.324	0.708	1.044	1.350	1.651				
0.800	-0.432	-0.402	-0.304	-0.138	0.150	0.517	0.874	1.197	1.505				
1.000	-0.439	-0.413	-0.330	-0.189	0.063	0.410	0.781	1.120	1.429				
1.200	-0.436	-0.415	-0.342	-0.217	0.018	0.356	0.732	1.076	1.370				
1.500	-0.430	-0.407	-0.339	-0.227	-0.021	0.307	0.677	1.003	1.258				
2.000	-0.439	-0.413	-0.340	-0.221	-0.025	0.258	0.569	0.835	1.052				
2.500	-0.452	-0.434	-0.368	-0.254	-0.064	0.190	0.442	0.664	0.883				
3.000	-0.458	-0.447	-0.395	-0.302	-0.130	0.095	0.314	0.521	0.752				
4.000	-0.466	-0.459	-0.424	-0.362	-0.236	-0.058	0.134	0.334	0.587				
5.000	-0.469	-0.464	-0.439	-0.393	-0.298	-0.153	0.020	0.219	0.477				
6.000	-0.472	-0.469	-0.449	-0.411	-0.334	-0.212	-0.057	0.143	0.401				
8.000	-0.475	-0.473	-0.458	-0.430	-0.372	-0.278	-0.143	0.054	0.310				
10.000	-0.476	-0.473	-0.460	-0.438	-0.389	-0.312	-0.178	0.004	0.253				
15.000	-0.482	-0.480	-0.468	-0.447	-0.405	-0.343	-0.231	-0.070	0.146				
20.000	-0.488	-0.485	-0.476	-0.459	-0.420	-0.363	-0.269	-0.130	0.066				
30.000	-0.498	-0.498	-0.492	-0.480	-0.450	-0.404	-0.328	-0.215	-0.044				
40.000	-0.508	-0.508	-0.504	-0.495	-0.471	-0.433	-0.372	-0.276	-0.125				
60.000	-0.526	-0.525	-0.522	-0.518	-0.502	-0.476	-0.434	-0.366	-0.244				
80.000	-0.544	-0.547	-0.545	-0.537	-0.526	-0.510	-0.485	-0.438	-0.331				
100.000	-0.563	-0.562	-0.561	-0.559	-0.551	-0.542	-0.530	-0.499	-0.399				

TABLE 23

ANDERS-GREVESSE ABUNDANCES FOR $X = 0.35$ AND $Z = 0.002$

	Log R												
T6	-5.0	-4.5	-4.0	-3.5	-3.0	-2.5	-2.0	-1.5	-1.0	-0.5	0.0	0.5	1.0
0.006	-1.738	-1.960	-2.093	-2.135	-2.118	-2.000	-1.884	-1.658	-1.446	-1.213	-0.966	-0.676	-0.341
0.007	-0.971	-1.050	-1.103	-1.127	-1.115	-1.040	-0.921	-0.767	-0.591	-0.404	-0.205	0.017	0.253
0.008	-0.585	-0.469	-0.372	-0.296	-0.231	-0.152	-0.064	0.041	0.170	0.313	0.482	0.657	0.854
0.009	-0.519	-0.256	-0.007	0.228	0.411	0.544	0.645	0.739	0.840	0.947	1.068	1.204	1.365
0.010	-0.534	-0.247	0.079	0.443	0.762	1.008	1.168	1.284	1.380	1.475	1.568	1.685	1.821
0.011	-0.555	-0.286	0.057	0.472	0.892	1.243	1.493	1.675	1.788	1.879	1.974	2.074	2.190
0.012	-0.549	-0.313	0.012	0.427	0.882	1.310	1.665	1.912	2.083	2.204	2.308	2.409	2.519
0.014	-0.440	-0.258	0.004	0.345	0.779	1.247	1.725	2.118	2.424	2.641	2.798	2.923	3.040
0.016	-0.421	-0.198	0.077	0.402	0.773	1.211	1.684	2.142	2.566	2.885	3.118	3.290	3.429
0.018	-0.426	-0.216	0.073	0.440	0.849	1.255	1.679	2.147	2.615	3.022	3.334	3.561	3.736
0.020	-0.432	-0.239	0.049	0.431	0.869	1.325	1.755	2.193	2.658	3.104	3.483	3.765	3.980
0.025	-0.409	-0.241	0.037	0.425	0.881	1.392	1.901	2.399	2.869	3.332	3.755	4.123	4.416
0.030	-0.326	-0.168	0.101	0.482	0.956	1.462	1.991	2.527	3.057	3.558	4.004	4.394	4.712
0.035	-0.161	0.008	0.265	0.609	1.063	1.564	2.094	2.631	3.180	3.711	4.193	4.601	4.933
0.040	-0.120	0.175	0.492	0.833	1.234	1.693	2.197	2.723	3.268	3.808	4.307	4.731	5.069
0.045	-0.159	0.184	0.575	1.014	1.428	1.845	2.302	2.804	3.330				
0.050	-0.198	0.102	0.498	0.991	1.509	1.961	2.403	2.872	3.372				
0.055	-0.232	0.044	0.416	0.886	1.433	1.960	2.450	2.915	3.395				
0.060	-0.256	-0.007	0.340	0.787	1.309	1.865	2.420	2.921	3.399				
0.070	-0.283	-0.063	0.255	0.668	1.164	1.697	2.272	2.839	3.358				
0.080	-0.295	-0.100	0.198	0.599	1.083	1.607	2.166	2.739	3.293				
0.090	-0.285	-0.102	0.189	0.587	1.056	1.575	2.126	2.690	3.255				
0.100	-0.271	-0.091	0.198	0.596	1.061	1.579	2.125	2.681	3.246				
0.120	-0.233	-0.043	0.251	0.652	1.111	1.626	2.161	2.716	3.271				
0.150	-0.181	-0.047	0.259	0.738	1.206	1.702	2.211	2.735	3.249				
0.200	-0.186	0.045	0.355	0.745	1.181	1.625	2.069	2.510	2.941				
0.250	-0.269	-0.050	0.250	0.630	1.033	1.434	1.828	2.220	2.614				
0.300	-0.348	-0.146	0.141	0.515	0.896	1.272	1.632	1.993	2.368				
0.400	-0.459	-0.340	-0.094	0.279	0.669	1.034	1.365	1.697	2.044				
0.500	-0.497	-0.421	-0.234	0.063	0.459	0.854	1.195	1.519	1.849				
0.600	-0.510	-0.457	-0.308	-0.065	0.304	0.706	1.064	1.392	1.717				
0.800	-0.525	-0.489	-0.377	-0.189	0.119	0.503	0.878	1.221	1.546				
1.000	-0.533	-0.503	-0.410	-0.252	0.021	0.386	0.772	1.130	1.453				
1.200	-0.531	-0.505	-0.424	-0.287	-0.033	0.322	0.714	1.074	1.381				
1.500	-0.525	-0.514	-0.439	-0.300	-0.078	0.264	0.649	0.988	1.257				
2.000	-0.538	-0.509	-0.430	-0.301	-0.091	0.208	0.531	0.809	1.041				
2.500	-0.551	-0.532	-0.461	-0.339	-0.135	0.135	0.399	0.633	0.866				
3.000	-0.557	-0.544	-0.490	-0.394	-0.209	0.031	0.265	0.485	0.723				
4.000	-0.565	-0.557	-0.520	-0.455	-0.322	-0.130	0.077	0.291	0.544				
5.000	-0.568	-0.565	-0.537	-0.487	-0.387	-0.231	-0.040	0.168	0.424				
6.000	-0.571	-0.568	-0.546	-0.505	-0.425	-0.294	-0.120	0.082	0.341				
8.000	-0.574	-0.571	-0.555	-0.525	-0.465	-0.361	-0.217	-0.017	0.248				
10.000	-0.575	-0.572	-0.558	-0.534	-0.482	-0.396	-0.259	-0.070	0.191				
15.000	-0.581	-0.578	-0.565	-0.543	-0.498	-0.430	-0.315	-0.143	0.081				
20.000	-0.587	-0.585	-0.574	-0.556	-0.517	-0.453	-0.353	-0.204	-0.001				
30.000	-0.597	-0.596	-0.589	-0.577	-0.546	-0.498	-0.413	-0.291	-0.113				
40.000	-0.607	-0.605	-0.600	-0.592	-0.567	-0.526	-0.456	-0.351	-0.194				
60.000	-0.625	-0.624	-0.621	-0.616	-0.598	-0.567	-0.518	-0.440	-0.314				
80.000	-0.644	-0.644	-0.642	-0.637	-0.624	-0.600	-0.566	-0.510	-0.403				
100.000	-0.662	-0.660	-0.658	-0.657	-0.646	-0.631	-0.609	-0.570	-0.474				

TABLE 24

ANDERS-GREVESSE ABUNDANCES FOR $X = 0.00$ AND $Z = 0.002$

	Log R								
T6	-5.0	-4.5	-4.0	-3.5	-3.0	-2.5	-2.0	-1.5	-1.0
0.006	-4.103	-4.147	-4.181	-4.203	-4.190	-4.160	-4.074	-3.949	-3.793
0.007	-3.933	-3.918	-3.907	-3.900	-3.887	-3.895	-3.805	-3.653	-3.443
0.008	-3.728	-3.828	-3.869	-3.851	-3.804	-3.745	-3.632	-3.444	-3.209
0.009	-2.900	-3.148	-3.356	-3.525	-3.592	-3.588	-3.428	-3.188	-2.915
0.010	-2.227	-2.443	-2.640	-2.817	-2.960	-3.136	-3.106	-2.921	-2.639
0.011	-1.682	-1.861	-2.016	-2.145	-2.230	-2.299	-2.303	-2.246	-2.126
0.012	-1.268	-1.384	-1.480	-1.557	-1.607	-1.626	-1.616	-1.576	-1.527
0.014	-0.858	-0.771	-0.698	-0.638	-0.589	-0.554	-0.515	-0.471	-0.416
0.016	-0.807	-0.624	-0.417	-0.188	0.002	0.136	0.235	0.314	0.386
0.018	-0.813	-0.647	-0.409	-0.099	0.222	0.491	0.690	0.828	0.938
0.020	-0.831	-0.679	-0.445	-0.131	0.240	0.614	0.928	1.159	1.324
0.025	-0.833	-0.727	-0.532	-0.250	0.123	0.560	1.015	1.421	1.771
0.030	-0.644	-0.577	-0.427	-0.196	0.121	0.515	0.979	1.431	1.889
0.035	-0.322	-0.199	-0.044	0.145	0.389	0.685	1.059	1.473	1.950
0.040	-0.259	0.043	0.323	0.580	0.813	1.051	1.304	1.633	2.054
0.045	-0.303	0.043	0.425	0.843	1.180	1.440	1.660	1.906	2.239
0.050	-0.345	-0.066	0.326	0.829	1.319	1.702	1.981	2.214	2.486
0.055	-0.379	-0.135	0.227	0.707	1.255	1.767	2.170	2.467	2.733
0.060	-0.403	-0.175	0.159	0.601	1.124	1.692	2.211	2.616	2.932
0.070	-0.427	-0.226	0.074	0.474	0.965	1.502	2.087	2.644	3.107
0.080	-0.434	-0.255	0.026	0.411	0.885	1.404	1.972	2.554	3.099
0.090	-0.423	-0.255	0.016	0.391	0.865	1.378	1.934	2.505	3.074
0.100	-0.404	-0.233	0.034	0.396	0.881	1.395	1.943	2.496	3.069
0.120	-0.348	-0.180	0.093	0.472	0.946	1.454	1.992	2.550	3.116
0.150	-0.267	-0.069	0.223	0.608	1.068	1.574	2.093	2.635	3.171
0.200	-0.262	-0.015	0.303	0.692	1.129	1.589	2.052	2.514	2.962
0.250	-0.359	-0.099	0.222	0.602	1.013	1.425	1.832	2.240	2.650
0.300	-0.451	-0.209	0.102	0.483	0.877	1.261	1.635	2.012	2.401
0.400	-0.575	-0.429	-0.167	0.210	0.626	1.011	1.360	1.706	2.067
0.500	-0.615	-0.518	-0.327	-0.042	0.397	0.818	1.180	1.521	1.860
0.600	-0.635	-0.570	-0.408	-0.147	0.235	0.657	1.038	1.382	1.719
0.800	-0.651	-0.607	-0.483	-0.279	0.042	0.442	0.839	1.198	1.536
1.000	-0.657	-0.625	-0.521	-0.347	-0.063	0.318	0.722	1.097	1.434
1.200	-0.665	-0.630	-0.538	-0.390	-0.124	0.249	0.656	1.034	1.356
1.500	-0.651	-0.621	-0.539	-0.405	-0.173	0.182	0.584	0.942	1.228
2.000	-0.664	-0.634	-0.550	-0.413	-0.187	0.127	0.465	0.759	1.005
2.500	-0.678	-0.660	-0.586	-0.455	-0.238	0.052	0.334	0.581	0.824
3.000	-0.685	-0.672	-0.615	-0.514	-0.321	-0.059	0.194	0.427	0.673
4.000	-0.693	-0.685	-0.647	-0.578	-0.440	-0.231	-0.004	0.225	0.477
5.000	-0.697	-0.694	-0.665	-0.610	-0.505	-0.337	-0.131	0.093	0.346
6.000	-0.699	-0.696	-0.673	-0.630	-0.546	-0.405	-0.219	-0.003	0.254
8.000	-0.703	-0.700	-0.682	-0.650	-0.587	-0.477	-0.318	-0.115	0.157
10.000	-0.703	-0.701	-0.686	-0.659	-0.606	-0.510	-0.368	-0.173	0.102
15.000	-0.709	-0.707	-0.694	-0.669	-0.620	-0.543	-0.426	-0.245	-0.011
20.000	-0.716	-0.715	-0.704	-0.681	-0.638	-0.570	-0.464	-0.305	-0.094
30.000	-0.726	-0.726	-0.719	-0.703	-0.674	-0.621	-0.526	-0.395	-0.208
40.000	-0.735	-0.736	-0.730	-0.718	-0.698	-0.650	-0.570	-0.455	-0.289
60.000	-0.754	-0.753	-0.749	-0.743	-0.727	-0.688	-0.630	-0.541	-0.407
80.000	-0.772	-0.770	-0.768	-0.766	-0.748	-0.720	-0.676	-0.608	-0.497
100.000	-0.791	-0.789	-0.788	-0.786	-0.771	-0.750	-0.718	-0.665	-0.570

TABLE 25

ANDERS-GREVESSE ABUNDANCES FOR $X = 0.70$ AND $Z = 0.004$

	Log R												
T6	-5.0	-4.5	-4.0	-3.5	-3.0	-2.5	-2.0	-1.5	-1.0	-0.5	0.0	0.5	1.0
0.006	-1.579	-1.729	-1.814	-1.833	-1.800	-1.613	-1.454	-1.243	-1.056	-0.819	-0.572	-0.305	0.000
0.007	-0.715	-0.788	-0.822	-0.817	-0.758	-0.658	-0.531	-0.363	-0.180	0.005	0.210	0.432	0.667
0.008	-0.214	-0.112	-0.025	0.045	0.109	0.201	0.300	0.420	0.560	0.713	0.879	1.064	1.266
0.009	-0.081	0.202	0.443	0.641	0.795	0.905	1.001	1.101	1.202	1.318	1.448	1.602	1.776
0.010	-0.085	0.255	0.599	0.947	1.214	1.408	1.543	1.642	1.731	1.827	1.936	2.064	2.209
0.011	-0.117	0.224	0.605	1.025	1.414	1.705	1.906	2.048	2.145	2.235	2.331	2.435	2.570
0.012	-0.151	0.173	0.556	0.998	1.448	1.834	2.128	2.321	2.463	2.568	2.668	2.773	2.892
0.014	-0.165	0.097	0.444	0.876	1.357	1.840	2.271	2.612	2.863	3.040	3.170	3.293	3.412
0.016	-0.177	0.075	0.400	0.798	1.256	1.768	2.256	2.704	3.070	3.335	3.525	3.675	3.809
0.018	-0.189	0.044	0.363	0.768	1.233	1.720	2.213	2.715	3.164	3.516	3.778	3.969	4.127
0.020	-0.198	0.020	0.332	0.741	1.205	1.696	2.205	2.717	3.210	3.635	3.958	4.195	4.387
0.025	-0.177	0.019	0.322	0.734	1.213	1.733	2.266	2.796	3.324	3.825	4.251	4.593	4.843
0.030	-0.109	0.079	0.381	0.795	1.288	1.809	2.353	2.903	3.464	3.987	4.454	4.840	5.142
0.035	-0.022	0.188	0.495	0.896	1.380	1.911	2.455	3.008	3.576	4.114	4.601	5.001	5.316
0.040	-0.006	0.275	0.621	1.033	1.502	2.016	2.547	3.093	3.650	4.189	4.675	5.077	5.386
0.045	-0.032	0.281	0.670	1.136	1.608	2.100	2.613	3.142	3.682				
0.050	-0.063	0.230	0.620	1.106	1.623	2.137	2.641	3.154	3.670				
0.055	-0.095	0.189	0.564	1.031	1.554	2.093	2.617	3.126	3.628				
0.060	-0.120	0.150	0.507	0.951	1.462	2.003	2.550	3.076	3.571				
0.070	-0.146	0.089	0.419	0.845	1.343	1.862	2.411	2.956	3.472				
0.080	-0.162	0.054	0.366	0.774	1.263	1.781	2.322	2.868	3.399				
0.090	-0.157	0.048	0.352	0.756	1.235	1.747	2.285	2.827	3.361				
0.100	-0.154	0.062	0.364	0.754	1.236	1.745	2.277	2.815	3.348				
0.120	-0.131	0.082	0.388	0.787	1.263	1.763	2.281	2.808	3.328				
0.150	-0.080	0.129	0.433	0.830	1.297	1.783	2.266	2.741	3.197				
0.200	-0.068	0.135	0.421	0.791	1.216	1.652	2.076	2.471	2.838				
0.250	-0.152	0.054	0.337	0.696	1.092	1.485	1.867	2.215	2.542				
0.300	-0.235	-0.039	0.239	0.599	0.985	1.362	1.707	2.023	2.327				
0.400	-0.353	-0.226	0.028	0.406	0.808	1.177	1.489	1.772	2.053				
0.500	-0.397	-0.325	-0.126	0.200	0.624	1.025	1.345	1.625	1.892				
0.600	-0.409	-0.360	-0.203	0.062	0.468	0.891	1.233	1.522	1.791				
0.800	-0.422	-0.384	-0.265	-0.065	0.272	0.684	1.057	1.371	1.654				
1.000	-0.428	-0.395	-0.294	-0.124	0.173	0.562	0.953	1.290	1.584				
1.200	-0.425	-0.398	-0.307	-0.154	0.122	0.499	0.898	1.247	1.537				
1.500	-0.416	-0.385	-0.302	-0.167	0.079	0.448	0.847	1.187	1.446				
2.000	-0.427	-0.389	-0.297	-0.151	0.079	0.405	0.754	1.039	1.248				
2.500	-0.445	-0.418	-0.330	-0.182	0.053	0.352	0.635	0.864	1.062				
3.000	-0.452	-0.437	-0.366	-0.239	-0.016	0.256	0.499	0.705	0.908				
4.000	-0.463	-0.454	-0.407	-0.321	-0.151	0.071	0.283	0.477	0.702				
5.000	-0.467	-0.461	-0.427	-0.365	-0.239	-0.057	0.135	0.329	0.563				
6.000	-0.470	-0.467	-0.440	-0.391	-0.292	-0.142	0.031	0.228	0.468				
8.000	-0.474	-0.471	-0.453	-0.419	-0.347	-0.237	-0.089	0.109	0.357				
10.000	-0.475	-0.471	-0.456	-0.429	-0.372	-0.283	-0.139	0.047	0.293				
15.000	-0.481	-0.478	-0.463	-0.436	-0.388	-0.318	-0.199	-0.034	0.175				
20.000	-0.488	-0.484	-0.472	-0.451	-0.404	-0.339	-0.241	-0.103	0.085				
30.000	-0.498	-0.498	-0.490	-0.477	-0.442	-0.391	-0.313	-0.202	-0.034				
40.000	-0.508	-0.508	-0.503	-0.493	-0.467	-0.426	-0.363	-0.268	-0.118				
60.000	-0.526	-0.525	-0.522	-0.517	-0.501	-0.473	-0.430	-0.362	-0.239				
80.000	-0.544	-0.547	-0.545	-0.537	-0.526	-0.508	-0.482	-0.435	-0.327				
100.000	-0.563	-0.562	-0.561	-0.559	-0.550	-0.541	-0.528	-0.496	-0.396				

TABLE 26

ANDERS-GREVESSE ABUNDANCES FOR $X = 0.35$ AND $Z = 0.004$

	Log R												
T6	-5.0	-4.5	-4.0	-3.5	-3.0	-2.5	-2.0	-1.5	-1.0	-0.5	0.0	0.5	1.0
0.006	-1.734	-1.955	-2.087	-2.128	-2.109	-1.991	-1.874	-1.646	-1.430	-1.193	-0.938	-0.638	-0.288
0.007	-0.968	-1.047	-1.099	-1.123	-1.110	-1.034	-0.915	-0.759	-0.580	-0.390	-0.187	0.040	0.281
0.008	-0.581	-0.465	-0.369	-0.293	-0.227	-0.147	-0.058	0.048	0.179	0.325	0.497	0.676	0.877
0.009	-0.513	-0.251	-0.003	0.232	0.415	0.549	0.651	0.746	0.849	0.959	1.084	1.226	1.392
0.010	-0.527	-0.239	0.087	0.450	0.768	1.014	1.174	1.291	1.389	1.487	1.585	1.707	1.846
0.011	-0.546	-0.274	0.069	0.484	0.902	1.252	1.502	1.683	1.799	1.894	1.991	2.094	2.215
0.012	-0.540	-0.301	0.026	0.442	0.896	1.322	1.675	1.923	2.095	2.219	2.325	2.429	2.543
0.014	-0.428	-0.243	0.021	0.366	0.799	1.268	1.740	2.133	2.438	2.655	2.814	2.941	3.061
0.016	-0.406	-0.180	0.096	0.423	0.794	1.230	1.703	2.159	2.581	2.901	3.134	3.307	3.446
0.018	-0.409	-0.195	0.095	0.462	0.867	1.273	1.698	2.165	2.633	3.038	3.349	3.576	3.749
0.020	-0.415	-0.217	0.072	0.452	0.887	1.340	1.771	2.209	2.675	3.121	3.497	3.778	3.991
0.025	-0.393	-0.221	0.059	0.446	0.899	1.407	1.915	2.414	2.883	3.346	3.765	4.131	4.422
0.030	-0.308	-0.148	0.122	0.502	0.972	1.477	2.006	2.542	3.070	3.569	4.012	4.401	4.717
0.035	-0.145	0.026	0.284	0.629	1.080	1.579	2.108	2.645	3.192	3.720	4.200	4.607	4.936
0.040	-0.103	0.190	0.507	0.848	1.248	1.708	2.210	2.735	3.278	3.816	4.313	4.735	5.072
0.045	-0.137	0.203	0.592	1.029	1.442	1.859	2.315	2.815	3.339				
0.050	-0.175	0.126	0.521	1.009	1.524	1.974	2.415	2.883	3.381				
0.055	-0.209	0.071	0.444	0.912	1.454	1.977	2.463	2.927	3.404				
0.060	-0.233	0.020	0.370	0.815	1.337	1.888	2.438	2.935	3.409				
0.070	-0.259	-0.033	0.286	0.700	1.195	1.727	2.296	2.858	3.372				
0.080	-0.271	-0.069	0.232	0.632	1.114	1.638	2.193	2.762	3.310				
0.090	-0.260	-0.070	0.225	0.622	1.088	1.606	2.155	2.715	3.273				
0.100	-0.245	-0.056	0.236	0.633	1.095	1.609	2.152	2.705	3.264				
0.120	-0.200	-0.007	0.290	0.691	1.146	1.656	2.185	2.735	3.284				
0.150	-0.122	0.014	0.317	0.787	1.249	1.740	2.242	2.759	3.264				
0.200	-0.110	0.130	0.443	0.828	1.259	1.702	2.141	2.570	2.980				
0.250	-0.208	0.034	0.349	0.738	1.144	1.546	1.937	2.310	2.673				
0.300	-0.303	-0.074	0.238	0.635	1.027	1.409	1.764	2.103	2.441				
0.400	-0.438	-0.294	-0.014	0.403	0.820	1.198	1.523	1.829	2.139				
0.500	-0.485	-0.396	-0.180	0.164	0.604	1.025	1.363	1.665	1.959				
0.600	-0.498	-0.437	-0.265	0.018	0.436	0.874	1.237	1.547	1.840				
0.800	-0.515	-0.472	-0.340	-0.119	0.233	0.657	1.047	1.380	1.681				
1.000	-0.523	-0.486	-0.375	-0.189	0.125	0.529	0.933	1.288	1.597				
1.200	-0.520	-0.488	-0.390	-0.226	0.068	0.457	0.871	1.236	1.540				
1.500	-0.511	-0.495	-0.405	-0.241	0.018	0.399	0.812	1.167	1.440				
2.000	-0.527	-0.486	-0.388	-0.231	0.011	0.352	0.712	1.010	1.233				
2.500	-0.544	-0.517	-0.425	-0.267	-0.018	0.297	0.592	0.832	1.043				
3.000	-0.552	-0.534	-0.461	-0.332	-0.096	0.194	0.452	0.670	0.882				
4.000	-0.562	-0.551	-0.502	-0.414	-0.237	0.001	0.229	0.438	0.663				
5.000	-0.566	-0.561	-0.526	-0.460	-0.327	-0.133	0.078	0.282	0.515				
6.000	-0.569	-0.566	-0.538	-0.486	-0.383	-0.222	-0.030	0.171	0.412				
8.000	-0.573	-0.569	-0.550	-0.514	-0.440	-0.318	-0.160	0.041	0.298				
10.000	-0.573	-0.570	-0.554	-0.525	-0.465	-0.366	-0.218	-0.023	0.235				
15.000	-0.580	-0.576	-0.560	-0.532	-0.480	-0.402	-0.279	-0.104	0.113				
20.000	-0.586	-0.584	-0.571	-0.547	-0.500	-0.426	-0.321	-0.174	0.020				
30.000	-0.597	-0.595	-0.587	-0.573	-0.537	-0.483	-0.396	-0.276	-0.102				
40.000	-0.607	-0.605	-0.600	-0.590	-0.563	-0.519	-0.447	-0.343	-0.187				
60.000	-0.625	-0.624	-0.620	-0.615	-0.596	-0.564	-0.514	-0.435	-0.309				
80.000	-0.644	-0.644	-0.642	-0.636	-0.623	-0.599	-0.564	-0.506	-0.399				
100.000	-0.662	-0.660	-0.658	-0.657	-0.645	-0.630	-0.607	-0.567	-0.470				

TABLE 27

ANDERS-GREVESSE ABUNDANCES FOR $X = 0.00$ AND $Z = 0.004$

	Log R								
T6	-5.0	-4.5	-4.0	-3.5	-3.0	-2.5	-2.0	-1.5	-1.0
0.006	-3.826	-3.871	-3.904	-3.926	-3.913	-3.882	-3.793	-3.665	-3.506
0.007	-3.661	-3.642	-3.629	-3.621	-3.607	-3.616	-3.524	-3.370	-3.156
0.008	-3.564	-3.612	-3.620	-3.587	-3.535	-3.471	-3.355	-3.162	-2.923
0.009	-2.861	-3.084	-3.252	-3.365	-3.380	-3.336	-3.157	-2.906	-2.627
0.010	-2.211	-2.420	-2.605	-2.767	-2.885	-3.008	-2.917	-2.688	-2.381
0.011	-1.669	-1.844	-1.992	-2.114	-2.189	-2.244	-2.228	-2.138	-1.975
0.012	-1.256	-1.368	-1.460	-1.532	-1.576	-1.588	-1.568	-1.513	-1.457
0.014	-0.844	-0.753	-0.675	-0.612	-0.558	-0.520	-0.477	-0.427	-0.364
0.016	-0.787	-0.599	-0.389	-0.156	0.039	0.176	0.280	0.365	0.443
0.018	-0.789	-0.618	-0.375	-0.061	0.263	0.535	0.738	0.884	1.004
0.020	-0.808	-0.646	-0.406	-0.088	0.285	0.659	0.976	1.213	1.388
0.025	-0.806	-0.694	-0.493	-0.205	0.173	0.611	1.066	1.480	1.835
0.030	-0.619	-0.546	-0.392	-0.156	0.166	0.564	1.031	1.491	1.950
0.035	-0.303	-0.178	-0.019	0.172	0.420	0.723	1.106	1.531	2.009
0.040	-0.240	0.061	0.340	0.597	0.833	1.075	1.338	1.678	2.106
0.045	-0.279	0.064	0.443	0.858	1.195	1.457	1.683	1.938	2.278
0.050	-0.319	-0.037	0.352	0.849	1.334	1.716	1.997	2.235	2.515
0.055	-0.354	-0.104	0.259	0.735	1.277	1.782	2.184	2.484	2.753
0.060	-0.377	-0.144	0.192	0.632	1.152	1.713	2.227	2.631	2.949
0.070	-0.400	-0.194	0.109	0.509	0.998	1.533	2.111	2.662	3.121
0.080	-0.408	-0.221	0.064	0.448	0.919	1.436	2.000	2.577	3.116
0.090	-0.397	-0.220	0.056	0.431	0.900	1.412	1.964	2.531	3.093
0.100	-0.377	-0.197	0.075	0.440	0.918	1.427	1.970	2.521	3.088
0.120	-0.313	-0.140	0.135	0.514	0.984	1.486	2.018	2.569	3.131
0.150	-0.205	-0.009	0.280	0.661	1.110	1.610	2.121	2.655	3.185
0.200	-0.185	0.072	0.391	0.773	1.201	1.655	2.112	2.562	2.994
0.250	-0.299	-0.016	0.319	0.706	1.116	1.527	1.928	2.318	2.701
0.300	-0.406	-0.138	0.197	0.597	1.001	1.388	1.756	2.110	2.466
0.400	-0.556	-0.386	-0.092	0.326	0.769	1.166	1.507	1.828	2.153
0.500	-0.603	-0.495	-0.277	0.050	0.531	0.977	1.338	1.657	1.964
0.600	-0.624	-0.552	-0.367	-0.071	0.355	0.811	1.201	1.529	1.836
0.800	-0.642	-0.591	-0.448	-0.213	0.148	0.584	0.999	1.350	1.665
1.000	-0.648	-0.608	-0.487	-0.285	0.037	0.452	0.873	1.248	1.573
1.200	-0.654	-0.613	-0.505	-0.331	-0.028	0.379	0.804	1.189	1.510
1.500	-0.638	-0.600	-0.503	-0.347	-0.081	0.312	0.739	1.115	1.407
2.000	-0.653	-0.612	-0.509	-0.344	-0.086	0.266	0.642	0.957	1.198
2.500	-0.671	-0.647	-0.551	-0.384	-0.122	0.214	0.527	0.782	1.004
3.000	-0.679	-0.663	-0.587	-0.454	-0.207	0.105	0.385	0.617	0.836
4.000	-0.690	-0.680	-0.629	-0.538	-0.356	-0.097	0.154	0.378	0.604
5.000	-0.694	-0.691	-0.654	-0.583	-0.445	-0.237	-0.008	0.214	0.445
6.000	-0.698	-0.694	-0.665	-0.610	-0.503	-0.330	-0.123	0.092	0.333
8.000	-0.702	-0.698	-0.677	-0.639	-0.562	-0.432	-0.258	-0.052	0.213
10.000	-0.702	-0.699	-0.682	-0.650	-0.588	-0.478	-0.324	-0.122	0.150
15.000	-0.708	-0.705	-0.688	-0.657	-0.600	-0.513	-0.386	-0.200	0.026
20.000	-0.715	-0.714	-0.700	-0.672	-0.620	-0.541	-0.428	-0.271	-0.069
30.000	-0.726	-0.726	-0.717	-0.699	-0.665	-0.605	-0.506	-0.378	-0.195
40.000	-0.735	-0.736	-0.729	-0.716	-0.693	-0.642	-0.560	-0.445	-0.280
60.000	-0.754	-0.753	-0.749	-0.742	-0.725	-0.685	-0.626	-0.536	-0.402
80.000	-0.772	-0.770	-0.768	-0.766	-0.747	-0.719	-0.674	-0.604	-0.493
100.000	-0.791	-0.789	-0.788	-0.786	-0.770	-0.749	-0.716	-0.663	-0.567

TABLE 28

ANDERS-GREVESSE ABUNDANCES FOR $X = 0.70$ AND $Z = 0.01$

	Log R												
T6	-5.0	-4.5	-4.0	-3.5	-3.0	-2.5	-2.0	-1.5	-1.0	-0.5	0.0	0.5	1.0
0.006	-1.573	-1.721	-1.804	-1.822	-1.787	-1.601	-1.442	-1.229	-1.025	-0.778	-0.515	-0.225	0.118
0.007	-0.711	-0.784	-0.817	-0.811	-0.752	-0.650	-0.521	-0.351	-0.164	0.029	0.241	0.471	0.716
0.008	-0.209	-0.108	-0.021	0.050	0.115	0.208	0.309	0.430	0.574	0.732	0.904	1.095	1.305
0.009	-0.073	0.209	0.449	0.647	0.802	0.912	1.010	1.112	1.217	1.338	1.474	1.635	1.815
0.010	-0.074	0.266	0.610	0.956	1.223	1.417	1.553	1.654	1.747	1.848	1.963	2.097	2.249
0.011	-0.103	0.240	0.622	1.041	1.427	1.717	1.919	2.062	2.164	2.257	2.358	2.467	2.606
0.012	-0.136	0.191	0.576	1.018	1.466	1.848	2.142	2.338	2.482	2.590	2.694	2.804	2.928
0.014	-0.145	0.122	0.472	0.904	1.382	1.861	2.291	2.632	2.882	3.061	3.195	3.322	3.443
0.016	-0.152	0.104	0.432	0.832	1.289	1.795	2.283	2.727	3.092	3.357	3.547	3.699	3.833
0.018	-0.160	0.077	0.398	0.801	1.261	1.746	2.239	2.739	3.187	3.537	3.799	3.989	4.145
0.020	-0.168	0.056	0.369	0.773	1.233	1.720	2.229	2.741	3.233	3.655	3.976	4.211	4.401
0.025	-0.150	0.052	0.358	0.767	1.240	1.757	2.290	2.818	3.343	3.841	4.266	4.605	4.853
0.030	-0.079	0.113	0.415	0.826	1.315	1.834	2.379	2.929	3.484	4.002	4.467	4.850	5.148
0.035	0.006	0.221	0.528	0.928	1.408	1.937	2.479	3.029	3.596	4.128	4.612	5.008	5.321
0.040	0.023	0.303	0.649	1.060	1.527	2.039	2.570	3.113	3.665	4.202	4.684	5.083	5.388
0.045	0.005	0.316	0.702	1.164	1.635	2.125	2.638	3.161	3.698				
0.050	-0.024	0.271	0.660	1.142	1.654	2.166	2.668	3.177	3.690				
0.055	-0.054	0.235	0.612	1.077	1.596	2.131	2.651	3.156	3.653				
0.060	-0.079	0.197	0.557	1.001	1.512	2.052	2.592	3.113	3.601				
0.070	-0.103	0.140	0.476	0.903	1.399	1.921	2.465	3.005	3.510				
0.080	-0.117	0.110	0.428	0.836	1.323	1.841	2.380	2.923	3.442				
0.090	-0.112	0.106	0.418	0.824	1.298	1.809	2.345	2.883	3.405				
0.100	-0.106	0.124	0.435	0.825	1.301	1.806	2.335	2.870	3.390				
0.120	-0.069	0.151	0.461	0.863	1.336	1.826	2.337	2.858	3.365				
0.150	0.026	0.233	0.533	0.927	1.388	1.868	2.349	2.819	3.258				
0.200	0.063	0.282	0.574	0.940	1.361	1.800	2.232	2.627	2.964				
0.250	-0.049	0.193	0.500	0.873	1.277	1.677	2.072	2.418	2.710				
0.300	-0.157	0.078	0.392	0.783	1.192	1.585	1.942	2.252	2.518				
0.400	-0.313	-0.134	0.172	0.604	1.037	1.432	1.756	2.028	2.267				
0.500	-0.373	-0.270	-0.017	0.386	0.865	1.298	1.626	1.892	2.120				
0.600	-0.386	-0.319	-0.117	0.219	0.697	1.167	1.521	1.795	2.028				
0.800	-0.403	-0.347	-0.190	0.067	0.474	0.945	1.342	1.646	1.900				
1.000	-0.409	-0.359	-0.223	-0.002	0.361	0.805	1.224	1.558	1.831				
1.200	-0.404	-0.362	-0.238	-0.034	0.301	0.731	1.158	1.510	1.791				
1.500	-0.391	-0.346	-0.233	-0.053	0.254	0.674	1.104	1.458	1.724				
2.000	-0.404	-0.344	-0.219	-0.031	0.248	0.632	1.026	1.338	1.551				
2.500	-0.430	-0.382	-0.256	-0.051	0.243	0.598	0.923	1.172	1.357				
3.000	-0.441	-0.412	-0.302	-0.113	0.184	0.517	0.793	1.005	1.185				
4.000	-0.455	-0.440	-0.364	-0.227	0.023	0.309	0.547	0.739	0.929				
5.000	-0.462	-0.453	-0.398	-0.298	-0.106	0.138	0.357	0.548	0.748				
6.000	-0.466	-0.461	-0.419	-0.341	-0.191	0.013	0.215	0.409	0.621				
8.000	-0.471	-0.467	-0.440	-0.389	-0.286	-0.137	0.038	0.239	0.471				
10.000	-0.472	-0.467	-0.445	-0.407	-0.327	-0.209	-0.044	0.153	0.391				
15.000	-0.478	-0.473	-0.451	-0.412	-0.347	-0.258	-0.121	0.054	0.249				
20.000	-0.486	-0.482	-0.463	-0.429	-0.365	-0.281	-0.170	-0.035	0.137				
30.000	-0.498	-0.497	-0.486	-0.466	-0.420	-0.355	-0.272	-0.165	-0.004				
40.000	-0.507	-0.508	-0.501	-0.488	-0.455	-0.407	-0.340	-0.245	-0.097				
60.000	-0.526	-0.525	-0.521	-0.515	-0.496	-0.465	-0.419	-0.349	-0.225				
80.000	-0.544	-0.547	-0.544	-0.536	-0.523	-0.504	-0.475	-0.425	-0.316				
100.000	-0.563	-0.562	-0.561	-0.558	-0.548	-0.537	-0.522	-0.488	-0.386				

TABLE 29

ANDERS-GREVESSE ABUNDANCES FOR $X = 0.35$ AND $Z = 0.01$

	Log R												
T6	-5.0	-4.5	-4.0	-3.5	-3.0	-2.5	-2.0	-1.5	-1.0	-0.5	0.0	0.5	1.0
0.006	-1.726	-1.944	-2.071	-2.109	-2.088	-1.970	-1.849	-1.620	-1.397	-1.150	-0.879	-0.560	-0.178
0.007	-0.962	-1.041	-1.092	-1.115	-1.099	-1.022	-0.900	-0.742	-0.559	-0.362	-0.151	0.085	0.338
0.008	-0.574	-0.459	-0.363	-0.287	-0.219	-0.138	-0.047	0.062	0.196	0.349	0.527	0.714	0.924
0.009	-0.502	-0.242	0.006	0.240	0.423	0.558	0.662	0.760	0.866	0.983	1.115	1.267	1.442
0.010	-0.513	-0.224	0.101	0.462	0.780	1.025	1.187	1.307	1.409	1.512	1.619	1.749	1.896
0.011	-0.530	-0.254	0.091	0.505	0.921	1.269	1.520	1.701	1.822	1.923	2.026	2.135	2.264
0.012	-0.523	-0.280	0.051	0.468	0.921	1.343	1.695	1.944	2.120	2.249	2.361	2.470	2.591
0.014	-0.407	-0.217	0.053	0.402	0.834	1.303	1.768	2.161	2.466	2.685	2.849	2.981	3.106
0.016	-0.379	-0.149	0.132	0.464	0.834	1.267	1.738	2.194	2.614	2.933	3.168	3.343	3.483
0.018	-0.377	-0.158	0.135	0.501	0.904	1.309	1.734	2.202	2.669	3.073	3.382	3.608	3.780
0.020	-0.384	-0.177	0.116	0.493	0.922	1.371	1.803	2.242	2.710	3.155	3.528	3.807	4.017
0.025	-0.364	-0.184	0.099	0.486	0.934	1.438	1.944	2.445	2.914	3.375	3.788	4.152	4.439
0.030	-0.274	-0.109	0.162	0.540	1.005	1.509	2.036	2.574	3.098	3.594	4.031	4.418	4.731
0.035	-0.115	0.060	0.321	0.666	1.113	1.610	2.138	2.673	3.217	3.740	4.216	4.620	4.945
0.040	-0.071	0.219	0.535	0.876	1.276	1.736	2.238	2.761	3.302	3.834	4.328	4.746	5.079
0.045	-0.097	0.239	0.623	1.055	1.468	1.886	2.341	2.840	3.359				
0.050	-0.132	0.171	0.562	1.044	1.551	1.999	2.441	2.908	3.401				
0.055	-0.165	0.121	0.496	0.959	1.494	2.009	2.491	2.952	3.425				
0.060	-0.189	0.073	0.425	0.868	1.388	1.933	2.473	2.966	3.433				
0.070	-0.213	0.022	0.347	0.762	1.254	1.785	2.346	2.899	3.403				
0.080	-0.223	-0.007	0.300	0.698	1.176	1.699	2.247	2.811	3.348				
0.090	-0.213	-0.008	0.294	0.693	1.153	1.669	2.214	2.767	3.313				
0.100	-0.197	0.009	0.310	0.707	1.165	1.670	2.209	2.757	3.303				
0.120	-0.140	0.061	0.364	0.768	1.218	1.718	2.237	2.778	3.317				
0.150	-0.017	0.123	0.422	0.877	1.331	1.812	2.305	2.811	3.302				
0.200	0.018	0.271	0.587	0.964	1.386	1.825	2.265	2.687	3.068				
0.250	-0.107	0.167	0.503	0.903	1.311	1.717	2.114	2.477	2.801				
0.300	-0.226	0.039	0.385	0.812	1.218	1.615	1.975	2.299	2.594				
0.400	-0.399	-0.207	0.123	0.592	1.040	1.440	1.770	2.056	2.320				
0.500	-0.461	-0.345	-0.080	0.335	0.830	1.282	1.626	1.908	2.160				
0.600	-0.476	-0.397	-0.184	0.162	0.646	1.131	1.507	1.800	2.054				
0.800	-0.497	-0.437	-0.270	0.006	0.420	0.898	1.313	1.637	1.909				
1.000	-0.503	-0.448	-0.304	-0.072	0.302	0.757	1.186	1.540	1.830				
1.200	-0.498	-0.452	-0.322	-0.109	0.240	0.675	1.116	1.485	1.783				
1.500	-0.486	-0.455	-0.336	-0.130	0.188	0.615	1.057	1.427	1.709				
2.000	-0.506	-0.442	-0.310	-0.112	0.175	0.570	0.975	1.302	1.531				
2.500	-0.529	-0.483	-0.352	-0.136	0.171	0.540	0.877	1.138	1.336				
3.000	-0.540	-0.509	-0.399	-0.208	0.104	0.454	0.747	0.971	1.159				
4.000	-0.554	-0.538	-0.460	-0.321	-0.064	0.242	0.498	0.703	0.895				
5.000	-0.561	-0.553	-0.497	-0.393	-0.193	0.065	0.304	0.506	0.708				
6.000	-0.565	-0.560	-0.516	-0.436	-0.280	-0.063	0.158	0.359	0.573				
8.000	-0.570	-0.566	-0.537	-0.484	-0.378	-0.216	-0.030	0.178	0.419				
10.000	-0.570	-0.565	-0.543	-0.502	-0.420	-0.291	-0.119	0.087	0.339				
15.000	-0.577	-0.570	-0.547	-0.506	-0.437	-0.338	-0.195	-0.010	0.194				
20.000	-0.585	-0.582	-0.561	-0.525	-0.458	-0.363	-0.244	-0.099	0.077				
30.000	-0.597	-0.595	-0.583	-0.563	-0.514	-0.445	-0.351	-0.235	-0.070				
40.000	-0.607	-0.605	-0.598	-0.585	-0.551	-0.499	-0.422	-0.318	-0.164				
60.000	-0.625	-0.624	-0.620	-0.613	-0.591	-0.556	-0.502	-0.422	-0.294				
80.000	-0.643	-0.644	-0.641	-0.635	-0.621	-0.594	-0.556	-0.497	-0.387				
100.000	-0.662	-0.660	-0.658	-0.656	-0.643	-0.627	-0.602	-0.559	-0.460				

TABLE 30

ANDERS-GREVESSE ABUNDANCES FOR $X = 0.00$ AND $Z = 0.01$

	Log R								
T6	-5.0	-4.5	-4.0	-3.5	-3.0	-2.5	-2.0	-1.5	-1.0
0.006	-3.444	-3.489	-3.523	-3.545	-3.532	-3.500	-3.409	-3.279	-3.118
0.007	-3.283	-3.262	-3.247	-3.238	-3.224	-3.233	-3.140	-2.983	-2.767
0.008	-3.276	-3.279	-3.259	-3.216	-3.158	-3.092	-2.974	-2.778	-2.534
0.009	-2.768	-2.936	-3.041	-3.084	-3.047	-2.972	-2.779	-2.521	-2.237
0.010	-2.176	-2.369	-2.530	-2.658	-2.728	-2.770	-2.613	-2.345	-2.015
0.011	-1.645	-1.810	-1.945	-2.051	-2.107	-2.134	-2.081	-1.938	-1.715
0.012	-1.235	-1.341	-1.425	-1.488	-1.522	-1.519	-1.480	-1.395	-1.331
0.014	-0.818	-0.720	-0.637	-0.570	-0.509	-0.468	-0.418	-0.357	-0.277
0.016	-0.752	-0.557	-0.341	-0.103	0.098	0.239	0.348	0.440	0.530
0.018	-0.747	-0.568	-0.317	0.003	0.331	0.607	0.817	0.973	1.105
0.020	-0.767	-0.591	-0.340	-0.015	0.361	0.737	1.058	1.306	1.495
0.025	-0.759	-0.636	-0.424	-0.124	0.262	0.703	1.158	1.583	1.946
0.030	-0.573	-0.490	-0.326	-0.081	0.248	0.655	1.130	1.603	2.066
0.035	-0.270	-0.138	0.026	0.222	0.479	0.795	1.193	1.639	2.124
0.040	-0.203	0.094	0.371	0.629	0.871	1.122	1.404	1.766	2.207
0.045	-0.233	0.104	0.477	0.886	1.222	1.490	1.728	2.001	2.358
0.050	-0.271	0.014	0.400	0.885	1.362	1.742	2.028	2.280	2.575
0.055	-0.305	-0.046	0.318	0.787	1.317	1.813	2.214	2.518	2.796
0.060	-0.329	-0.085	0.255	0.691	1.204	1.755	2.262	2.664	2.984
0.070	-0.350	-0.133	0.177	0.578	1.061	1.592	2.160	2.700	3.153
0.080	-0.357	-0.154	0.139	0.522	0.986	1.501	2.056	2.625	3.155
0.090	-0.347	-0.153	0.133	0.511	0.970	1.480	2.025	2.584	3.134
0.100	-0.327	-0.131	0.153	0.525	0.992	1.494	2.029	2.575	3.130
0.120	-0.250	-0.068	0.214	0.594	1.062	1.554	2.074	2.613	3.165
0.150	-0.097	0.099	0.384	0.758	1.192	1.682	2.181	2.701	3.218
0.200	-0.057	0.215	0.536	0.906	1.321	1.767	2.218	2.659	3.068
0.250	-0.200	0.113	0.468	0.863	1.275	1.686	2.087	2.466	2.814
0.300	-0.331	-0.027	0.338	0.765	1.184	1.580	1.952	2.290	2.604
0.400	-0.520	-0.303	0.039	0.507	0.980	1.397	1.741	2.042	2.322
0.500	-0.580	-0.450	-0.186	0.211	0.741	1.220	1.589	1.888	2.154
0.600	-0.605	-0.515	-0.293	0.060	0.546	1.051	1.458	1.771	2.042
0.800	-0.623	-0.557	-0.381	-0.096	0.321	0.807	1.251	1.596	1.884
1.000	-0.628	-0.571	-0.418	-0.170	0.205	0.665	1.114	1.490	1.797
1.200	-0.632	-0.577	-0.439	-0.218	0.139	0.586	1.037	1.428	1.744
1.500	-0.613	-0.561	-0.436	-0.239	0.081	0.518	0.973	1.367	1.670
2.000	-0.633	-0.568	-0.433	-0.226	0.074	0.473	0.895	1.243	1.494
2.500	-0.657	-0.614	-0.481	-0.256	0.064	0.451	0.808	1.086	1.299
3.000	-0.668	-0.639	-0.528	-0.334	-0.010	0.364	0.680	0.920	1.119
4.000	-0.683	-0.667	-0.588	-0.447	-0.183	0.147	0.428	0.649	0.846
5.000	-0.689	-0.683	-0.625	-0.516	-0.310	-0.034	0.227	0.447	0.650
6.000	-0.694	-0.688	-0.644	-0.560	-0.400	-0.166	0.073	0.291	0.507
8.000	-0.699	-0.695	-0.665	-0.609	-0.498	-0.326	-0.122	0.094	0.344
10.000	-0.699	-0.694	-0.670	-0.627	-0.541	-0.400	-0.219	-0.003	0.263
15.000	-0.705	-0.700	-0.675	-0.630	-0.554	-0.444	-0.294	-0.096	0.118
20.000	-0.714	-0.712	-0.691	-0.649	-0.575	-0.471	-0.341	-0.185	-0.004
30.000	-0.725	-0.725	-0.713	-0.689	-0.641	-0.563	-0.456	-0.331	-0.159
40.000	-0.735	-0.735	-0.727	-0.711	-0.681	-0.620	-0.532	-0.417	-0.256
60.000	-0.754	-0.752	-0.748	-0.740	-0.720	-0.676	-0.613	-0.521	-0.387
80.000	-0.772	-0.770	-0.768	-0.764	-0.745	-0.714	-0.666	-0.594	-0.481
100.000	-0.791	-0.789	-0.787	-0.785	-0.768	-0.745	-0.710	-0.654	-0.556

TABLE 31

ANDERS-GREVESSE ABUNDANCES FOR $X = 0.70$ AND $Z = 0.02$

	Log R												
T6	-5.0	-4.5	-4.0	-3.5	-3.0	-2.5	-2.0	-1.5	-1.0	-0.5	0.0	0.5	1.0
0.006	-1.565	-1.711	-1.791	-1.807	-1.770	-1.586	-1.427	-1.213	-0.988	-0.728	-0.444	-0.126	0.254
0.007	-0.706	-0.778	-0.810	-0.803	-0.743	-0.641	-0.510	-0.337	-0.147	0.057	0.277	0.516	0.774
0.008	-0.204	-0.103	-0.016	0.056	0.121	0.215	0.318	0.442	0.589	0.754	0.933	1.131	1.349
0.009	-0.065	0.216	0.455	0.652	0.809	0.920	1.020	1.124	1.233	1.360	1.502	1.671	1.860
0.010	-0.062	0.277	0.620	0.966	1.232	1.428	1.565	1.669	1.766	1.871	1.992	2.133	2.295
0.011	-0.088	0.257	0.638	1.057	1.441	1.731	1.933	2.078	2.185	2.283	2.388	2.503	2.648
0.012	-0.120	0.210	0.596	1.038	1.483	1.864	2.157	2.356	2.503	2.616	2.725	2.841	2.970
0.014	-0.125	0.148	0.501	0.933	1.409	1.885	2.313	2.654	2.904	3.086	3.224	3.356	3.480
0.016	-0.126	0.134	0.465	0.868	1.324	1.824	2.311	2.753	3.118	3.384	3.575	3.729	3.863
0.018	-0.131	0.111	0.434	0.836	1.293	1.775	2.269	2.768	3.214	3.563	3.826	4.015	4.170
0.020	-0.138	0.092	0.408	0.809	1.264	1.748	2.257	2.769	3.261	3.681	3.999	4.233	4.421
0.025	-0.123	0.086	0.395	0.803	1.271	1.784	2.317	2.844	3.366	3.860	4.284	4.622	4.866
0.030	-0.047	0.149	0.451	0.860	1.345	1.863	2.408	2.958	3.508	4.020	4.483	4.864	5.157
0.035	0.035	0.254	0.563	0.962	1.439	1.967	2.509	3.054	3.619	4.145	4.626	5.018	5.327
0.040	0.053	0.333	0.678	1.089	1.556	2.067	2.598	3.137	3.685	4.218	4.696	5.090	5.391
0.045	0.043	0.352	0.736	1.193	1.664	2.154	2.666	3.184	3.719				
0.050	0.018	0.314	0.701	1.178	1.686	2.197	2.698	3.204	3.715				
0.055	-0.011	0.283	0.661	1.123	1.640	2.171	2.688	3.189	3.683				
0.060	-0.036	0.247	0.610	1.053	1.563	2.101	2.637	3.154	3.638				
0.070	-0.057	0.196	0.536	0.965	1.459	1.982	2.523	3.059	3.557				
0.080	-0.069	0.171	0.496	0.904	1.387	1.907	2.443	2.985	3.495				
0.090	-0.064	0.169	0.489	0.898	1.368	1.877	2.411	2.946	3.458				
0.100	-0.057	0.189	0.509	0.903	1.374	1.874	2.400	2.932	3.442				
0.120	-0.004	0.222	0.538	0.944	1.414	1.898	2.402	2.917	3.414				
0.150	0.131	0.336	0.634	1.025	1.480	1.954	2.432	2.900	3.331				
0.200	0.187	0.420	0.717	1.077	1.491	1.930	2.368	2.770	3.098				
0.250	0.048	0.320	0.647	1.029	1.435	1.839	2.244	2.599	2.879				
0.300	-0.083	0.184	0.525	0.939	1.363	1.766	2.135	2.454	2.706				
0.400	-0.269	-0.041	0.306	0.770	1.218	1.633	1.973	2.248	2.470				
0.500	-0.347	-0.205	0.095	0.556	1.064	1.515	1.857	2.123	2.331				
0.600	-0.362	-0.269	-0.025	0.371	0.897	1.394	1.760	2.030	2.244				
0.800	-0.381	-0.303	-0.109	0.200	0.659	1.168	1.582	1.883	2.120				
1.000	-0.387	-0.315	-0.145	0.125	0.537	1.018	1.456	1.790	2.050				
1.200	-0.380	-0.317	-0.159	0.094	0.472	0.936	1.382	1.737	2.011				
1.500	-0.364	-0.302	-0.157	0.070	0.426	0.876	1.323	1.685	1.954				
2.000	-0.379	-0.295	-0.138	0.090	0.410	0.832	1.251	1.579	1.800				
2.500	-0.412	-0.338	-0.174	0.079	0.415	0.805	1.160	1.425	1.611				
3.000	-0.426	-0.376	-0.228	0.019	0.370	0.741	1.039	1.261	1.433				
4.000	-0.445	-0.418	-0.308	-0.114	0.204	0.533	0.787	0.980	1.151				
5.000	-0.455	-0.439	-0.357	-0.209	0.048	0.337	0.575	0.766	0.945				
6.000	-0.461	-0.452	-0.389	-0.273	-0.066	0.184	0.408	0.602	0.794				
8.000	-0.467	-0.462	-0.422	-0.347	-0.203	-0.014	0.186	0.392	0.611				
10.000	-0.468	-0.461	-0.430	-0.376	-0.267	-0.114	0.075	0.284	0.513				
15.000	-0.475	-0.465	-0.433	-0.379	-0.295	-0.180	-0.021	0.165	0.348				
20.000	-0.484	-0.478	-0.450	-0.399	-0.312	-0.205	-0.080	0.056	0.210				
30.000	-0.497	-0.496	-0.480	-0.451	-0.388	-0.306	-0.214	-0.111	0.041				
40.000	-0.507	-0.507	-0.498	-0.479	-0.438	-0.379	-0.305	-0.210	-0.065				
60.000	-0.526	-0.524	-0.520	-0.512	-0.489	-0.453	-0.402	-0.328	-0.203				
80.000	-0.544	-0.547	-0.543	-0.534	-0.519	-0.496	-0.463	-0.410	-0.297				
100.000	-0.563	-0.562	-0.560	-0.557	-0.545	-0.532	-0.513	-0.476	-0.370				

TABLE 32

ANDERS-GREVESSE ABUNDANCES FOR $X = 0.35$ AND $Z = 0.02$

	Log R												
T6	-5.0	-4.5	-4.0	-3.5	-3.0	-2.5	-2.0	-1.5	-1.0	-0.5	0.0	0.5	1.0
0.006	-1.716	-1.928	-2.050	-2.083	-2.058	-1.942	-1.816	-1.586	-1.356	-1.096	-0.805	-0.463	-0.048
0.007	-0.954	-1.033	-1.082	-1.104	-1.086	-1.007	-0.882	-0.722	-0.534	-0.330	-0.111	0.136	0.401
0.008	-0.566	-0.452	-0.356	-0.279	-0.211	-0.128	-0.035	0.078	0.217	0.377	0.560	0.756	0.975
0.009	-0.490	-0.231	0.015	0.249	0.432	0.568	0.674	0.775	0.886	1.008	1.148	1.310	1.495
0.010	-0.499	-0.209	0.116	0.475	0.793	1.038	1.202	1.325	1.431	1.539	1.655	1.794	1.950
0.011	-0.514	-0.235	0.112	0.526	0.939	1.287	1.539	1.719	1.847	1.954	2.064	2.180	2.318
0.012	-0.506	-0.259	0.074	0.494	0.945	1.365	1.716	1.967	2.147	2.283	2.400	2.517	2.645
0.014	-0.386	-0.190	0.084	0.436	0.868	1.336	1.798	2.191	2.498	2.719	2.889	3.027	3.158
0.016	-0.352	-0.116	0.169	0.503	0.874	1.304	1.775	2.232	2.650	2.971	3.208	3.387	3.529
0.018	-0.346	-0.121	0.175	0.543	0.943	1.348	1.774	2.244	2.711	3.113	3.422	3.647	3.820
0.020	-0.354	-0.137	0.159	0.535	0.961	1.407	1.840	2.279	2.750	3.197	3.566	3.845	4.051
0.025	-0.334	-0.147	0.140	0.529	0.973	1.473	1.976	2.479	2.950	3.411	3.817	4.178	4.462
0.030	-0.239	-0.069	0.204	0.580	1.042	1.545	2.070	2.609	3.130	3.623	4.056	4.440	4.750
0.035	-0.084	0.096	0.359	0.705	1.149	1.646	2.173	2.708	3.247	3.764	4.237	4.638	4.958
0.040	-0.039	0.249	0.565	0.907	1.308	1.770	2.271	2.792	3.331	3.856	4.346	4.759	5.088
0.045	-0.055	0.276	0.656	1.083	1.496	1.916	2.371	2.870	3.384				
0.050	-0.086	0.217	0.605	1.079	1.580	2.027	2.470	2.937	3.427				
0.055	-0.118	0.174	0.549	1.007	1.534	2.044	2.522	2.983	3.453				
0.060	-0.142	0.129	0.484	0.923	1.440	1.979	2.512	3.001	3.464				
0.070	-0.164	0.082	0.413	0.829	1.317	1.845	2.399	2.945	3.441				
0.080	-0.173	0.058	0.373	0.771	1.245	1.766	2.307	2.867	3.395				
0.090	-0.163	0.059	0.370	0.770	1.227	1.739	2.279	2.827	3.362				
0.100	-0.148	0.077	0.389	0.788	1.242	1.740	2.273	2.817	3.352				
0.120	-0.077	0.133	0.442	0.848	1.299	1.791	2.299	2.831	3.359				
0.150	0.085	0.232	0.527	0.970	1.418	1.890	2.376	2.872	3.351				
0.200	0.137	0.403	0.720	1.089	1.502	1.938	2.378	2.801	3.169				
0.250	-0.014	0.287	0.640	1.045	1.454	1.862	2.266	2.634	2.940				
0.300	-0.154	0.139	0.510	0.958	1.374	1.783	2.154	2.480	2.754				
0.400	-0.358	-0.120	0.251	0.752	1.215	1.633	1.976	2.260	2.501				
0.500	-0.436	-0.287	0.023	0.493	1.020	1.492	1.846	2.123	2.352				
0.600	-0.453	-0.350	-0.099	0.301	0.832	1.348	1.735	2.022	2.254				
0.800	-0.476	-0.395	-0.193	0.132	0.591	1.108	1.541	1.862	2.117				
1.000	-0.480	-0.403	-0.227	0.049	0.468	0.957	1.406	1.761	2.038				
1.200	-0.475	-0.408	-0.244	0.015	0.403	0.869	1.329	1.702	1.993				
1.500	-0.459	-0.407	-0.257	-0.009	0.354	0.808	1.267	1.646	1.932				
2.000	-0.482	-0.394	-0.230	0.008	0.332	0.762	1.193	1.538	1.777				
2.500	-0.512	-0.440	-0.272	-0.007	0.339	0.742	1.109	1.388	1.589				
3.000	-0.526	-0.475	-0.325	-0.078	0.288	0.674	0.991	1.226	1.407				
4.000	-0.545	-0.517	-0.405	-0.210	0.116	0.466	0.740	0.945	1.121				
5.000	-0.555	-0.539	-0.456	-0.305	-0.039	0.267	0.524	0.727	0.909				
6.000	-0.560	-0.550	-0.486	-0.367	-0.154	0.111	0.353	0.557	0.753				
8.000	-0.567	-0.560	-0.519	-0.442	-0.295	-0.091	0.122	0.336	0.565				
10.000	-0.566	-0.560	-0.528	-0.471	-0.358	-0.194	0.005	0.223	0.466				
15.000	-0.574	-0.563	-0.529	-0.473	-0.382	-0.257	-0.091	0.107	0.299				
20.000	-0.583	-0.578	-0.548	-0.494	-0.402	-0.283	-0.147	-0.001	0.156				
30.000	-0.596	-0.594	-0.577	-0.547	-0.481	-0.392	-0.288	-0.177	-0.021				
40.000	-0.606	-0.604	-0.594	-0.576	-0.532	-0.469	-0.385	-0.280	-0.130				
60.000	-0.625	-0.623	-0.618	-0.610	-0.584	-0.543	-0.484	-0.401	-0.271				
80.000	-0.643	-0.644	-0.640	-0.633	-0.616	-0.586	-0.544	-0.481	-0.369				
100.000	-0.662	-0.660	-0.657	-0.654	-0.640	-0.621	-0.593	-0.546	-0.444				

TABLE 33

ANDERS-GREVESSE ABUNDANCES FOR $X = 0.00$ AND $Z = 0.02$

	Log R								
T6	-5.0	-4.5	-4.0	-3.5	-3.0	-2.5	-2.0	-1.5	-1.0
0.006	-3.149	-3.194	-3.228	-3.251	-3.237	-3.205	-3.113	-2.982	-2.821
0.007	-2.989	-2.967	-2.951	-2.942	-2.928	-2.937	-2.844	-2.687	-2.469
0.008	-3.019	-3.003	-2.971	-2.924	-2.865	-2.798	-2.679	-2.482	-2.237
0.009	-2.652	-2.768	-2.827	-2.831	-2.771	-2.683	-2.485	-2.225	-1.939
0.010	-2.134	-2.306	-2.438	-2.530	-2.556	-2.543	-2.353	-2.068	-1.727
0.011	-1.617	-1.770	-1.891	-1.979	-2.014	-2.011	-1.925	-1.741	-1.480
0.012	-1.214	-1.313	-1.390	-1.444	-1.466	-1.447	-1.386	-1.272	-1.200
0.014	-0.794	-0.690	-0.603	-0.535	-0.466	-0.423	-0.366	-0.291	-0.195
0.016	-0.718	-0.517	-0.296	-0.057	0.148	0.292	0.406	0.506	0.607
0.018	-0.708	-0.520	-0.264	0.061	0.391	0.671	0.886	1.049	1.193
0.020	-0.730	-0.539	-0.279	0.052	0.431	0.808	1.134	1.391	1.591
0.025	-0.714	-0.581	-0.358	-0.046	0.349	0.790	1.247	1.680	2.052
0.030	-0.527	-0.434	-0.260	-0.007	0.331	0.747	1.230	1.714	2.182
0.035	-0.234	-0.097	0.073	0.275	0.540	0.870	1.285	1.750	2.241
0.040	-0.166	0.128	0.404	0.663	0.912	1.174	1.475	1.860	2.315
0.045	-0.186	0.145	0.511	0.915	1.252	1.526	1.777	2.072	2.446
0.050	-0.220	0.067	0.448	0.923	1.391	1.771	2.065	2.330	2.644
0.055	-0.253	0.014	0.378	0.839	1.358	1.846	2.247	2.557	2.847
0.060	-0.277	-0.022	0.320	0.752	1.258	1.799	2.300	2.701	3.026
0.070	-0.297	-0.067	0.249	0.651	1.130	1.654	2.213	2.744	3.191
0.080	-0.304	-0.084	0.218	0.603	1.061	1.572	2.119	2.680	3.201
0.090	-0.294	-0.082	0.215	0.598	1.049	1.556	2.093	2.644	3.184
0.100	-0.276	-0.062	0.236	0.616	1.075	1.570	2.096	2.638	3.181
0.120	-0.185	0.007	0.296	0.682	1.148	1.633	2.140	2.668	3.209
0.150	0.007	0.205	0.487	0.856	1.281	1.763	2.250	2.757	3.262
0.200	0.061	0.345	0.668	1.030	1.434	1.872	2.320	2.758	3.155
0.250	-0.110	0.228	0.598	1.000	1.411	1.824	2.228	2.608	2.939
0.300	-0.261	0.069	0.457	0.903	1.334	1.740	2.121	2.458	2.752
0.400	-0.482	-0.219	0.161	0.659	1.149	1.583	1.939	2.236	2.494
0.500	-0.556	-0.398	-0.092	0.363	0.922	1.421	1.801	2.094	2.339
0.600	-0.583	-0.471	-0.214	0.188	0.717	1.255	1.678	1.985	2.235
0.800	-0.603	-0.518	-0.309	0.022	0.479	1.002	1.468	1.814	2.086
1.000	-0.606	-0.527	-0.343	-0.054	0.361	0.853	1.324	1.704	1.999
1.200	-0.608	-0.533	-0.363	-0.097	0.296	0.771	1.240	1.638	1.948
1.500	-0.586	-0.517	-0.362	-0.121	0.241	0.704	1.175	1.578	1.886
2.000	-0.610	-0.521	-0.354	-0.108	0.226	0.656	1.105	1.473	1.736
2.500	-0.641	-0.574	-0.403	-0.128	0.230	0.647	1.033	1.332	1.550
3.000	-0.655	-0.606	-0.457	-0.207	0.172	0.582	0.922	1.175	1.368
4.000	-0.674	-0.647	-0.534	-0.338	-0.005	0.371	0.672	0.895	1.077
5.000	-0.683	-0.670	-0.585	-0.429	-0.156	0.171	0.452	0.672	0.860
6.000	-0.689	-0.679	-0.613	-0.492	-0.273	0.012	0.274	0.495	0.696
8.000	-0.696	-0.690	-0.647	-0.567	-0.413	-0.196	0.036	0.260	0.498
10.000	-0.695	-0.689	-0.656	-0.595	-0.478	-0.300	-0.090	0.139	0.399
15.000	-0.701	-0.692	-0.657	-0.596	-0.498	-0.359	-0.183	0.029	0.233
20.000	-0.712	-0.708	-0.677	-0.617	-0.516	-0.384	-0.235	-0.077	0.086
30.000	-0.725	-0.724	-0.707	-0.673	-0.606	-0.506	-0.387	-0.265	-0.106
40.000	-0.735	-0.735	-0.724	-0.702	-0.661	-0.587	-0.491	-0.376	-0.219
60.000	-0.754	-0.752	-0.746	-0.736	-0.712	-0.663	-0.594	-0.499	-0.362
80.000	-0.772	-0.770	-0.767	-0.762	-0.740	-0.706	-0.654	-0.578	-0.461
100.000	-0.791	-0.789	-0.787	-0.783	-0.765	-0.740	-0.701	-0.641	-0.540

TABLE 34

ANDERS-GREVESSE ABUNDANCES FOR $X = 0.70$ AND $Z = 0.03$

	Log R												
T6	-5.0	-4.5	-4.0	-3.5	-3.0	-2.5	-2.0	-1.5	-1.0	-0.5	0.0	0.5	1.0
0.006	-1.558	-1.701	-1.779	-1.793	-1.754	-1.572	-1.416	-1.202	-0.957	-0.687	-0.387	-0.049	0.355
0.007	-0.702	-0.773	-0.805	-0.797	-0.736	-0.634	-0.501	-0.327	-0.135	0.078	0.305	0.551	0.820
0.008	-0.200	-0.099	-0.013	0.060	0.126	0.221	0.325	0.451	0.600	0.771	0.954	1.159	1.383
0.009	-0.058	0.221	0.459	0.657	0.814	0.926	1.027	1.134	1.245	1.376	1.524	1.698	1.893
0.010	-0.054	0.285	0.627	0.973	1.239	1.435	1.573	1.679	1.780	1.889	2.013	2.160	2.330
0.011	-0.078	0.268	0.650	1.068	1.451	1.741	1.944	2.091	2.201	2.302	2.410	2.530	2.680
0.012	-0.108	0.222	0.609	1.051	1.496	1.876	2.169	2.370	2.520	2.635	2.749	2.869	3.002
0.014	-0.111	0.165	0.520	0.952	1.427	1.902	2.329	2.671	2.921	3.105	3.247	3.383	3.510
0.016	-0.108	0.155	0.488	0.892	1.347	1.844	2.332	2.772	3.137	3.405	3.597	3.752	3.889
0.018	-0.110	0.135	0.459	0.862	1.316	1.797	2.291	2.789	3.236	3.584	3.847	4.037	4.192
0.020	-0.116	0.118	0.435	0.834	1.288	1.769	2.278	2.790	3.282	3.701	4.019	4.252	4.438
0.025	-0.104	0.111	0.422	0.829	1.295	1.804	2.338	2.865	3.384	3.875	4.298	4.636	4.879
0.030	-0.025	0.174	0.478	0.885	1.369	1.886	2.431	2.981	3.527	4.035	4.497	4.875	5.165
0.035	0.056	0.279	0.589	0.988	1.463	1.990	2.532	3.074	3.637	4.159	4.638	5.026	5.333
0.040	0.074	0.354	0.700	1.112	1.578	2.088	2.619	3.157	3.701	4.231	4.706	5.095	5.394
0.045	0.070	0.378	0.760	1.214	1.685	2.175	2.688	3.202	3.736				
0.050	0.048	0.344	0.730	1.204	1.709	2.220	2.720	3.225	3.735				
0.055	0.020	0.318	0.696	1.155	1.670	2.199	2.714	3.215	3.707				
0.060	-0.004	0.284	0.649	1.090	1.599	2.136	2.670	3.185	3.667				
0.070	-0.023	0.237	0.581	1.010	1.503	2.025	2.564	3.099	3.593				
0.080	-0.034	0.216	0.546	0.954	1.435	1.954	2.489	3.031	3.536				
0.090	-0.028	0.215	0.542	0.952	1.420	1.927	2.459	2.993	3.500				
0.100	-0.022	0.236	0.563	0.960	1.428	1.924	2.448	2.978	3.483				
0.120	0.041	0.273	0.593	1.002	1.472	1.952	2.451	2.962	3.453				
0.150	0.203	0.408	0.705	1.094	1.545	2.016	2.491	2.957	3.385				
0.200	0.269	0.513	0.813	1.169	1.579	2.016	2.456	2.862	3.190				
0.250	0.113	0.405	0.744	1.131	1.537	1.943	2.351	2.712	2.992				
0.300	-0.034	0.254	0.611	1.038	1.470	1.878	2.253	2.579	2.829				
0.400	-0.238	0.023	0.393	0.873	1.327	1.752	2.103	2.385	2.603				
0.500	-0.327	-0.155	0.176	0.667	1.186	1.645	1.995	2.265	2.467				
0.600	-0.344	-0.230	0.043	0.475	1.024	1.532	1.904	2.176	2.382				
0.800	-0.365	-0.268	-0.048	0.293	0.781	1.308	1.730	2.031	2.260				
1.000	-0.369	-0.281	-0.086	0.215	0.654	1.154	1.601	1.936	2.189				
1.200	-0.362	-0.281	-0.098	0.185	0.586	1.067	1.523	1.880	2.150				
1.500	-0.344	-0.267	-0.099	0.161	0.542	1.005	1.462	1.827	2.096				
2.000	-0.360	-0.258	-0.079	0.177	0.521	0.960	1.390	1.726	1.952				
2.500	-0.398	-0.304	-0.114	0.170	0.529	0.936	1.305	1.579	1.768				
3.000	-0.414	-0.346	-0.171	0.112	0.491	0.880	1.190	1.418	1.588				
4.000	-0.437	-0.398	-0.262	-0.029	0.327	0.676	0.939	1.133	1.297				
5.000	-0.449	-0.426	-0.322	-0.138	0.159	0.471	0.718	0.909	1.080				
6.000	-0.456	-0.442	-0.362	-0.215	0.029	0.304	0.539	0.734	0.918				
8.000	-0.464	-0.457	-0.405	-0.310	-0.136	0.079	0.294	0.504	0.716				
10.000	-0.465	-0.457	-0.418	-0.348	-0.216	-0.039	0.167	0.383	0.607				
15.000	-0.471	-0.458	-0.419	-0.353	-0.251	-0.117	0.057	0.251	0.427				
20.000	-0.483	-0.474	-0.437	-0.373	-0.269	-0.145	-0.008	0.129	0.272				
30.000	-0.496	-0.494	-0.474	-0.436	-0.360	-0.264	-0.166	-0.064	0.082				
40.000	-0.507	-0.506	-0.495	-0.472	-0.422	-0.353	-0.274	-0.178	-0.035				
60.000	-0.526	-0.524	-0.518	-0.508	-0.482	-0.441	-0.386	-0.309	-0.181				
80.000	-0.544	-0.547	-0.542	-0.532	-0.515	-0.489	-0.452	-0.395	-0.280				
100.000	-0.563	-0.562	-0.560	-0.555	-0.543	-0.526	-0.504	-0.463	-0.354				

TABLE 35

ANDERS-GREVESSE ABUNDANCES FOR $X = 0.35$ AND $Z = 0.03$

	Log R												
T6	-5.0	-4.5	-4.0	-3.5	-3.0	-2.5	-2.0	-1.5	-1.0	-0.5	0.0	0.5	1.0
0.006	-1.707	-1.913	-2.031	-2.059	-2.032	-1.916	-1.788	-1.556	-1.320	-1.051	-0.744	-0.384	0.052
0.007	-0.949	-1.026	-1.075	-1.095	-1.074	-0.994	-0.867	-0.705	-0.514	-0.306	-0.080	0.174	0.451
0.008	-0.560	-0.446	-0.351	-0.274	-0.204	-0.120	-0.026	0.090	0.233	0.398	0.585	0.787	1.014
0.009	-0.481	-0.224	0.022	0.255	0.439	0.576	0.683	0.787	0.900	1.027	1.173	1.342	1.533
0.010	-0.489	-0.199	0.126	0.485	0.802	1.048	1.212	1.338	1.446	1.559	1.681	1.826	1.989
0.011	-0.502	-0.221	0.126	0.540	0.952	1.300	1.553	1.732	1.866	1.977	2.091	2.212	2.357
0.012	-0.493	-0.244	0.091	0.511	0.961	1.381	1.732	1.985	2.168	2.307	2.428	2.551	2.685
0.014	-0.372	-0.172	0.105	0.459	0.890	1.359	1.819	2.214	2.522	2.745	2.920	3.061	3.198
0.016	-0.334	-0.094	0.194	0.530	0.900	1.330	1.801	2.259	2.677	2.999	3.239	3.420	3.565
0.018	-0.325	-0.096	0.203	0.572	0.971	1.376	1.803	2.275	2.742	3.144	3.453	3.679	3.852
0.020	-0.333	-0.110	0.190	0.565	0.989	1.433	1.868	2.306	2.781	3.228	3.596	3.875	4.079
0.025	-0.314	-0.121	0.170	0.559	1.001	1.500	2.001	2.506	2.977	3.438	3.840	4.199	4.481
0.030	-0.214	-0.041	0.234	0.610	1.070	1.573	2.097	2.636	3.154	3.646	4.075	4.459	4.766
0.035	-0.061	0.122	0.387	0.734	1.177	1.673	2.200	2.735	3.270	3.783	4.254	4.653	4.969
0.040	-0.015	0.271	0.587	0.931	1.331	1.795	2.297	2.817	3.354	3.875	4.362	4.771	5.096
0.045	-0.025	0.303	0.679	1.103	1.517	1.939	2.395	2.894	3.405				
0.050	-0.053	0.250	0.635	1.104	1.601	2.048	2.492	2.960	3.448				
0.055	-0.084	0.212	0.587	1.041	1.563	2.069	2.545	3.007	3.475				
0.060	-0.108	0.170	0.527	0.963	1.476	2.012	2.540	3.028	3.488				
0.070	-0.128	0.125	0.460	0.877	1.362	1.888	2.438	2.980	3.471				
0.080	-0.137	0.106	0.426	0.825	1.296	1.815	2.352	2.909	3.431				
0.090	-0.126	0.108	0.425	0.828	1.281	1.791	2.327	2.872	3.400				
0.100	-0.112	0.126	0.446	0.847	1.299	1.792	2.322	2.862	3.391				
0.120	-0.033	0.185	0.498	0.907	1.360	1.846	2.347	2.873	3.393				
0.150	0.155	0.307	0.601	1.035	1.481	1.948	2.428	2.918	3.391				
0.200	0.217	0.490	0.809	1.173	1.580	2.013	2.453	2.878	3.243				
0.250	0.048	0.366	0.729	1.137	1.545	1.955	2.363	2.735	3.037				
0.300	-0.106	0.204	0.590	1.050	1.471	1.887	2.264	2.595	2.864				
0.400	-0.328	-0.059	0.334	0.851	1.320	1.748	2.101	2.389	2.622				
0.500	-0.417	-0.241	0.096	0.596	1.137	1.618	1.980	2.259	2.479				
0.600	-0.435	-0.313	-0.036	0.397	0.951	1.480	1.875	2.162	2.385				
0.800	-0.460	-0.362	-0.135	0.221	0.703	1.239	1.683	2.004	2.250				
1.000	-0.462	-0.368	-0.169	0.134	0.578	1.085	1.545	1.902	2.172				
1.200	-0.456	-0.371	-0.185	0.103	0.513	0.994	1.464	1.840	2.127				
1.500	-0.439	-0.370	-0.197	0.080	0.467	0.933	1.400	1.783	2.070				
2.000	-0.464	-0.357	-0.171	0.094	0.439	0.886	1.328	1.682	1.927				
2.500	-0.498	-0.406	-0.213	0.083	0.451	0.869	1.251	1.540	1.744				
3.000	-0.514	-0.445	-0.269	0.013	0.408	0.811	1.141	1.382	1.562				
4.000	-0.536	-0.496	-0.360	-0.126	0.239	0.610	0.892	1.099	1.268				
5.000	-0.549	-0.525	-0.420	-0.234	0.072	0.402	0.669	0.872	1.046				
6.000	-0.556	-0.541	-0.459	-0.309	-0.058	0.232	0.486	0.692	0.879				
8.000	-0.564	-0.555	-0.502	-0.405	-0.226	0.004	0.232	0.451	0.673				
10.000	-0.563	-0.555	-0.515	-0.443	-0.306	-0.117	0.099	0.325	0.564				
15.000	-0.570	-0.556	-0.514	-0.446	-0.338	-0.192	-0.010	0.197	0.383				
20.000	-0.582	-0.574	-0.535	-0.467	-0.357	-0.219	-0.071	0.076	0.222				
30.000	-0.595	-0.592	-0.571	-0.532	-0.452	-0.348	-0.237	-0.127	0.022				
40.000	-0.606	-0.604	-0.591	-0.568	-0.516	-0.442	-0.352	-0.247	-0.099				
60.000	-0.625	-0.623	-0.617	-0.606	-0.577	-0.531	-0.468	-0.381	-0.249				
80.000	-0.643	-0.644	-0.640	-0.631	-0.612	-0.579	-0.533	-0.466	-0.351				
100.000	-0.662	-0.660	-0.657	-0.653	-0.638	-0.616	-0.584	-0.533	-0.428				

TABLE 36

ANDERS-GREVESSE ABUNDANCES FOR $X = 0.00$ AND $Z = 0.03$

	Log R								
T6	-5.0	-4.5	-4.0	-3.5	-3.0	-2.5	-2.0	-1.5	-1.0
0.006	-2.975	-3.020	-3.054	-3.077	-3.063	-3.030	-2.939	-2.808	-2.646
0.007	-2.816	-2.793	-2.777	-2.768	-2.753	-2.763	-2.670	-2.513	-2.295
0.008	-2.859	-2.836	-2.800	-2.752	-2.692	-2.624	-2.506	-2.308	-2.063
0.009	-2.562	-2.648	-2.685	-2.672	-2.604	-2.511	-2.312	-2.051	-1.765
0.010	-2.099	-2.254	-2.366	-2.433	-2.435	-2.397	-2.193	-1.901	-1.557
0.011	-1.595	-1.739	-1.848	-1.923	-1.944	-1.921	-1.815	-1.610	-1.331
0.012	-1.199	-1.293	-1.365	-1.412	-1.426	-1.394	-1.317	-1.184	-1.108
0.014	-0.778	-0.670	-0.581	-0.513	-0.438	-0.394	-0.331	-0.247	-0.139
0.016	-0.696	-0.490	-0.268	-0.028	0.181	0.324	0.442	0.548	0.657
0.018	-0.681	-0.489	-0.229	0.098	0.430	0.711	0.928	1.097	1.249
0.020	-0.705	-0.506	-0.239	0.095	0.476	0.854	1.182	1.444	1.651
0.025	-0.683	-0.543	-0.313	0.007	0.406	0.849	1.306	1.744	2.122
0.030	-0.494	-0.394	-0.215	0.045	0.389	0.812	1.300	1.789	2.259
0.035	-0.210	-0.067	0.107	0.313	0.585	0.924	1.350	1.827	2.323
0.040	-0.139	0.153	0.429	0.689	0.942	1.213	1.527	1.927	2.392
0.045	-0.152	0.174	0.536	0.936	1.274	1.553	1.815	2.124	2.511
0.050	-0.183	0.105	0.482	0.949	1.413	1.793	2.093	2.369	2.696
0.055	-0.216	0.056	0.420	0.877	1.387	1.870	2.272	2.586	2.886
0.060	-0.239	0.023	0.368	0.796	1.296	1.831	2.328	2.729	3.058
0.070	-0.258	-0.020	0.301	0.705	1.179	1.699	2.252	2.777	3.221
0.080	-0.266	-0.034	0.276	0.662	1.116	1.625	2.165	2.722	3.237
0.090	-0.255	-0.031	0.274	0.661	1.107	1.611	2.144	2.690	3.222
0.100	-0.239	-0.012	0.295	0.682	1.136	1.627	2.147	2.685	3.221
0.120	-0.140	0.060	0.354	0.745	1.212	1.693	2.191	2.710	3.245
0.150	0.078	0.277	0.559	0.925	1.345	1.824	2.302	2.800	3.298
0.200	0.139	0.430	0.755	1.112	1.510	1.944	2.389	2.826	3.219
0.250	-0.051	0.303	0.682	1.087	1.498	1.911	2.318	2.701	3.028
0.300	-0.215	0.131	0.532	0.988	1.426	1.838	2.225	2.566	2.855
0.400	-0.454	-0.161	0.241	0.754	1.251	1.694	2.059	2.359	2.609
0.500	-0.537	-0.357	-0.024	0.463	1.034	1.543	1.930	2.225	2.461
0.600	-0.567	-0.436	-0.155	0.277	0.828	1.382	1.813	2.121	2.362
0.800	-0.587	-0.486	-0.256	0.105	0.584	1.125	1.605	1.952	2.216
1.000	-0.589	-0.492	-0.286	0.028	0.465	0.973	1.457	1.840	2.129
1.200	-0.590	-0.497	-0.304	-0.011	0.401	0.890	1.370	1.771	2.079
1.500	-0.566	-0.482	-0.305	-0.034	0.351	0.825	1.303	1.711	2.020
2.000	-0.593	-0.486	-0.296	-0.023	0.331	0.776	1.236	1.612	1.883
2.500	-0.628	-0.541	-0.345	-0.038	0.339	0.771	1.171	1.481	1.704
3.000	-0.643	-0.579	-0.403	-0.117	0.291	0.716	1.070	1.330	1.523
4.000	-0.666	-0.627	-0.490	-0.255	0.117	0.515	0.825	1.049	1.226
5.000	-0.677	-0.657	-0.551	-0.358	-0.045	0.307	0.598	0.819	1.000
6.000	-0.685	-0.670	-0.587	-0.435	-0.176	0.136	0.410	0.633	0.827
8.000	-0.693	-0.685	-0.631	-0.529	-0.344	-0.099	0.149	0.379	0.611
10.000	-0.692	-0.685	-0.643	-0.567	-0.426	-0.220	0.008	0.245	0.501
15.000	-0.698	-0.685	-0.642	-0.569	-0.453	-0.293	-0.099	0.123	0.322
20.000	-0.710	-0.705	-0.665	-0.590	-0.469	-0.317	-0.153	0.007	0.159
30.000	-0.724	-0.723	-0.701	-0.658	-0.576	-0.459	-0.331	-0.210	-0.058
40.000	-0.734	-0.734	-0.721	-0.694	-0.644	-0.559	-0.456	-0.339	-0.186
60.000	-0.754	-0.752	-0.745	-0.733	-0.705	-0.650	-0.577	-0.478	-0.340
80.000	-0.772	-0.770	-0.766	-0.760	-0.736	-0.698	-0.642	-0.563	-0.443
100.000	-0.791	-0.789	-0.786	-0.782	-0.762	-0.734	-0.692	-0.629	-0.524

TABLE 37

COX-TABOR ABUNDANCES FOR $X = 0.70$ AND $Z = 0.001$

	Log R												
T6	-5.0	-4.5	-4.0	-3.5	-3.0	-2.5	-2.0	-1.5	-1.0	-0.5	0.0	0.5	1.0
0.006	-1.585	-1.736	-1.822	-1.842	-1.810	-1.624	-1.465	-1.256	-1.082	-0.853	-0.618	-0.371	-0.096
0.007	-0.720	-0.792	-0.827	-0.823	-0.765	-0.665	-0.540	-0.374	-0.195	-0.017	0.181	0.396	0.624
0.008	-0.220	-0.117	-0.030	0.041	0.102	0.194	0.291	0.409	0.546	0.694	0.855	1.034	1.231
0.009	-0.089	0.196	0.438	0.636	0.790	0.898	0.992	1.090	1.188	1.299	1.423	1.570	1.739
0.010	-0.097	0.243	0.588	0.937	1.204	1.399	1.533	1.630	1.716	1.808	1.912	2.034	2.173
0.011	-0.133	0.206	0.586	1.006	1.399	1.691	1.894	2.034	2.128	2.214	2.307	2.406	2.537
0.012	-0.168	0.153	0.534	0.976	1.429	1.819	2.114	2.306	2.446	2.547	2.644	2.745	2.861
0.014	-0.188	0.068	0.413	0.845	1.331	1.819	2.252	2.594	2.846	3.021	3.148	3.269	3.387
0.016	-0.206	0.042	0.365	0.763	1.224	1.742	2.231	2.682	3.051	3.316	3.506	3.657	3.791
0.018	-0.223	0.006	0.325	0.732	1.204	1.694	2.189	2.693	3.144	3.498	3.761	3.954	4.113
0.020	-0.232	-0.022	0.291	0.707	1.177	1.671	2.182	2.696	3.191	3.619	3.944	4.184	4.377
0.025	-0.208	-0.021	0.280	0.697	1.183	1.709	2.242	2.775	3.308	3.813	4.241	4.585	4.837
0.030	-0.143	0.040	0.342	0.761	1.259	1.784	2.328	2.879	3.447	3.975	4.445	4.834	5.139
0.035	-0.053	0.151	0.456	0.862	1.354	1.887	2.433	2.988	3.559	4.104	4.592	4.996	5.313
0.040	-0.036	0.244	0.590	1.001	1.474	1.991	2.526	3.077	3.637	4.179	4.668	5.074	5.384
0.045	-0.065	0.245	0.635	1.106	1.580	2.077	2.592	3.126	3.669				
0.050	-0.098	0.190	0.580	1.070	1.592	2.109	2.616	3.135	3.655				
0.055	-0.131	0.145	0.517	0.985	1.512	2.057	2.588	3.103	3.610				
0.060	-0.158	0.105	0.458	0.901	1.415	1.957	2.512	3.047	3.550				
0.070	-0.190	0.037	0.363	0.788	1.288	1.805	2.362	2.916	3.443				
0.080	-0.209	-0.004	0.303	0.713	1.207	1.722	2.270	2.822	3.367				
0.090	-0.204	-0.012	0.287	0.693	1.178	1.691	2.232	2.781	3.329				
0.100	-0.205	-0.005	0.292	0.686	1.174	1.692	2.228	2.772	3.318				
0.120	-0.193	0.013	0.315	0.715	1.196	1.710	2.236	2.772	3.303				
0.150	-0.193	0.020	0.329	0.733	1.208	1.701	2.193	2.682	3.159				
0.200	-0.220	-0.037	0.241	0.614	1.047	1.489	1.918	2.335	2.749				
0.250	-0.278	-0.119	0.128	0.463	0.851	1.251	1.641	2.024	2.412				
0.300	-0.329	-0.191	0.032	0.341	0.695	1.063	1.426	1.791	2.169				
0.400	-0.400	-0.322	-0.144	0.135	0.465	0.801	1.137	1.486	1.853				
0.500	-0.424	-0.377	-0.246	-0.030	0.282	0.626	0.963	1.309	1.659				
0.600	-0.432	-0.398	-0.294	-0.119	0.165	0.507	0.852	1.192	1.532				
0.800	-0.442	-0.418	-0.338	-0.201	0.038	0.359	0.701	1.035	1.369				
1.000	-0.448	-0.429	-0.361	-0.245	-0.030	0.280	0.624	0.958	1.280				
1.200	-0.445	-0.429	-0.370	-0.268	-0.071	0.229	0.578	0.909	1.209				
1.500	-0.441	-0.425	-0.371	-0.277	-0.103	0.183	0.522	0.832	1.097				
2.000	-0.449	-0.432	-0.375	-0.278	-0.111	0.140	0.427	0.686	0.918				
2.500	-0.458	-0.446	-0.396	-0.310	-0.156	0.068	0.309	0.535	0.771				
3.000	-0.463	-0.454	-0.416	-0.348	-0.215	-0.024	0.188	0.403	0.655				
4.000	-0.468	-0.463	-0.438	-0.391	-0.296	-0.152	0.028	0.239	0.520				
5.000	-0.471	-0.466	-0.447	-0.411	-0.339	-0.221	-0.061	0.149	0.429				
6.000	-0.473	-0.470	-0.454	-0.423	-0.361	-0.260	-0.115	0.093	0.366				
8.000	-0.475	-0.474	-0.461	-0.436	-0.384	-0.301	-0.173	0.024	0.285				
10.000	-0.477	-0.474	-0.463	-0.443	-0.398	-0.327	-0.199	-0.021	0.231				
15.000	-0.483	-0.482	-0.472	-0.453	-0.416	-0.359	-0.251	-0.092	0.129				
20.000	-0.488	-0.486	-0.478	-0.465	-0.431	-0.378	-0.287	-0.146	0.056				
30.000	-0.498	-0.498	-0.493	-0.483	-0.455	-0.412	-0.338	-0.223	-0.050				
40.000	-0.508	-0.508	-0.504	-0.496	-0.474	-0.438	-0.376	-0.280	-0.129				
60.000	-0.526	-0.525	-0.522	-0.518	-0.503	-0.477	-0.436	-0.369	-0.246				
80.000	-0.544	-0.547	-0.545	-0.538	-0.527	-0.511	-0.486	-0.440	-0.333				
100.000	-0.563	-0.562	-0.561	-0.560	-0.551	-0.542	-0.531	-0.501	-0.401				

TABLE 38

COX-TABOR ABUNDANCES FOR $X = 0.35$ AND $Z = 0.001$

	Log R												
T6	-5.0	-4.5	-4.0	-3.5	-3.0	-2.5	-2.0	-1.5	-1.0	-0.5	0.0	0.5	1.0
0.006	-1.741	-1.965	-2.099	-2.142	-2.125	-2.007	-1.893	-1.669	-1.460	-1.232	-0.992	-0.708	-0.386
0.007	-0.974	-1.053	-1.106	-1.131	-1.119	-1.045	-0.928	-0.775	-0.601	-0.417	-0.223	-0.005	0.226
0.008	-0.589	-0.472	-0.376	-0.300	-0.235	-0.156	-0.069	0.034	0.161	0.300	0.468	0.638	0.832
0.009	-0.525	-0.261	-0.011	0.225	0.407	0.540	0.640	0.733	0.831	0.935	1.052	1.181	1.338
0.010	-0.542	-0.256	0.070	0.436	0.755	1.002	1.161	1.276	1.370	1.464	1.551	1.665	1.797
0.011	-0.564	-0.298	0.043	0.458	0.881	1.233	1.482	1.666	1.777	1.866	1.957	2.055	2.168
0.012	-0.559	-0.326	-0.003	0.410	0.867	1.297	1.655	1.901	2.071	2.190	2.292	2.390	2.498
0.014	-0.453	-0.275	-0.017	0.323	0.757	1.226	1.711	2.105	2.411	2.628	2.783	2.906	3.022
0.016	-0.438	-0.217	0.055	0.378	0.751	1.192	1.666	2.125	2.551	2.871	3.104	3.277	3.416
0.018	-0.446	-0.239	0.049	0.418	0.829	1.237	1.662	2.129	2.600	3.008	3.322	3.550	3.726
0.020	-0.452	-0.265	0.022	0.408	0.851	1.311	1.740	2.178	2.643	3.091	3.472	3.755	3.972
0.025	-0.428	-0.265	0.011	0.399	0.861	1.376	1.887	2.384	2.855	3.321	3.747	4.116	4.412
0.030	-0.347	-0.191	0.077	0.459	0.936	1.445	1.977	2.511	3.044	3.549	3.997	4.389	4.708
0.035	-0.177	-0.012	0.243	0.587	1.046	1.549	2.079	2.618	3.169	3.704	4.188	4.597	4.930
0.040	-0.134	0.159	0.476	0.816	1.217	1.678	2.183	2.712	3.259	3.801	4.303	4.728	5.067
0.045	-0.173	0.169	0.560	1.001	1.416	1.833	2.291	2.794	3.322				
0.050	-0.213	0.084	0.480	0.975	1.497	1.950	2.391	2.862	3.365				
0.055	-0.247	0.023	0.394	0.865	1.416	1.948	2.440	2.907	3.388				
0.060	-0.274	-0.030	0.316	0.763	1.287	1.848	2.407	2.911	3.391				
0.070	-0.306	-0.090	0.226	0.641	1.139	1.673	2.253	2.825	3.349				
0.080	-0.320	-0.132	0.164	0.568	1.055	1.580	2.144	2.722	3.282				
0.090	-0.309	-0.134	0.154	0.556	1.029	1.550	2.104	2.672	3.243				
0.100	-0.298	-0.126	0.161	0.563	1.033	1.557	2.105	2.664	3.235				
0.120	-0.262	-0.075	0.218	0.616	1.083	1.605	2.145	2.703	3.263				
0.150	-0.234	-0.102	0.208	0.697	1.173	1.677	2.192	2.723	3.241				
0.200	-0.261	-0.039	0.271	0.670	1.119	1.573	2.026	2.479	2.923				
0.250	-0.333	-0.140	0.144	0.521	0.933	1.346	1.755	2.168	2.584				
0.300	-0.396	-0.226	0.034	0.386	0.761	1.143	1.526	1.920	2.325				
0.400	-0.483	-0.388	-0.180	0.143	0.495	0.853	1.212	1.589	1.979				
0.500	-0.510	-0.447	-0.294	-0.051	0.289	0.659	1.021	1.390	1.763				
0.600	-0.521	-0.475	-0.352	-0.153	0.158	0.525	0.891	1.253	1.614				
0.800	-0.535	-0.504	-0.409	-0.251	0.016	0.360	0.722	1.075	1.425				
1.000	-0.542	-0.519	-0.441	-0.308	-0.069	0.263	0.628	0.980	1.313				
1.200	-0.540	-0.519	-0.452	-0.339	-0.122	0.201	0.568	0.916	1.227				
1.500	-0.537	-0.528	-0.466	-0.352	-0.161	0.144	0.500	0.824	1.102				
2.000	-0.548	-0.528	-0.464	-0.358	-0.178	0.091	0.391	0.663	0.910				
2.500	-0.557	-0.543	-0.489	-0.395	-0.228	0.009	0.265	0.505	0.755				
3.000	-0.562	-0.552	-0.511	-0.438	-0.296	-0.092	0.134	0.365	0.626				
4.000	-0.567	-0.561	-0.533	-0.483	-0.382	-0.229	-0.035	0.193	0.473				
5.000	-0.570	-0.567	-0.545	-0.505	-0.428	-0.302	-0.124	0.095	0.372				
6.000	-0.572	-0.569	-0.551	-0.517	-0.452	-0.343	-0.181	0.028	0.303				
8.000	-0.574	-0.572	-0.558	-0.532	-0.478	-0.384	-0.248	-0.049	0.221				
10.000	-0.576	-0.573	-0.561	-0.539	-0.492	-0.412	-0.281	-0.096	0.167				
15.000	-0.582	-0.579	-0.569	-0.550	-0.510	-0.447	-0.337	-0.167	0.062				
20.000	-0.587	-0.585	-0.577	-0.561	-0.528	-0.470	-0.373	-0.222	-0.013				
30.000	-0.597	-0.596	-0.590	-0.579	-0.551	-0.507	-0.423	-0.300	-0.119				
40.000	-0.607	-0.605	-0.601	-0.593	-0.569	-0.531	-0.462	-0.356	-0.198				
60.000	-0.625	-0.624	-0.621	-0.617	-0.599	-0.569	-0.520	-0.443	-0.316				
80.000	-0.644	-0.644	-0.642	-0.637	-0.625	-0.601	-0.568	-0.512	-0.405				
100.000	-0.662	-0.660	-0.658	-0.657	-0.646	-0.632	-0.610	-0.571	-0.475				

TABLE 39

COX-TABOR ABUNDANCES FOR $X = 0.00$ AND $Z = 0.001$

	Log R								
T6	-5.0	-4.5	-4.0	-3.5	-3.0	-2.5	-2.0	-1.5	-1.0
0.006	-4.476	-4.525	-4.564	-4.592	-4.585	-4.560	-4.476	-4.359	-4.222
0.007	-4.287	-4.281	-4.278	-4.278	-4.271	-4.283	-4.197	-4.056	-3.868
0.008	-3.878	-4.066	-4.169	-4.186	-4.159	-4.109	-4.004	-3.837	-3.625
0.009	-2.930	-3.194	-3.441	-3.670	-3.817	-3.893	-3.781	-3.576	-3.330
0.010	-2.242	-2.464	-2.670	-2.861	-3.025	-3.249	-3.303	-3.203	-2.976
0.011	-1.696	-1.879	-2.040	-2.176	-2.270	-2.353	-2.375	-2.349	-2.280
0.012	-1.282	-1.402	-1.504	-1.586	-1.642	-1.669	-1.669	-1.643	-1.601
0.014	-0.875	-0.794	-0.725	-0.671	-0.629	-0.599	-0.564	-0.527	-0.481
0.016	-0.830	-0.652	-0.450	-0.225	-0.042	0.087	0.179	0.252	0.315
0.018	-0.840	-0.681	-0.448	-0.143	0.176	0.443	0.638	0.767	0.864
0.020	-0.859	-0.718	-0.492	-0.182	0.189	0.564	0.876	1.100	1.254
0.025	-0.861	-0.764	-0.578	-0.304	0.065	0.503	0.960	1.359	1.706
0.030	-0.671	-0.609	-0.465	-0.239	0.074	0.462	0.922	1.368	1.825
0.035	-0.339	-0.221	-0.069	0.117	0.359	0.648	1.012	1.414	1.887
0.040	-0.275	0.027	0.306	0.562	0.792	1.025	1.269	1.585	2.000
0.045	-0.318	0.027	0.410	0.830	1.168	1.426	1.640	1.875	2.201
0.050	-0.361	-0.087	0.305	0.813	1.306	1.690	1.967	2.194	2.458
0.055	-0.396	-0.159	0.201	0.684	1.239	1.757	2.161	2.455	2.716
0.060	-0.422	-0.201	0.132	0.575	1.101	1.675	2.198	2.604	2.919
0.070	-0.451	-0.256	0.042	0.443	0.938	1.478	2.069	2.631	3.097
0.080	-0.462	-0.291	-0.012	0.376	0.855	1.376	1.949	2.537	3.087
0.090	-0.449	-0.290	-0.022	0.354	0.835	1.351	1.911	2.488	3.062
0.100	-0.433	-0.270	-0.007	0.355	0.850	1.370	1.923	2.478	3.057
0.120	-0.379	-0.216	0.056	0.437	0.915	1.429	1.974	2.537	3.108
0.150	-0.325	-0.124	0.172	0.563	1.035	1.548	2.075	2.624	3.164
0.200	-0.340	-0.103	0.217	0.618	1.071	1.544	2.016	2.488	2.948
0.250	-0.424	-0.189	0.118	0.497	0.919	1.344	1.766	2.194	2.624
0.300	-0.498	-0.289	-0.004	0.357	0.748	1.141	1.538	1.946	2.363
0.400	-0.598	-0.476	-0.250	0.080	0.462	0.841	1.215	1.605	2.007
0.500	-0.628	-0.553	-0.385	-0.122	0.239	0.635	1.016	1.398	1.779
0.600	-0.642	-0.586	-0.449	-0.230	0.099	0.489	0.874	1.249	1.621
0.800	-0.662	-0.622	-0.514	-0.339	-0.055	0.311	0.693	1.061	1.421
1.000	-0.667	-0.641	-0.554	-0.404	-0.151	0.201	0.586	0.955	1.299
1.200	-0.674	-0.646	-0.569	-0.443	-0.213	0.131	0.517	0.882	1.206
1.500	-0.663	-0.639	-0.570	-0.457	-0.253	0.065	0.440	0.782	1.075
2.000	-0.673	-0.652	-0.585	-0.471	-0.274	0.011	0.327	0.615	0.875
2.500	-0.684	-0.671	-0.613	-0.511	-0.333	-0.078	0.195	0.450	0.712
3.000	-0.689	-0.679	-0.636	-0.558	-0.408	-0.187	0.054	0.301	0.571
4.000	-0.696	-0.689	-0.660	-0.606	-0.501	-0.334	-0.125	0.118	0.399
5.000	-0.698	-0.696	-0.673	-0.629	-0.546	-0.412	-0.223	0.012	0.288
6.000	-0.700	-0.697	-0.678	-0.642	-0.573	-0.456	-0.284	-0.063	0.210
8.000	-0.703	-0.701	-0.685	-0.657	-0.600	-0.500	-0.350	-0.150	0.126
10.000	-0.704	-0.703	-0.689	-0.665	-0.616	-0.526	-0.391	-0.201	0.073
15.000	-0.710	-0.709	-0.697	-0.676	-0.634	-0.563	-0.452	-0.273	-0.033
20.000	-0.716	-0.716	-0.706	-0.687	-0.651	-0.590	-0.488	-0.326	-0.108
30.000	-0.726	-0.726	-0.720	-0.706	-0.680	-0.631	-0.538	-0.405	-0.215
40.000	-0.736	-0.736	-0.730	-0.719	-0.700	-0.654	-0.576	-0.460	-0.293
60.000	-0.754	-0.753	-0.749	-0.743	-0.728	-0.689	-0.632	-0.544	-0.410
80.000	-0.772	-0.770	-0.768	-0.766	-0.749	-0.721	-0.678	-0.610	-0.499
100.000	-0.791	-0.789	-0.788	-0.786	-0.771	-0.751	-0.719	-0.667	-0.572

TABLE 40

COX-TABOR ABUNDANCES FOR $X = 0.70$ AND $Z = 0.02$

	Log R												
T6	-5.0	-4.5	-4.0	-3.5	-3.0	-2.5	-2.0	-1.5	-1.0	-0.5	0.0	0.5	1.0
0.006	-1.572	-1.719	-1.801	-1.818	-1.782	-1.597	-1.437	-1.224	-1.000	-0.740	-0.456	-0.139	0.237
0.007	-0.709	-0.781	-0.814	-0.808	-0.748	-0.646	-0.517	-0.346	-0.158	0.044	0.261	0.498	0.754
0.008	-0.207	-0.105	-0.019	0.053	0.118	0.211	0.312	0.435	0.579	0.741	0.916	1.111	1.326
0.009	-0.069	0.212	0.452	0.649	0.805	0.916	1.014	1.117	1.223	1.347	1.485	1.649	1.834
0.010	-0.069	0.271	0.614	0.960	1.226	1.421	1.558	1.660	1.755	1.858	1.974	2.111	2.269
0.011	-0.097	0.247	0.628	1.048	1.433	1.723	1.925	2.069	2.173	2.268	2.371	2.483	2.624
0.012	-0.130	0.198	0.584	1.026	1.473	1.855	2.149	2.346	2.491	2.601	2.708	2.820	2.946
0.014	-0.139	0.130	0.482	0.915	1.393	1.872	2.301	2.642	2.891	3.072	3.208	3.337	3.460
0.016	-0.143	0.113	0.442	0.845	1.304	1.808	2.296	2.739	3.104	3.370	3.561	3.713	3.847
0.018	-0.150	0.088	0.409	0.814	1.273	1.758	2.252	2.752	3.200	3.550	3.812	4.002	4.157
0.020	-0.159	0.065	0.380	0.785	1.243	1.728	2.239	2.752	3.246	3.668	3.987	4.222	4.411
0.025	-0.144	0.058	0.364	0.773	1.248	1.764	2.297	2.826	3.351	3.849	4.274	4.614	4.860
0.030	-0.068	0.123	0.423	0.833	1.322	1.843	2.389	2.938	3.493	4.009	4.475	4.857	5.153
0.035	0.018	0.230	0.536	0.937	1.419	1.948	2.489	3.036	3.604	4.135	4.619	5.013	5.324
0.040	0.046	0.317	0.657	1.066	1.533	2.047	2.579	3.122	3.673	4.210	4.690	5.086	5.390
0.045	0.044	0.346	0.724	1.179	1.647	2.139	2.651	3.171	3.709				
0.050	0.020	0.310	0.693	1.169	1.675	2.183	2.683	3.191	3.705				
0.055	-0.009	0.279	0.654	1.115	1.633	2.163	2.679	3.181	3.675				
0.060	-0.039	0.235	0.595	1.041	1.553	2.092	2.627	3.144	3.630				
0.070	-0.072	0.178	0.517	0.947	1.445	1.969	2.511	3.049	3.548				
0.080	-0.094	0.139	0.463	0.876	1.365	1.888	2.428	2.972	3.485				
0.090	-0.091	0.136	0.456	0.868	1.343	1.856	2.394	2.933	3.448				
0.100	-0.085	0.158	0.477	0.874	1.350	1.856	2.384	2.917	3.432				
0.120	-0.026	0.198	0.513	0.922	1.392	1.878	2.386	2.911	3.412				
0.150	0.100	0.310	0.611	1.004	1.465	1.946	2.430	2.907	3.343				
0.200	0.148	0.381	0.682	1.050	1.476	1.931	2.387	2.801	3.134				
0.250	0.016	0.286	0.612	0.995	1.412	1.838	2.268	2.640	2.919				
0.300	-0.110	0.154	0.492	0.904	1.333	1.750	2.146	2.484	2.738				
0.400	-0.293	-0.076	0.264	0.728	1.174	1.591	1.943	2.239	2.475				
0.500	-0.363	-0.232	0.058	0.507	1.003	1.448	1.797	2.085	2.316				
0.600	-0.372	-0.288	-0.056	0.325	0.829	1.319	1.692	1.984	2.220				
0.800	-0.394	-0.317	-0.132	0.163	0.603	1.099	1.516	1.835	2.089				
1.000	-0.403	-0.342	-0.177	0.093	0.498	0.979	1.416	1.754	2.017				
1.200	-0.392	-0.340	-0.193	0.049	0.432	0.900	1.356	1.712	1.980				
1.500	-0.374	-0.321	-0.187	0.028	0.379	0.843	1.304	1.671	1.935				
2.000	-0.382	-0.304	-0.155	0.066	0.382	0.817	1.253	1.593	1.817				
2.500	-0.413	-0.339	-0.179	0.064	0.402	0.804	1.181	1.462	1.648				
3.000	-0.429	-0.377	-0.230	0.011	0.356	0.735	1.058	1.297	1.469				
4.000	-0.448	-0.423	-0.316	-0.127	0.180	0.504	0.775	0.990	1.174				
5.000	-0.456	-0.441	-0.364	-0.225	0.017	0.297	0.548	0.764	0.962				
6.000	-0.462	-0.452	-0.391	-0.279	-0.086	0.155	0.388	0.602	0.810				
8.000	-0.468	-0.462	-0.421	-0.343	-0.198	-0.007	0.194	0.402	0.622				
10.000	-0.469	-0.462	-0.431	-0.374	-0.257	-0.097	0.092	0.292	0.514				
15.000	-0.475	-0.468	-0.437	-0.385	-0.299	-0.181	-0.026	0.152	0.335				
20.000	-0.485	-0.480	-0.454	-0.407	-0.324	-0.221	-0.098	0.038	0.198				
30.000	-0.497	-0.496	-0.482	-0.455	-0.397	-0.320	-0.229	-0.122	0.034				
40.000	-0.507	-0.507	-0.499	-0.482	-0.443	-0.386	-0.313	-0.216	-0.069				
60.000	-0.526	-0.524	-0.520	-0.512	-0.491	-0.455	-0.405	-0.331	-0.205				
80.000	-0.544	-0.547	-0.543	-0.534	-0.520	-0.497	-0.465	-0.411	-0.298				
100.000	-0.563	-0.562	-0.560	-0.557	-0.546	-0.532	-0.514	-0.477	-0.370				

TABLE 41

COX-TABOR ABUNDANCES FOR $X = 0.35$ AND $Z = 0.02$

	Log R												
T6	-5.0	-4.5	-4.0	-3.5	-3.0	-2.5	-2.0	-1.5	-1.0	-0.5	0.0	0.5	1.0
0.006	-1.724	-1.940	-2.065	-2.101	-2.077	-1.958	-1.833	-1.601	-1.371	-1.111	-0.821	-0.478	-0.067
0.007	-0.958	-1.037	-1.088	-1.110	-1.094	-1.015	-0.891	-0.733	-0.547	-0.346	-0.129	0.115	0.379
0.008	-0.570	-0.455	-0.360	-0.283	-0.216	-0.134	-0.042	0.069	0.205	0.361	0.540	0.732	0.947
0.009	-0.495	-0.236	0.010	0.244	0.427	0.563	0.667	0.767	0.875	0.993	1.128	1.284	1.463
0.010	-0.507	-0.218	0.107	0.468	0.785	1.030	1.193	1.314	1.418	1.523	1.634	1.767	1.918
0.011	-0.523	-0.246	0.100	0.514	0.929	1.277	1.528	1.707	1.833	1.936	2.042	2.154	2.287
0.012	-0.517	-0.272	0.060	0.478	0.931	1.353	1.704	1.954	2.132	2.264	2.377	2.490	2.614
0.014	-0.400	-0.209	0.063	0.414	0.847	1.317	1.781	2.174	2.480	2.700	2.867	3.002	3.130
0.016	-0.370	-0.138	0.144	0.477	0.850	1.283	1.756	2.212	2.631	2.951	3.188	3.364	3.505
0.018	-0.366	-0.146	0.148	0.517	0.919	1.325	1.752	2.222	2.689	3.092	3.402	3.627	3.800
0.020	-0.377	-0.167	0.128	0.507	0.935	1.385	1.817	2.256	2.727	3.175	3.546	3.826	4.034
0.025	-0.356	-0.176	0.107	0.493	0.942	1.448	1.955	2.455	2.926	3.390	3.802	4.165	4.450
0.030	-0.261	-0.096	0.175	0.549	1.014	1.519	2.049	2.585	3.108	3.604	4.042	4.429	4.741
0.035	-0.100	0.073	0.332	0.675	1.124	1.623	2.151	2.684	3.225	3.748	4.226	4.630	4.952
0.040	-0.044	0.235	0.544	0.885	1.284	1.746	2.249	2.770	3.312	3.842	4.336	4.753	5.084
0.045	-0.051	0.273	0.647	1.070	1.480	1.899	2.355	2.852	3.368				
0.050	-0.081	0.216	0.601	1.072	1.570	2.014	2.454	2.920	3.412				
0.055	-0.113	0.173	0.544	1.001	1.530	2.039	2.515	2.973	3.443				
0.060	-0.145	0.117	0.469	0.912	1.430	1.971	2.502	2.985	3.453				
0.070	-0.181	0.062	0.392	0.809	1.301	1.832	2.389	2.937	3.433				
0.080	-0.198	0.025	0.337	0.739	1.221	1.748	2.293	2.856	3.386				
0.090	-0.192	0.024	0.335	0.739	1.199	1.719	2.261	2.816	3.353				
0.100	-0.177	0.043	0.354	0.757	1.214	1.721	2.257	2.805	3.343				
0.120	-0.099	0.109	0.416	0.822	1.278	1.769	2.282	2.824	3.356				
0.150	0.053	0.201	0.499	0.948	1.400	1.880	2.370	2.876	3.358				
0.200	0.098	0.363	0.685	1.063	1.489	1.938	2.393	2.827	3.197				
0.250	-0.045	0.250	0.602	1.012	1.431	1.860	2.286	2.670	2.974				
0.300	-0.181	0.107	0.475	0.923	1.344	1.765	2.159	2.505	2.780				
0.400	-0.382	-0.155	0.209	0.710	1.169	1.587	1.940	2.245	2.501				
0.500	-0.451	-0.313	-0.015	0.443	0.955	1.422	1.782	2.081	2.333				
0.600	-0.463	-0.368	-0.129	0.255	0.767	1.271	1.665	1.973	2.229				
0.800	-0.489	-0.409	-0.214	0.096	0.537	1.041	1.478	1.815	2.086				
1.000	-0.496	-0.429	-0.258	0.016	0.433	0.921	1.371	1.730	2.007				
1.200	-0.487	-0.428	-0.277	-0.036	0.358	0.837	1.304	1.680	1.965				
1.500	-0.469	-0.428	-0.290	-0.055	0.302	0.773	1.248	1.632	1.915				
2.000	-0.484	-0.403	-0.247	-0.017	0.304	0.745	1.194	1.552	1.795				
2.500	-0.512	-0.441	-0.277	-0.021	0.325	0.737	1.127	1.424	1.627				
3.000	-0.528	-0.475	-0.327	-0.084	0.275	0.667	1.006	1.261	1.445				
4.000	-0.547	-0.522	-0.413	-0.221	0.094	0.435	0.722	0.951	1.142				
5.000	-0.556	-0.541	-0.462	-0.320	-0.071	0.224	0.493	0.720	0.923				
6.000	-0.561	-0.550	-0.487	-0.373	-0.175	0.080	0.330	0.554	0.767				
8.000	-0.567	-0.561	-0.518	-0.439	-0.288	-0.082	0.132	0.346	0.576				
10.000	-0.567	-0.561	-0.528	-0.469	-0.349	-0.175	0.024	0.233	0.468				
15.000	-0.575	-0.565	-0.533	-0.479	-0.386	-0.259	-0.096	0.094	0.285				
20.000	-0.584	-0.579	-0.552	-0.502	-0.415	-0.300	-0.167	-0.021	0.142				
30.000	-0.596	-0.594	-0.579	-0.552	-0.491	-0.407	-0.305	-0.190	-0.029				
40.000	-0.606	-0.604	-0.595	-0.579	-0.538	-0.477	-0.394	-0.288	-0.135				
60.000	-0.625	-0.623	-0.619	-0.611	-0.586	-0.546	-0.488	-0.404	-0.274				
80.000	-0.643	-0.644	-0.641	-0.633	-0.617	-0.588	-0.546	-0.483	-0.370				
100.000	-0.662	-0.660	-0.657	-0.655	-0.641	-0.622	-0.594	-0.547	-0.445				

TABLE 42

COX-TABOR ABUNDANCES FOR $X = 0.00$ AND $Z = 0.02$

	Log R								
T6	-5.0	-4.5	-4.0	-3.5	-3.0	-2.5	-2.0	-1.5	-1.0
0.006	-3.286	-3.340	-3.382	-3.412	-3.404	-3.371	-3.270	-3.130	-2.967
0.007	-3.112	-3.094	-3.084	-3.081	-3.072	-3.086	-2.990	-2.832	-2.619
0.008	-3.126	-3.121	-3.097	-3.054	-3.000	-2.932	-2.813	-2.618	-2.375
0.009	-2.699	-2.838	-2.919	-2.942	-2.893	-2.806	-2.611	-2.354	-2.069
0.010	-2.154	-2.334	-2.479	-2.587	-2.634	-2.637	-2.460	-2.184	-1.843
0.011	-1.632	-1.790	-1.916	-2.011	-2.054	-2.065	-1.993	-1.824	-1.571
0.012	-1.227	-1.329	-1.409	-1.467	-1.493	-1.481	-1.429	-1.326	-1.248
0.014	-0.810	-0.710	-0.627	-0.560	-0.495	-0.452	-0.398	-0.329	-0.239
0.016	-0.739	-0.541	-0.324	-0.088	0.116	0.258	0.371	0.468	0.563
0.018	-0.734	-0.551	-0.298	0.026	0.359	0.637	0.850	1.009	1.147
0.020	-0.758	-0.577	-0.321	0.009	0.391	0.770	1.094	1.346	1.540
0.025	-0.738	-0.614	-0.402	-0.103	0.292	0.736	1.196	1.628	1.994
0.030	-0.554	-0.465	-0.298	-0.051	0.278	0.687	1.163	1.644	2.111
0.035	-0.250	-0.119	0.046	0.245	0.507	0.828	1.226	1.677	2.162
0.040	-0.169	0.117	0.387	0.643	0.887	1.144	1.433	1.797	2.237
0.045	-0.177	0.145	0.505	0.905	1.237	1.507	1.750	2.028	2.386
0.050	-0.213	0.069	0.446	0.918	1.384	1.759	2.047	2.299	2.596
0.055	-0.246	0.013	0.373	0.835	1.354	1.844	2.241	2.541	2.818
0.060	-0.278	-0.034	0.305	0.739	1.248	1.792	2.290	2.686	3.004
0.070	-0.315	-0.088	0.227	0.630	1.113	1.641	2.205	2.737	3.181
0.080	-0.329	-0.120	0.178	0.567	1.033	1.552	2.104	2.670	3.193
0.090	-0.324	-0.122	0.174	0.563	1.017	1.531	2.075	2.633	3.176
0.100	-0.306	-0.099	0.196	0.582	1.045	1.547	2.080	2.624	3.172
0.120	-0.208	-0.022	0.265	0.655	1.124	1.609	2.120	2.661	3.208
0.150	-0.027	0.172	0.458	0.832	1.261	1.751	2.240	2.758	3.267
0.200	0.021	0.305	0.632	1.002	1.418	1.870	2.330	2.779	3.178
0.250	-0.141	0.192	0.561	0.965	1.386	1.816	2.242	2.639	2.970
0.300	-0.288	0.038	0.423	0.866	1.301	1.719	2.119	2.477	2.775
0.400	-0.506	-0.254	0.120	0.615	1.103	1.535	1.897	2.214	2.488
0.500	-0.571	-0.430	-0.128	0.336	0.859	1.351	1.733	2.046	2.315
0.600	-0.586	-0.483	-0.240	0.144	0.654	1.180	1.605	1.932	2.207
0.800	-0.618	-0.530	-0.328	-0.011	0.429	0.939	1.407	1.765	2.054
1.000	-0.622	-0.557	-0.380	-0.091	0.327	0.819	1.292	1.674	1.969
1.200	-0.621	-0.560	-0.403	-0.150	0.245	0.737	1.217	1.618	1.922
1.500	-0.597	-0.534	-0.391	-0.167	0.184	0.664	1.155	1.564	1.870
2.000	-0.612	-0.532	-0.373	-0.136	0.194	0.636	1.102	1.484	1.755
2.500	-0.641	-0.573	-0.407	-0.142	0.213	0.639	1.047	1.367	1.590
3.000	-0.657	-0.607	-0.458	-0.210	0.159	0.570	0.931	1.206	1.406
4.000	-0.677	-0.652	-0.542	-0.348	-0.026	0.338	0.647	0.895	1.096
5.000	-0.684	-0.671	-0.591	-0.443	-0.187	0.125	0.414	0.659	0.870
6.000	-0.690	-0.679	-0.615	-0.498	-0.293	-0.020	0.248	0.488	0.707
8.000	-0.696	-0.691	-0.647	-0.564	-0.406	-0.185	0.049	0.272	0.510
10.000	-0.696	-0.690	-0.656	-0.593	-0.469	-0.278	-0.066	0.153	0.401
15.000	-0.703	-0.695	-0.662	-0.602	-0.503	-0.361	-0.187	0.015	0.216
20.000	-0.713	-0.710	-0.681	-0.626	-0.530	-0.403	-0.257	-0.100	0.069
30.000	-0.725	-0.724	-0.709	-0.678	-0.617	-0.523	-0.406	-0.281	-0.116
40.000	-0.735	-0.735	-0.725	-0.705	-0.667	-0.597	-0.502	-0.385	-0.226
60.000	-0.754	-0.752	-0.747	-0.737	-0.714	-0.666	-0.598	-0.503	-0.368
80.000	-0.772	-0.770	-0.767	-0.763	-0.741	-0.707	-0.656	-0.580	-0.463
100.000	-0.791	-0.789	-0.787	-0.784	-0.766	-0.740	-0.702	-0.643	-0.541

TABLE 43

ROSS-ALLER ABUNDANCES FOR $X = 0.70$ AND $Z = 0.02$

	Log R												
T6	-5.0	-4.5	-4.0	-3.5	-3.0	-2.5	-2.0	-1.5	-1.0	-0.5	0.0	0.5	1.0
0.006	-1.562	-1.707	-1.786	-1.800	-1.763	-1.580	-1.424	-1.211	-0.986	-0.727	-0.444	-0.126	0.250
0.007	-0.706	-0.777	-0.809	-0.802	-0.742	-0.640	-0.509	-0.335	-0.146	0.058	0.278	0.517	0.775
0.008	-0.204	-0.103	-0.016	0.056	0.122	0.217	0.320	0.444	0.591	0.756	0.935	1.134	1.352
0.009	-0.065	0.216	0.455	0.653	0.810	0.922	1.023	1.127	1.237	1.364	1.507	1.676	1.865
0.010	-0.062	0.279	0.622	0.968	1.235	1.431	1.568	1.673	1.772	1.878	1.999	2.141	2.302
0.011	-0.087	0.258	0.640	1.060	1.444	1.734	1.937	2.083	2.191	2.290	2.395	2.512	2.657
0.012	-0.118	0.212	0.599	1.042	1.487	1.868	2.161	2.361	2.509	2.622	2.732	2.849	2.979
0.014	-0.123	0.152	0.506	0.940	1.415	1.890	2.318	2.659	2.909	3.091	3.231	3.364	3.489
0.016	-0.124	0.139	0.472	0.877	1.334	1.831	2.318	2.758	3.122	3.388	3.581	3.736	3.872
0.018	-0.128	0.116	0.440	0.845	1.302	1.784	2.277	2.773	3.219	3.569	3.832	4.022	4.178
0.020	-0.134	0.096	0.413	0.816	1.273	1.757	2.265	2.776	3.267	3.687	4.007	4.241	4.428
0.025	-0.120	0.091	0.400	0.808	1.277	1.790	2.324	2.853	3.375	3.870	4.293	4.631	4.874
0.030	-0.049	0.149	0.453	0.863	1.349	1.868	2.415	2.965	3.516	4.029	4.492	4.871	5.162
0.035	0.031	0.252	0.563	0.964	1.442	1.971	2.514	3.062	3.626	4.153	4.634	5.023	5.331
0.040	0.046	0.329	0.677	1.090	1.559	2.072	2.604	3.145	3.692	4.225	4.702	5.093	5.394
0.045	0.032	0.346	0.732	1.192	1.664	2.156	2.670	3.189	3.725				
0.050	0.005	0.305	0.696	1.177	1.686	2.199	2.701	3.209	3.720				
0.055	-0.025	0.272	0.653	1.120	1.639	2.171	2.689	3.192	3.686				
0.060	-0.050	0.236	0.602	1.049	1.561	2.102	2.639	3.157	3.642				
0.070	-0.069	0.183	0.525	0.957	1.455	1.982	2.524	3.062	3.561				
0.080	-0.080	0.160	0.485	0.894	1.381	1.904	2.442	2.987	3.499				
0.090	-0.073	0.158	0.478	0.886	1.359	1.871	2.409	2.946	3.461				
0.100	-0.067	0.178	0.497	0.891	1.366	1.867	2.396	2.932	3.444				
0.120	-0.020	0.206	0.523	0.929	1.402	1.887	2.395	2.913	3.413				
0.150	0.103	0.308	0.608	1.003	1.461	1.937	2.417	2.886	3.319				
0.200	0.154	0.384	0.679	1.040	1.456	1.894	2.333	2.739	3.075				
0.250	0.025	0.287	0.609	0.990	1.396	1.796	2.203	2.565	2.857				
0.300	-0.097	0.162	0.495	0.904	1.324	1.726	2.101	2.428	2.693				
0.400	-0.272	-0.051	0.288	0.745	1.190	1.609	1.959	2.247	2.478				
0.500	-0.348	-0.210	0.085	0.539	1.045	1.504	1.861	2.141	2.356				
0.600	-0.365	-0.273	-0.031	0.363	0.889	1.395	1.777	2.061	2.280				
0.800	-0.383	-0.304	-0.110	0.197	0.658	1.180	1.610	1.923	2.162				
1.000	-0.388	-0.315	-0.144	0.126	0.538	1.028	1.480	1.825	2.085				
1.200	-0.384	-0.320	-0.159	0.099	0.480	0.948	1.401	1.761	2.031				
1.500	-0.369	-0.308	-0.162	0.070	0.432	0.884	1.330	1.688	1.948				
2.000	-0.385	-0.305	-0.150	0.079	0.403	0.820	1.229	1.547	1.764				
2.500	-0.416	-0.350	-0.191	0.060	0.394	0.778	1.120	1.380	1.571				
3.000	-0.428	-0.384	-0.243	-0.004	0.343	0.710	1.003	1.223	1.401				
4.000	-0.446	-0.419	-0.313	-0.127	0.187	0.520	0.778	0.969	1.141				
5.000	-0.456	-0.440	-0.358	-0.212	0.046	0.343	0.585	0.771	0.945				
6.000	-0.461	-0.452	-0.389	-0.272	-0.061	0.197	0.423	0.612	0.797				
8.000	-0.468	-0.462	-0.422	-0.347	-0.200	-0.006	0.196	0.398	0.609				
10.000	-0.468	-0.462	-0.432	-0.377	-0.267	-0.113	0.077	0.281	0.504				
15.000	-0.475	-0.467	-0.437	-0.385	-0.303	-0.190	-0.035	0.147	0.332				
20.000	-0.485	-0.479	-0.453	-0.406	-0.324	-0.221	-0.099	0.037	0.196				
30.000	-0.497	-0.496	-0.482	-0.455	-0.396	-0.318	-0.228	-0.122	0.033				
40.000	-0.507	-0.507	-0.499	-0.482	-0.442	-0.386	-0.313	-0.217	-0.070				
60.000	-0.526	-0.524	-0.520	-0.512	-0.491	-0.455	-0.406	-0.332	-0.206				
80.000	-0.544	-0.547	-0.543	-0.534	-0.520	-0.498	-0.465	-0.412	-0.300				
100.000	-0.563	-0.562	-0.560	-0.557	-0.546	-0.533	-0.515	-0.477	-0.372				

TABLE 44

ROSS-ALLER ABUNDANCES FOR $X = 0.35$ AND $Z = 0.02$

	Log R												
T6	-5.0	-4.5	-4.0	-3.5	-3.0	-2.5	-2.0	-1.5	-1.0	-0.5	0.0	0.5	1.0
0.006	-1.712	-1.921	-2.041	-2.072	-2.046	-1.932	-1.807	-1.580	-1.351	-1.093	-0.803	-0.461	-0.051
0.007	-0.954	-1.031	-1.081	-1.101	-1.083	-1.004	-0.879	-0.718	-0.531	-0.328	-0.109	0.136	0.402
0.008	-0.566	-0.452	-0.356	-0.279	-0.210	-0.127	-0.033	0.080	0.220	0.380	0.563	0.759	0.978
0.009	-0.490	-0.231	0.015	0.250	0.434	0.570	0.676	0.779	0.889	1.012	1.154	1.316	1.501
0.010	-0.499	-0.208	0.117	0.478	0.796	1.041	1.206	1.330	1.437	1.545	1.662	1.801	1.958
0.011	-0.513	-0.233	0.114	0.529	0.943	1.291	1.544	1.725	1.854	1.962	2.073	2.189	2.327
0.012	-0.504	-0.257	0.077	0.498	0.949	1.370	1.721	1.973	2.154	2.291	2.408	2.527	2.656
0.014	-0.384	-0.186	0.090	0.443	0.875	1.344	1.804	2.197	2.504	2.726	2.898	3.037	3.170
0.016	-0.350	-0.111	0.176	0.512	0.884	1.313	1.783	2.239	2.656	2.977	3.216	3.396	3.539
0.018	-0.344	-0.117	0.182	0.552	0.954	1.359	1.785	2.253	2.718	3.120	3.429	3.656	3.831
0.020	-0.351	-0.133	0.165	0.543	0.970	1.417	1.851	2.288	2.759	3.205	3.575	3.855	4.062
0.025	-0.331	-0.143	0.146	0.534	0.979	1.481	1.985	2.488	2.960	3.420	3.829	4.191	4.473
0.030	-0.241	-0.069	0.205	0.583	1.046	1.550	2.077	2.617	3.140	3.634	4.068	4.452	4.760
0.035	-0.088	0.093	0.358	0.707	1.153	1.650	2.178	2.715	3.256	3.775	4.247	4.648	4.965
0.040	-0.047	0.244	0.562	0.907	1.310	1.774	2.277	2.800	3.340	3.865	4.354	4.766	5.093
0.045	-0.068	0.268	0.651	1.081	1.496	1.918	2.375	2.875	3.391				
0.050	-0.101	0.206	0.598	1.076	1.579	2.027	2.472	2.941	3.432				
0.055	-0.134	0.160	0.539	1.002	1.533	2.043	2.522	2.985	3.456				
0.060	-0.159	0.116	0.475	0.918	1.437	1.978	2.512	3.005	3.467				
0.070	-0.178	0.067	0.400	0.819	1.311	1.844	2.400	2.946	3.444				
0.080	-0.185	0.045	0.361	0.761	1.237	1.762	2.306	2.868	3.397				
0.090	-0.172	0.048	0.358	0.758	1.217	1.732	2.275	2.827	3.364				
0.100	-0.157	0.065	0.376	0.775	1.232	1.733	2.270	2.816	3.355				
0.120	-0.092	0.117	0.426	0.835	1.286	1.780	2.292	2.828	3.359				
0.150	0.059	0.205	0.502	0.949	1.400	1.875	2.364	2.864	3.346				
0.200	0.107	0.369	0.685	1.057	1.471	1.909	2.350	2.778	3.153				
0.250	-0.036	0.257	0.606	1.011	1.418	1.825	2.232	2.606	2.923				
0.300	-0.167	0.119	0.484	0.926	1.339	1.748	2.125	2.460	2.745				
0.400	-0.361	-0.129	0.234	0.728	1.190	1.611	1.965	2.262	2.511				
0.500	-0.437	-0.290	0.016	0.479	1.004	1.482	1.851	2.144	2.378				
0.600	-0.455	-0.354	-0.104	0.295	0.824	1.349	1.753	2.053	2.291				
0.800	-0.477	-0.398	-0.195	0.130	0.590	1.118	1.568	1.901	2.158				
1.000	-0.482	-0.403	-0.226	0.048	0.469	0.966	1.428	1.794	2.071				
1.200	-0.478	-0.411	-0.245	0.020	0.412	0.880	1.346	1.724	2.011				
1.500	-0.464	-0.410	-0.258	-0.009	0.361	0.816	1.273	1.648	1.925				
2.000	-0.488	-0.403	-0.242	-0.004	0.323	0.751	1.171	1.506	1.740				
2.500	-0.515	-0.450	-0.288	-0.028	0.318	0.715	1.070	1.343	1.547				
3.000	-0.528	-0.482	-0.340	-0.102	0.261	0.644	0.955	1.187	1.374				
4.000	-0.545	-0.517	-0.410	-0.223	0.098	0.453	0.731	0.935	1.110				
5.000	-0.555	-0.539	-0.457	-0.308	-0.041	0.273	0.536	0.734	0.911				
6.000	-0.561	-0.551	-0.486	-0.367	-0.150	0.124	0.370	0.569	0.757				
8.000	-0.567	-0.561	-0.519	-0.442	-0.291	-0.082	0.133	0.343	0.563				
10.000	-0.567	-0.561	-0.529	-0.472	-0.358	-0.192	0.007	0.221	0.458				
15.000	-0.575	-0.565	-0.533	-0.479	-0.390	-0.268	-0.105	0.088	0.282				
20.000	-0.584	-0.579	-0.551	-0.501	-0.415	-0.300	-0.168	-0.022	0.141				
30.000	-0.596	-0.594	-0.579	-0.551	-0.490	-0.406	-0.304	-0.190	-0.030				
40.000	-0.606	-0.604	-0.595	-0.578	-0.537	-0.476	-0.393	-0.288	-0.136				
60.000	-0.625	-0.623	-0.618	-0.610	-0.586	-0.546	-0.488	-0.404	-0.274				
80.000	-0.643	-0.644	-0.641	-0.633	-0.617	-0.588	-0.546	-0.483	-0.371				
100.000	-0.662	-0.660	-0.657	-0.655	-0.641	-0.622	-0.594	-0.548	-0.446				

TABLE 45

ROSS-ALLER ABUNDANCES FOR $X = 0.00$ AND $Z = 0.02$

	Log R								
T6	-5.0	-4.5	-4.0	-3.5	-3.0	-2.5	-2.0	-1.5	-1.0
0.006	-3.080	-3.116	-3.140	-3.153	-3.134	-3.100	-3.010	-2.882	-2.727
0.007	-2.918	-2.895	-2.878	-2.866	-2.848	-2.855	-2.760	-2.600	-2.383
0.008	-2.966	-2.947	-2.912	-2.864	-2.801	-2.735	-2.614	-2.411	-2.164
0.009	-2.630	-2.737	-2.789	-2.786	-2.721	-2.632	-2.436	-2.172	-1.885
0.010	-2.127	-2.296	-2.423	-2.507	-2.524	-2.504	-2.311	-2.023	-1.684
0.011	-1.614	-1.767	-1.887	-1.973	-2.005	-1.996	-1.902	-1.713	-1.449
0.012	-1.212	-1.311	-1.387	-1.441	-1.461	-1.439	-1.372	-1.254	-1.187
0.014	-0.792	-0.686	-0.598	-0.530	-0.459	-0.416	-0.359	-0.281	-0.183
0.016	-0.716	-0.512	-0.289	-0.048	0.159	0.303	0.418	0.519	0.620
0.018	-0.705	-0.518	-0.259	0.070	0.403	0.685	0.900	1.066	1.210
0.020	-0.726	-0.535	-0.274	0.058	0.440	0.821	1.150	1.409	1.610
0.025	-0.714	-0.580	-0.355	-0.040	0.356	0.799	1.258	1.694	2.070
0.030	-0.530	-0.437	-0.262	-0.006	0.334	0.754	1.240	1.725	2.196
0.035	-0.240	-0.102	0.069	0.273	0.542	0.875	1.292	1.759	2.253
0.040	-0.176	0.121	0.400	0.661	0.911	1.176	1.480	1.868	2.326
0.045	-0.201	0.134	0.505	0.911	1.250	1.526	1.780	2.078	2.455
0.050	-0.237	0.054	0.439	0.918	1.389	1.770	2.065	2.334	2.651
0.055	-0.272	-0.003	0.366	0.833	1.355	1.843	2.245	2.557	2.851
0.060	-0.296	-0.038	0.308	0.744	1.254	1.797	2.299	2.700	3.028
0.070	-0.312	-0.084	0.233	0.640	1.123	1.652	2.212	2.744	3.192
0.080	-0.318	-0.098	0.205	0.591	1.051	1.567	2.116	2.680	3.202
0.090	-0.304	-0.093	0.202	0.584	1.037	1.547	2.088	2.643	3.185
0.100	-0.285	-0.073	0.223	0.602	1.064	1.562	2.090	2.636	3.183
0.120	-0.199	-0.009	0.280	0.666	1.134	1.622	2.132	2.664	3.208
0.150	-0.018	0.178	0.462	0.835	1.262	1.749	2.239	2.750	3.258
0.200	0.031	0.312	0.635	0.999	1.405	1.845	2.296	2.739	3.141
0.250	-0.131	0.200	0.566	0.967	1.378	1.791	2.197	2.583	2.924
0.300	-0.274	0.049	0.432	0.873	1.302	1.707	2.093	2.439	2.744
0.400	-0.484	-0.228	0.146	0.638	1.125	1.561	1.929	2.239	2.504
0.500	-0.557	-0.401	-0.098	0.351	0.907	1.411	1.805	2.115	2.365
0.600	-0.586	-0.476	-0.220	0.182	0.712	1.256	1.693	2.015	2.271
0.800	-0.604	-0.520	-0.313	0.018	0.477	1.010	1.492	1.851	2.126
1.000	-0.609	-0.526	-0.341	-0.053	0.362	0.860	1.342	1.734	2.031
1.200	-0.612	-0.535	-0.362	-0.093	0.304	0.782	1.256	1.658	1.967
1.500	-0.591	-0.524	-0.367	-0.122	0.248	0.713	1.181	1.580	1.880
2.000	-0.615	-0.531	-0.366	-0.120	0.218	0.646	1.084	1.441	1.698
2.500	-0.644	-0.584	-0.419	-0.149	0.209	0.621	0.996	1.286	1.507
3.000	-0.656	-0.613	-0.471	-0.232	0.144	0.551	0.887	1.136	1.333
4.000	-0.675	-0.647	-0.539	-0.351	-0.025	0.356	0.663	0.886	1.067
5.000	-0.683	-0.670	-0.586	-0.431	-0.159	0.176	0.464	0.682	0.863
6.000	-0.690	-0.680	-0.614	-0.492	-0.269	0.024	0.293	0.510	0.702
8.000	-0.696	-0.690	-0.647	-0.566	-0.410	-0.188	0.047	0.269	0.499
10.000	-0.696	-0.690	-0.657	-0.596	-0.478	-0.298	-0.088	0.138	0.391
15.000	-0.702	-0.694	-0.661	-0.602	-0.506	-0.370	-0.198	0.009	0.213
20.000	-0.713	-0.710	-0.680	-0.625	-0.530	-0.403	-0.258	-0.100	0.068
30.000	-0.725	-0.724	-0.708	-0.677	-0.615	-0.521	-0.404	-0.280	-0.116
40.000	-0.735	-0.735	-0.725	-0.704	-0.666	-0.596	-0.501	-0.385	-0.226
60.000	-0.754	-0.752	-0.747	-0.737	-0.714	-0.666	-0.598	-0.503	-0.366
80.000	-0.772	-0.770	-0.767	-0.763	-0.741	-0.707	-0.656	-0.581	-0.464
100.000	-0.791	-0.789	-0.787	-0.784	-0.766	-0.741	-0.702	-0.643	-0.542

REFERENCES

Abe, R. 1959, Prog. Theor. Phys., 22, 213
Alexander, D. R., Johnson, H. R., & Rypma, R. L. 1983, ApJ, 272, 773
Anders, E., & Grevesse, N. 1989, Geochim. Cosmochim. Acta, 53, 197
Andreasen, G. K. 1988, A&A, 201, 72
Andreasen, G. K., & Petersen, J. O. 1988, A&A, 192, L4
Bahcall, J. N., & Ulrich, R. K. 1988, Rev. Mod. Phys., 60, 297
Berrington, K. A., Burke, P. G., Butler, K., Seaton, M. J., Storey, P. J., Taylor, K. T., & Yan, Y. 1987, J. Phys. B, 20, 6397
Boercker, D. B. 1987, ApJ, 316, L95
Bolle, D. 1987, Phys. Rev. A, 36, 3259
———. 1989, Phys. Rev. A, 39, 2752
Cameron, A. G. W. 1973, Space Sci. Rev., 15, 121
Carson, T., Huebner, W., Magee, N., & Merts, A. 1984, ApJ, 283, 466
Carson, T. R., & Stothers, R. 1976, ApJ, 204, 461
———. 1988, ApJ, 328, 196
Carson, T. R., Stothers, R., & Vermury, S. K. 1981, ApJ, 244, 230
Christensen-Dalsgaard, J., Dappen, W., & Lebreton, Y. 1988, Nature, 336, 634
Christensen-Dalsgaard, J., Duval, T. L., Gough, D. O., Harvey, J. W., & Rhodes, E. J. 1985, Nature, 315, 378
Cowan, R. D. 1981, The Theory of Atomic Structure (Berkeley: Univ. California Press)
Cox, A. N. 1991, ApJ, 381, L71
Cox, A. N., Guzik, J. A., & Kidman, R. B. 1989, ApJ, 342, 1187
Cox, A. N., Guzik, J. A., & Raby, S. 1990, ApJ, 342, 1187
Cox, A. N., & Stewart, J. N. 1965, ApJS, 11, 22
———. 1969, ApJS, 19, 243
———. 1970a, ApJS, 19, 243
———. 1970b, ApJS, 19, 261
Cox, A. N., Stewart, J. N., & Eilers, D. D. 1965, ApJS, 11, 1
Cox, A. N., & Tabor, J. E. 1976, ApJS, 31, 271 (CT)
Dappen, W., Anderson, L., & Mihalas, D. 1987, ApJ, 319, 195
Dappen, W., Lebreton, Y., & Rogers, F. 1990, Sol. Phys., 128, 35
Dimitrijevic, M. S., & Konjevic, N. 1980, J. Quant. Spectrosc. Rad. Transf., 24, 451
———. 1986, A&A, 163, 297
———. 1986, A&A, 172, 345
D'yachkov, L. G., Kobzev, G. A., & Pankratov, P. M. 1988, J. Phys. B, 21, 1939
Ebeling, W., Kraeft, W. D., & Kremp, D. 1976, Theory of Bound States and Ionization Equilibrium in Plasmas and Solids (Berlin: Akademia)
Eggleton, P. P., Faulkner, J., & Flannery, B. P. 1973, A&A, 23, 325
Griem, H. R. 1960, ApJ, 132, 883
Griem, H. R. 1974, Spectral Line Broadening by Plasmas (New York: Academic)
Hejlesen, P. M. 1980, A&A, 84, 135
Huebner, W. F. 1986, in Physics of the Sun, Vol. 1, ed. P. A. Sturrock, T. E. Holzer, D. M. Mihalas, & R. K. Ulrich (Dordrecht: Reidel), 33
Huebner, W. F., Merts, A. L., Magee, N. H., & Argo, M. F. 1977, Los Alamos Scientific Report LA-6760-M
Hummer, D. G., & Mihalas, D. 1988, ApJ, 331, 794
Iglesias, C., DeWitt, H., Lebowitz, J., MacGowan, D., & Hubbard, W. B. 1985, Phys. Rev. A, 31, 1698
Iglesias, C. A., & Rogers, F. J. 1991a, ApJ, 371, 408
———. 1991b, ApJ, 371, L73
Iglesias, C. A., Rogers, F. J., & Wilson, B. G. 1987, ApJ, 322, L45 (IRW1)
———. 1990, ApJ, 360, 221 (IRW2)
Inglis, D., & Teller, E. 1939, ApJ, 90, 439
Johnson, R. R. 1967, J. Quant. Spectrosc. Rad. Transf., 7, 815
Korzennik, S. G., & Ulrich, R. K. 1989, ApJ, 339, 1144
Kurucz, R. L. 1970, Smithsonian Astrophys. Obs. Spec. Rep., 308
Lee, R. W. 1988, J. Quant. Spectrosc. Rad. Transf., 40, 561
Lenzuni, P., Chernoff, D. F., & Salpeter, E. E. 1991, ApJS, 76, 759
Magee, N. H., Merts, A. L., & Huebner, W. F. 1975, ApJ, 196, 617
———. 1984, ApJ, 283, 264
Mihalas, D., Dappen, W., & Hummer, D. G. 1988, ApJ, 331, 815
Moskalik, P., Buchler, J. R., & Marom, A. 1992, ApJ, in press
Petersen, J. O. 1989, A&A, 226, 151
———. 1990, A&A, 238, 160
Pisano, C., & McKellar, B. H. J. 1989, Phys. Rev. A, 40, 6597
Renzini, A., & Fusi-Pecci, F. 1988, ARA&A, 26, 199
Rogers, F. J. 1974, Phys. Rev. A, 10, 2441
———. 1976, Phys. Rev. A, 19, 375
———. 1977, Phys. Letters A, 61, 358
———. 1979, Phys. Rev. A, 19, 375
———. 1981, Phys. Rev. A, 23, 1008
———. 1986, ApJ, 310, 723
———. 1991, Nuovo Cimento, in press
Rogers, F. J., & DeWitt, H. 1973, Phys. Rev. A, 8, 1061
Rogers, F. J., Wilson, B. G., & Iglesias, C. A. 1988, Phys. Rev. A, 38, 5007
Ross, J. E., & Aller, L. H. 1976, Science, 191, 1223
Rozsnyai, B. F. 1989, ApJ, 341, 414
Ruzdjak, V., & Vujnovic, V. 1976, A&A, 54, 751
Sampson, D. H. 1959, ApJ, 129, 734
Seaton, M. J. 1987, J. Phys. B, 20, 6363
———. 1991, J. Phys. B, 23, 3255
Simon, N. R. 1982, ApJ, 260, L87
Simon, N. R., & Cox, A. N. 1991, ApJ, 376, 717
Sommerville, W. B. 1967, ApJ, 149, 811
Stellingwerf, R. F. 1974, ApJ, 195, 441
———. 1975, ApJ, 199, 705
———. 1978, AJ, 83, 1184
Stilley, J. L., & Callaway, J. 1970, ApJ, 160, 245
Swenson, F. J., Stringfellow, G., & Faulkner, J. 1990, ApJ, 348, L33
Weiss, A., Keady, J. J., & Magee, N. H. 1990, Atomic Data Nucl. Data, 45, 209
Wiese, W. L., Kelleher, D. E., & Paquette, D. R. 1972, Phys. Rev. A, 6, 1132
Wishart, A. W. 1979, MNRAS, 187, 59